THESIS FOR THE DEGREE OF DOCTOR OF PHYLOSOPHY (Ph.D.)

MOLECULAR ORGANIZATION OF THE ENDOCANNABINOID SYSTEM IN THE SPINAL DORSAL HORN OF RODENTS

Zoltán Hegyi

Supervisor: Miklós Antal MD, PhD, DSc

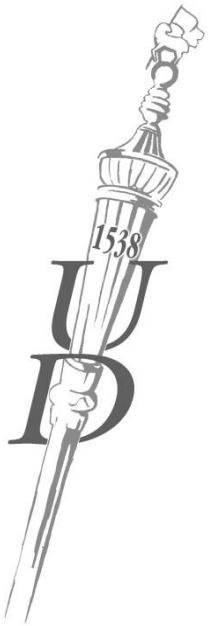

UNIVERSITY OF DEBRECEN

DOCTORAL SCHOOL OF NEUROSCIENCES

DEBRECEN, 2013.

CONTENTS

ABBREVIATIONS **5**

1. INTRODUCTION **7**

2. THEORETICAL BACKGROUND **10**

2.1. Endogenous cannabinoid ligands *10*

2.2. Endocannabinoid biosythesis and mobilization *12*

2.2.1. Biosynthesis of anandamide *12*

2.2.1.1. NAPE-PLD *12*

2.2.1.2. Alternative N-acyl-ethanolamine biosynthetic routes *14*

2.2.2. Biosynthesis of 2-AG *14*

2.3. Cannabinoid receptors *16*

2.3.1. CB1 receptor *16*

2.3.2. CB2 receptor *18*

2.4. Degradation of endocannabinoids *(Fig. 5)* *19*

2.4.1.1. Degradation of anandamide (Fig. 5a) *19*

2.4.1.2. Degradation of 2-AG (Fig. 5b) *21*

2.4.2. Oxidative degradation of endocannabinoids *22*

2.5. Roles of the endocannabinoid system in the retrograde modulation of synaptic transmission *22*

2.5.1. Endocannabinoid-mediated short term depression *23*

2.5.2. Endocannabinoid-mediated long term depression *25*

2.5.3. Role of anandamide in the endocannabinoid-mediated modulation of synaptic transmission *25*

3. MATERIALS AND METHODS **29**

3.1. Animals and preparation of tissue sections *29*

3.2. Immunohistochemistry *30*

3.2.1. Single immunostaining *30*

3.2.2. Double immunostaining *30*

3.2.3. Confocal microscopy and analysis *32*

3.2.4. Preembedding immunostaining with diaminobenzidine chromogen reaction for electron microscopy *33*

3.2.5. Preembedding nanogold immunostaining for electron microscopy *34*

3.2.6. Controls *35*

4. RESULTS 40

4.1. Distribution of CB1-R immunoreactivity in the superficial spinal dorsal horn *40*

4.2. Co-localization of CB1-R immunoreactivity with axonal and glial markers *41*

4.2.1. Co-localization of CB1-R immunoreactivity with markers of nociceptive primary afferents 41

4.2.2. Co-localization of CB1-R immunoreactivity with markers of axon terminals of glutamatergic and GABAergic spinal neurons 44

4.2.3. Co-localization of CB1-R immunoreactivity with markers of astrocytes and microglial cells 46

4.3. Distribution of CB1-receptors on the cell membrane of presynaptic axon terminals and glial processes *47*

4.4. Distribution of DGL-α and NAPE-PLD immunoreactivity in the superficial spinal dorsal horn *49*

4.5. Co-localization of DGL-α and NAPE-PLD immunoreactivity with axonal and glial markers *50*

4.5.1. Co-localization of DGL-α and NAPE-PLD immunoreactivity with markers of nociceptive primary afferents 51

4.5.2. Co-localization of DGL-α and NAPE-PLD immunoreactivity with markers of axon terminals of putative glutamatergic and GABAergic spinal neurons 52

4.5.3. Co-localization of DGL-α and NAPE-PLD immunoreactivity with markers of astrocytes and microglial cells 55

4.6. Ultrastructural localization of DGL-α and NAPE-PLD immunoreactivity *58*

5. DISCUSSION 63

5.1. CB1 receptors on central axon terminals of nociceptive primary afferents *63*

5.2. CB1 receptors on axon terminals of spinal neurons *65*

5.3. CB1 receptors on glial cells *66*

5.4. Enzymes synthesizing 2-AG and anandamide in the brain and spinal cordHiba! A könyvjelző nem létezik.

5.5. DGL-α and NAPE-PLD in axon terminals *67*

5.6. Differential distribution of DGL-α and NAPE-PLD in dendrites *67*

5.7. DGL-α and NAPE-PLD in glial cells *68*

6. SUMMARY **71**

7. REFERENCES **72**

8. LIST OF PUBLICATIONS **97**

9. KEY WORDS **101**

10. ACKNOWLEDGEMENT **102**

ABBREVIATIONS

2-AG – 2-arachidonoyl-glycerol

ABHD4, ABHD6, ABHD12 – serine hydrolase α/β hydrolase domain 4, 6 or 12

AEA – arachidonoyl-ethanolamide or anandamide

CB1-R – type 1 cannabinoid receptor

CB2-R – type 2 cannabinoid receptor

CGRP – calcitonine gene-related peptide

COX-2 – cyclooxigenase-2

DAB – 3, 3'-diamino-benzidine

DAG – diacylglycerol

DGL-α – diacylglycerol lipase α

DSE – depolarization-induced suppression of excitation

DSI – depolarization-induced suppression of inhibition

eCB – endocannabinoid

ERK – extracellular signal-regulated kinase

FAAH – fatty acid amide hydrolase

GABA – γ-aminobutyric acid

GAD65/67 – 65 and 67 kDa isoforms of glutamic acid decarboxylase

GDE1 – glycerophosphodiesterase-1

GFAP – glial fibrillary acidic protein

GIRK – G-protein coupled, inwardly rectifying potassium channel

GPCR – G-protein coupled receptor

GPR55 – G-protein coupled receptor 55

IB4 – isolectin B4

iNAT – calcium-insensitive N-acyltransferase

IP3 – inositol triphosphate

LOX-2 – lipoxygenase 2

LTD – long term depression

MAP kinase – mitogen-activated protein kinase

MGL – monoacylglycerol lipase

NAAA – N-acylethanolamin-hydrolyzing acid amidase

NADA – N-arachidonoyl dopamine

NAE – N-acyl ethanolamine

NAPE – N-acylphosphatidyl ethanolamine

NAPE-PLD – N-acylphosphatidyl ethanolamine-selective phospholipase D

NAT – N-acyltransferase

NMDA – N-methyl-D-aspartate

PB – phophate buffer

PBS – phosphate buffered saline

PIP_2 – phosphatidylinositol 4,5-bisphosphate

PKA – protein kinase A

PLA_1 – phospholipase A_1

PLC – phospholipase C

SEM – standard error of mean

TBS – Tris-buffered saline

THC – Δ9-tetrahydrocannabinol

TPBS – Tris-phosphate-buffered saline

TRPV1 – transient receptor potential cation channel V1

VGLUT2 – vesicular glutamate transporter 2

1. INTRODUCTION

Between 50 and 70 AD, a Greek physician, pharmacologist and botanist Pedanius Dioscorides wrote a five-volume book *De Materia Medica*, in which he described the use of more than 500 medicinal plants to cure certain diseases. This collection has been an inexhaustible source of drugs for more than 19 centuries, still containing powerful and effective medicinal plants with unknown mechanisms of action.

In 1962, Raphael Mechoulam, the young postdoctoral fellow at the Hebrew University in Jerusalem, decided to investigate one of the famous and promising plants in Dioscorides' Herbal: the Cannabis sativa, also known as the hemp, one of the most widely used drugs throughout the world. In two years, the major psychoactive component of the Cannabis has successfully been identified and named delta-9-tetrahydrocannabinol or THC (Gaoni and Mechoulam, 1964). As it turned out, the chemical structure of THC is remarkably different from the other plant-derived compounds. Based on its strong hydrophobic nature, the THC was thought to act by influencing the biophysical properties of cell membranes rather than via specific interactions with selective binding sites.

More than 20 years later, experiments with highly selective, enantiomerically pure THC analogues showed that their major pharmacological actions are enantioselective, and mediated by inhibiting cAMP accumulation (Howlett and Fleming, 1984). These findings suggested the existence of cannabinoid-binding receptor, which was identified and cloned only in 1990 by Matsuda and his co-workers (Matsuda *et al.*, 1990). The discovery of cannabinoid receptor (CB1-R) helped to explain the pharmacological effects of THC, but raised questions regarding the brain-derived, endogenous ligands of CB1-R. To the greatest surprise, in the early '90s not only one but two cannabimimetic compounds have been isolated: anandamide (arachidonoyl-ethanolamide; Devane et al, 1992) and 2-AG (2-arachidonoyl-glycerol; Mechoulam et al, 1995; Sugiura et al, 1995). In the past 20 years, biosynthetic and catabolic pathways and ezymes for anandamide and 2-AG, as well as additional cannabinoid sensitive receptors and an entire family of endogenous cannabinoid ligands have been elucidated. These cannabinoid-related ligands, receptors and enzymes together are known as the endocannabinoid system.

Although Cannabis has been used for centuries as a recreational drug, it was also prescribed as medicine against pain and spasm. However, biomedical research has only recently been focusing on the Cannabis' true therapeutic potential and the unexpectedly powerful endocannabinoid influence on different physiological and pathological functions, from cancer and epilepsy to fertility and obesity (Pacher et al, 2006.). One of the most interesting observations is that both exogenous cannabinoid compounds and endocannabinoid ligands effectively induce antinociception, which in potency and efficacy is comparable to the analgesic effects of morphine (Bloom et al, 1977). It has been demonstrated that the molecular players of the endocannabinoid system, primarily the CB1-Rs are localized at mutiple levels of the pain pathways suggesting that the endocannabinoid system may modulate pain processing at peripheral, spinal and supraspinal levels (Herkenham et al, 1991; Pertwee, 2001; Agarwal et al, 2007; Drew et al, 2008).

Considering the well-known gate control theory of pain, which has been proposed by Melzack and Wall (Melzack and Wall, 1965), neural networks in the dorsal horn of the spinal cord can be regarded as the primary area of the central nervous system that can effectively modulate nociceptive information processing. CB1-Rs are strongly expressed in the spinal dorsal horn, as it has been reported in immunocytochemical (Farquhar-Smith et al, 2000) and in situ hybridization studies (Mailleux and Vanderhaeghen, 1992). These molecular anatomical data helped to explain the cannabinoid-evoked antinociception after intrathecal administration of the cannabinoid agonist WIN 55,212-2 (Hohmann et al, 1995), as well as the cannabinoid-mediated suppression of C- and Aδ-fiber evoked responses in dorsal horn neurons (Strangman and Walker, 1999; Kelly and Chapman, 2001). However, the laminar distribution and cellular localization of CB1-Rs in laminae I-II of the spinal dorsal horn, which contains the primary pain processing neural network, remains controversial (Hohmann et al, 1999; Ong and Mackie, 1999; Salio et al, 2001, 2002; Farquhar-Smith et al, 2000).

Causing further difficulties in the understanding of the spinal endocannabinoid system, surprisingly little is known about the molecular anatomical background of the endocannabinoid mobilization at the level of the spinal cord. Nyilas et al. (2009) provided convincing experimental evidence for the ultrastructural localization of diacylglycerol lipase alpha (DGL-α), the synthesizing enzyme of 2-AG. However, the distribution of DGL-α among the cellular elements of the spinal cord remains largely unknown.

Investigation of the morphological substrate of anandamide biosynthesis could be even more complicated, since no less then five paralell metabolic pathways are involved in the biogenesis of N-acyethanolamides (Sun et al, 2004; Simon and Cravatt, 2006, 2008; Liu et al, 2006), the most important and best known being catalyzed by N-acylphosphatidylethanolamine-specific phospholipase D (NAPE-PLD; Okamoto et al, 2004). Previous studies have reported that NAPE-PLD is localized predominantly to intracellular membrane cisternae of axonal calcium stores (Egertova et al, 2008; Nyilas et al, 2008). However, experimental evidence for the somatodendritic localization of NAPE-PLD has also been provided (Cristino et al, 2008). To date, however, expression of NAPE-PLD in the spinal dorsal horn has not been investigated, thus the morphological background of spinal anandamide mobilization remains completely unknown.

2. THEORETICAL BACKGROUND

2.1. Endogenous cannabinoid ligands

Cannabinoids are chemical compounds of various origin capable of binding to cannabinoid receptors. Cannabinoids include

- phytocannabinoids isolated mainly from Cannabis sativa, the most famous being the Δ-9-tetrahydrocannabinol,

- synthetic compounds such as WIN55,212-2, and

- the endocannabinoids.

By definition, endocannabinoids are endogenously synthesized compounds which can interact with and activate cannabinoid receptors (Di Marzo and Fontan, 1995; Bisogno et al, 2005). These molecules are lipid mediators belonging to the class of eicosanoids and sharing some common features: they are either ethers, esters or amids of polyunsaturated long-chain fatty acids, and unlike classical neurotransmitters, endogenous cannabinoids are not stored in synaptic or secretory vesiculae, but instead, they are synthesized and released on demand (Di Marzo et al, 1998; Piomelli, 2007) (Fig. 1).

The first such compounds to be identified are anandamide (arachidonoyl-ethanolamine, AEA; Devane et al, 1992) and 2-arachidonoyl-glycerol (2-AG; Mechoulam et al, 1995; Sugiura et al, 1995).

Anandamide belongs to the family of N-acyl-ethanolamines (NAEs) and acts as partial or full agonist at CB1-R depending on the tissue and the biological response measured, and as weak agonist at CB2-R (Pertwee et al, 2010). In addition, anandamide is also endogenous ligand for vanilloid-1 receptor (TRPV1; Zygmunt et al, 1999; Smart et al, 2000) and for the deorphanized G-protein coupled receptor 55 (GPR55; Pertwee, 2002; Lauckner et al, 2008). The rodent brain contains 10-15 pmol anandamide / g tissue on average, but anandamide level is highly variable in different brain areas, from the diencephalic 10.2 pmol/g to the hippocampal 148 pmol/g (Felder et al, 1996, Bisogno et al, 1999). The level of anandamide, which has been measured in the spinal cord of male and female mice (27.6 and 20.2 pmol/g, respectively; Di Marzo et al, 2000), may

activate CB1 receptors, since it has been demonstrated, that CB1-R mediated intracellular signalization can safely be evoked with 7 pmol/g anandamide (Wang et al, 2003), suggesting that anandamide may serve as functional ligand of CB1-R in the spinal dorsal horn.

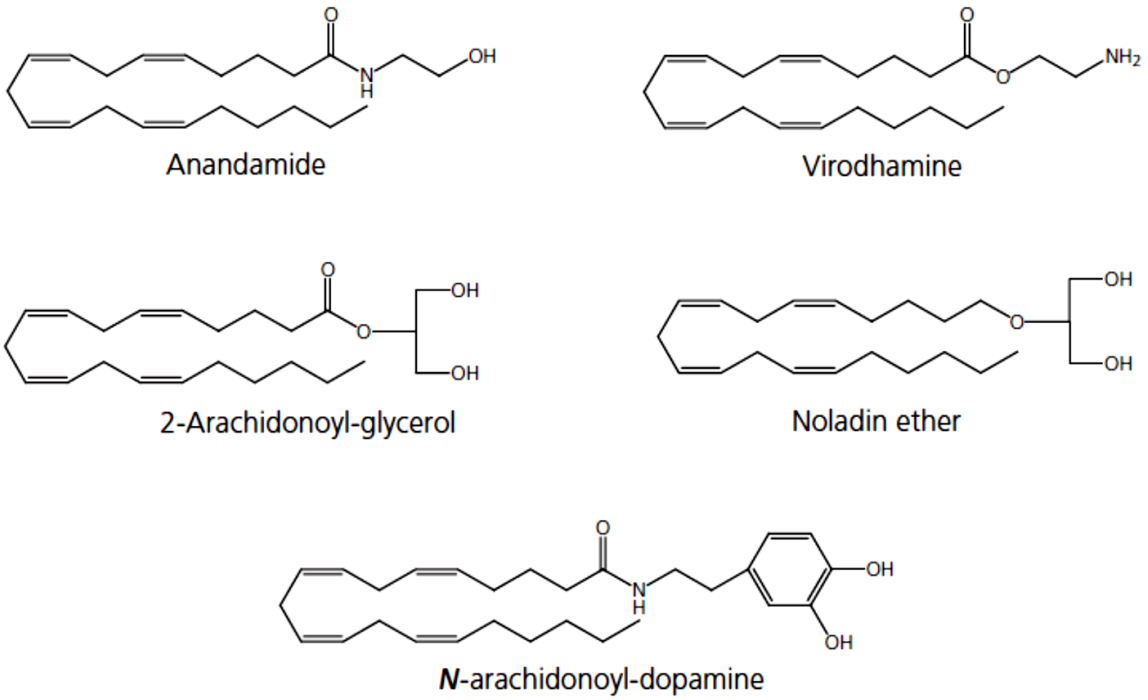

Fig. 1. Chemical structure of the five best-known endocannabinoids. (Di Marzo et al, 2005)

2-AG is the second endogenous cannabinoid ligand to be isolated, which acts as full agonist at both CB1-R and CB2-R (Sugiura et al, 1999, 2000). The tissue levels of 2-AG fall in the nanomolar range, with the highest level of 10.2 nmol/g in the hippocampus (Bisogno et al, 1999). In the lumbar spinal cord, however, surprisingly low level, only 0.432 nmol/g 2-AG was detected (Huang et al, 1999), which does not necessarily influence its ability to activate CB1-Rs, considering its high affinity to and efficacy at CB1-Rs.

It is important to note, that 2-AG serves as precursor or intermediate of several metabolic pathways, and is produced upon degradation of various phospho-, di- and triglycerides suggesting that only a fraction of 2-AG found in the central nervous system is involved in the endocannabinoid signalization (De Petrocelli et al, 2004).

In addition to anandamide and 2-AG, several endogenous cannabinoid ligands have been identified, such as 2-arachidonoyl-glyceryl esther (noladine; Hanus et al, 2001), N-arachidonoyldopamine (NADA; Bisogno et al, 2000) and virodhamine (Porter et al, 2002). However, their functional significance in the modulation of synaptic transmission has been less extensively studied.

2.2. Endocannabinoid biosythesis and mobilization

2.2.1. Biosynthesis of anandamide

Several biochemical pathways participate in the biosynthesis of anandamide and the other members of the NAEs' family (Fig. 2). The general precursors for NAEs are N-acylphosphatidyl-ethanolamines (NAPEs), which are synthesized by calcium-sensitive or –insensitive N-acyltransferases, NAT or iNAT, respectively (Astarita et al, 2008; Jin et al, 2009).

2.2.1.1. NAPE-PLD

Generally considered as the major route for NAE production, the second step of the canonical transacylation-phosphodiesterase pathway includes the enzymatic hydrolysis of NAPEs. This reaction is catalized by a calcium-sensitive NAPE-selective phospholipase D (NAPE-PLD; Di Marzo et al, 1994, 1996), which is different from other PLDs, since it is not involved in the transphosphatydilation, the characteristic reaction of PLD enzymes. Indeed, NAPE-PLD features phosphodiesterase activity, and belongs to the metallo-β-lactamase family (Okamoto et al, 2004). The contribution of NAPE-PLD in anandamide biosynthesis has been demonstrated in multiple experiments (Okamoto et al, 2005; Guo et al, 2005; Merkel et al, 2005), and it has been reported, that in osteoarthritis model of chronic pain, elevation of anandamide and NAPE-PLD protein levels are closely associated in the spinal cord. However, genetical invalidation of NAPE-PLD does not cause any notable change in the anandamide levels in the brain (Leung et al, 2006), providing direct evidence for additional, either paralell or compensatory NAE biosynthetic pathways.

NAPE-PLD expression has been confirmed in many regions of the central nervous system, including the cerebral cortex, basal ganglia, cerebellum, and brainstem with Western blot analysis and real-time PCR (Morishita et al, 2005). Furthermore, in immunohistochemical studies

NAPE-PLD was found in the somatodendrotic compartment of CA3 pyramidal cells of the hippocampus, and presynaptic to Purkinje cell dendritic spines in the cerebellum (Cristino et al, 2008). Presynaptic localization of NAPE-PLD immunoreactivity has also been described in hippocampal glutamatergic axon terminals, associated with the external surface of intracellular membrane compartments (Nyilas et al, 2008). Before our experiments, the expression of NAPE-PLD in the spinal cord had not been addressed.

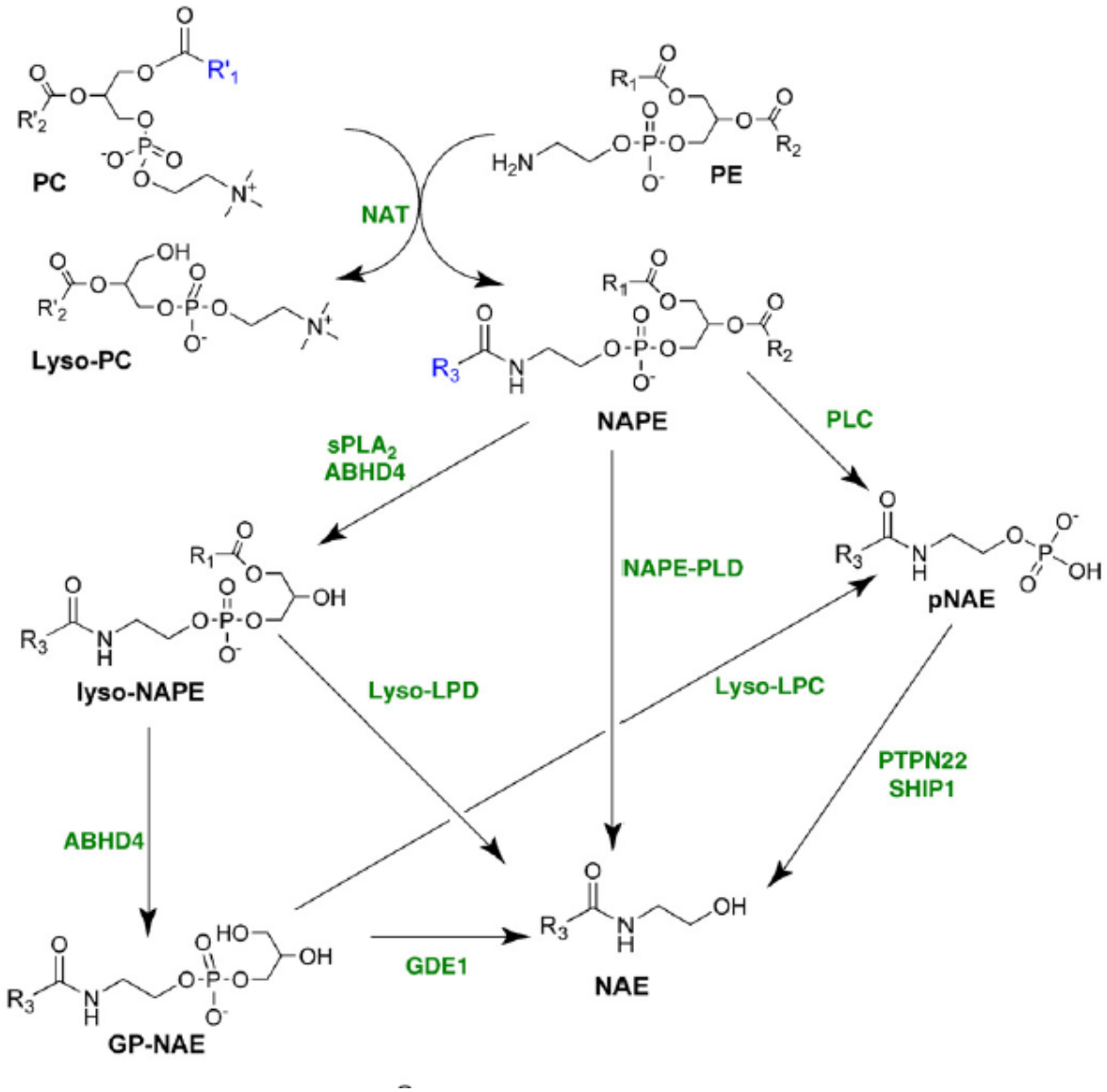

Fig. 2. N-acylethanolamine biosynthetic pathways. (Muccioli, 2010)

2.2.1.2. Alternative N-acyl-ethanolamine biosynthetic routes

As general precursors in anadamide biosythesis, NAPEs can be transformed into anandamide in two steps along the phospholipase-phosphatase pathway. First, PLC converts NAPEs into phospho-NAEs, which in turn are dephosphorylated by the protein tyrosin phosphatase N22 (PTPN22; Liu et al, 2006).

NAPEs can also be substrates for the group Ib secretory phospholipase A_2 (PLA_2) producing 2-lyso-NAPE intermediates, which can be converted into NAEs by a selective lyso-phospholipase D (Sun et al, 2004). Alternatively, α/β-hydrolase domain 4 (ABHD4) can convert 2-lyso-NAPEs into glycerophospho-NAEs, from which glycerophosphodiesterase 1 (GDE1) can sythesize NAEs (Simon et al, 2006).

Despite the alternative anandamide biosynthetic pathways and the results obtained from experiments with NAPE-PLD knockout animals, NAPE-PLD is still considered as the major anandamide-synthesizing enzyme during physiological conditions (Okamoto et al, 2009; Battista et al, 2012).

2.2.2. Biosynthesis of 2-AG

Stimulation of various receptors including G-protein coupled receptors and receptor tyrosine kinases results in the activation of phospholipase C (PLC), which triggers the cleavage of phosphatidylinositol-4,5-bisphosphate (PIP_2) into inositol-1,4,5-triphosphate (IP_3) and diacylglycerol (DAG) (Berridge et al, 2000; Brose et al, 2004). DAG remains bound to the membrane, and is subsequently hydrolyzed by *sn*-1 diacylglycerol lipases (DGL; Fig. 3) into 2-AG (Stella et al, 1997). Alternatively, as a much less well known pathway, PLA_1 may convert PIP_2 into lyso-phosphatidyl-inositol (lyso-PC), which is in turn transformed into 2-AG by a lyso-PC selective PLC (Ueda et al, 1993).

Two *sn*-1 DGL isoforms, DGL-α and β have been identified, both containing an N-terminal four transmembrane domain and an intracellular catalytic domain with a lipase-3 motif and a serine lipase motif (Bisogno et al, 2003). Although both isoform show similar catalytic activities, they are under the control of their own promoters which allow differential expression in different tissues and cell types. DGL-β shows broader and more homogenous distribution

across tissues, while DGL-α is much more abundant in the central nervous system (Farooqui et al, 1986; Bisogno et al, 2003).

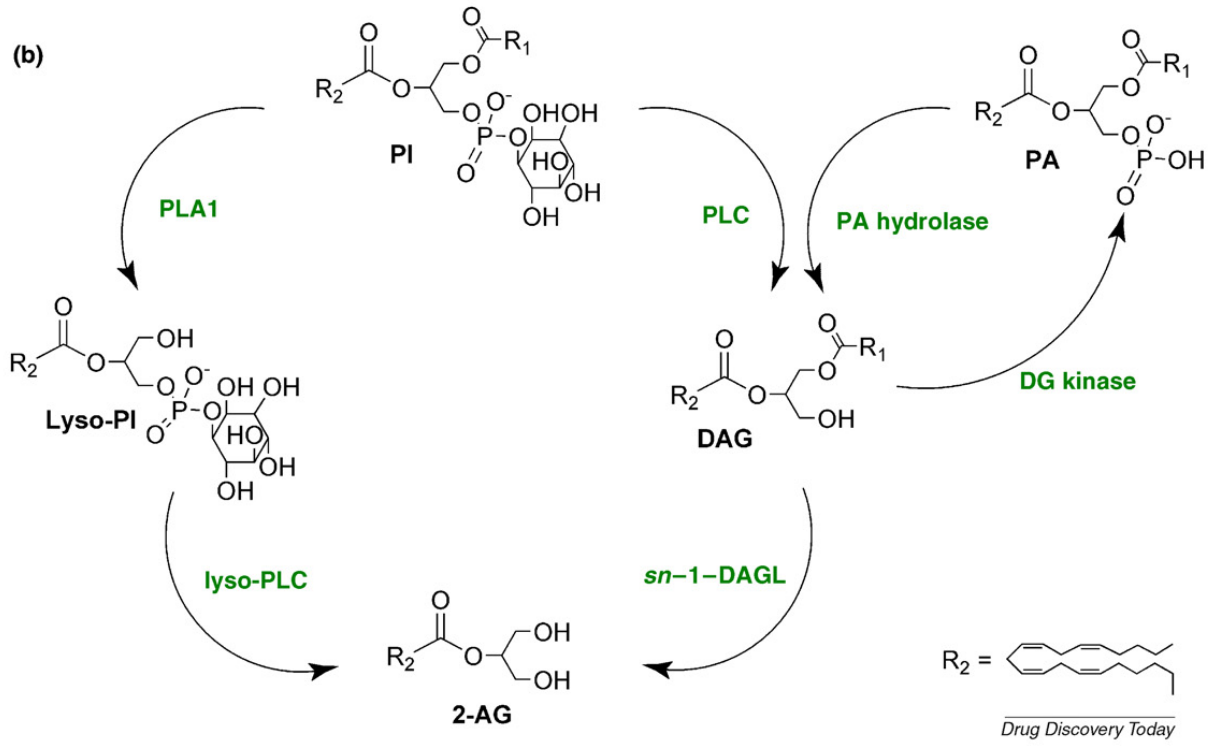

Fig. 3. 2-AG biosynthetic pathways. (Muccioli, 2010)

Since DGL-β was found to be associated to intracellular membrane compartments (Jung et al, 2011), and the endocannabinoid-mediated phenomena are not altered after genetic invalidation of DGL-β (Gao et al, 2010, Tanimura et al, 2010), it seems that the role of DGL-β in the retrograde 2-AG signalization cannot be very prominent. In DGL-α knockout mice, however, a reduction of 80% in 2-AG levels in the brain and spinal cord with the complete loss of retrograde cannabinoid signaling has been reported, indicating that this isoform is the major source of 2-AG utilized in intercellular 2-AG mediated communication (Gao et al, 2010). The distribution of DGL-α has been extensively documented in the forebrain (Suarez et al, 2011), hippocampus (Katona et al, 2006), amygdala (Yoshida et al, 2011), cerebellum (Yoshida et al, 2006). Although molecular architecture of 2-AG releasing apparatus has also been described at the level of the spinal cord

(Nyilas et al, 2009), the expression of DGL-α by glial cells, and consequently the ability of spinal astrocytes and microglial cells to release 2-AG has not been investigated.

2.3. Cannabinoid receptors

Cannabinoid receptors belong to the rhodopsin-like (1a) family of 7-transmembrane domain receptors (Foord et al, 2005). Although the cannabinoid receptor family has only two members, CB1 and CB2 receptors, cannabinoid ligands can also bind to a number of other receptors such as TRP channels, 5-HT_3 receptor, GPR55 and many more, which may play role in the diversification of the effects of cannabinoids (Pertwee et al, 2010).

2.3.1. CB1 receptor

CB1-Rs are among the most abundant G-protein coupled receptors in the brain (Herkenham et al, 1990), which primarily mediate the effects of both exogenous and enogenous cannabinoid compounds in the central nervous system (Elphick and Egertova, 2001). Matsuda and his co-workers (1990) showed that CB1-R is expressed in the central nervous system, which was confirmed by Herkenham et al. (1990) by using radioligand binding assays. Later it has been demonstrated that CB1-R is expressed in most areas of the central nervous system including the cerebral cortex (Tsou et al, 1998; Egertova and Elphick, 2000; Egertova et al, 2003), hippocampus (Katona et al, 2006; Kawamura et al, 2006), basal ganglia (Egertova and Elphick, 2000; Matyas et al, 2006), cerebellum (Tsou et al, 1998; Kawamura et al, 2006), where cannabinoids modulate functions like hypothermia, analgesia and impairments in memory, learning and motor coordination (Abood and Martin, 1996; Adams et al, 1996).

Although it has been shown that the dorsal horn of the spinal cord also contains CB1-Rs in high quantities, the available descriptions are rather contradictory. Farquhar-Smith et al. (2000) reported that CB1-R immunoreactivity is confined to a characteristic twin band corresponding to lamina I and the inner portion of lamina II, whereas others found a homogeneous immunostaining throughout laminae I and II (Ong & Mackie, 1999; Salio et al., 2001, 2002). There is general agreement that CB1-Rs are expressed by central terminals of primary afferents as well as by spinal interneurons in laminae I and II. The proportion among neural elements expressing CB1-R, however, is the subject of much discussion. Farquhar-Smith et al. (2000) found that dorsal

rhizotomy and hemisection of the spinal cord resulted in only a marginal decrease in CB1-R immunoreactivity, and observed very little co-localization of CB1-R with markers of primary afferents at the single fiber level, suggesting that CB1-Rs are primarily expressed by spinal interneurons. In contrast, Hohmann et al. (1999) found that dorsal rhizotomy induced a 50% loss in binding of radiolabeled cannabinoid agonist [^{3}H]CP55,490 in laminae I and II. In addition, localization of CB1-Rs on spinal dorsal horn neurons remains uncertain. Salio et al. (2001, 2002) claimed that CB1-Rs are expressed exclusively on the somatic and dendritic membranes of spinal neurons, whereas others reported that CB1-R immunoreactivity is restricted to axon terminals in the superficial spinal dorsal horn (Farquhar-Smith et al., 2000).

CB1-R belongs to the G-protein coupled receptors, therefore it can induce numerous intracellular signaling mechanisms which are characteristic to GPCRs (Fig. 4).

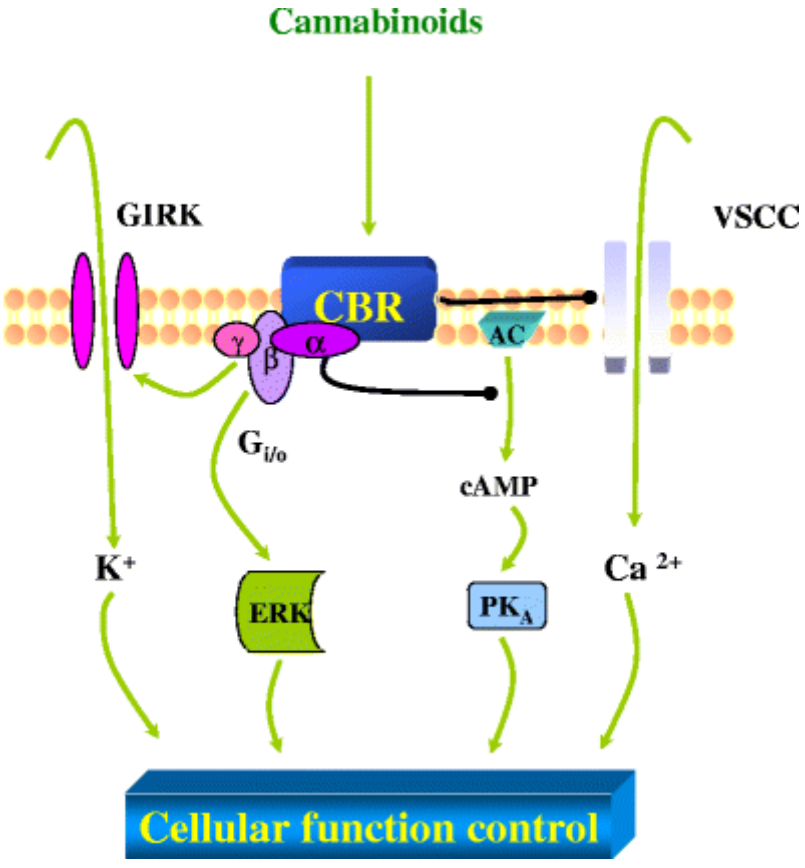

Fig. 4. Signal transduction pathways of CB1-R resulting in the modulation of G-proteins, various ion channels and activation of ERK cascade (Gómez-Ruiz et al, 2007).

Among the CB1-R induced signal transduction pathways, the functional inhibition of adenylyl cyclase activity and consequently the inhibition of cAMP production was first identified (Howlett and Fleming, 1984; Howlett, 1985, Bidaut-Russel and Howlett, 1991). This mechanism was described in cell lines overexpressing recombinant CB1-R (Matsuda et al, 1990; Vogel et al, 1993) as well as in cells exhibiting intrinsic CB1-R expression (Pinto et al, 1994). The CB1-R dependent reduction of cAMP appears to be sensitive to pertussis toxin indicating that this action is mediated by the α subunit of $G_{i/o}$ proteins (Howlett et al, 1986), which in turn activates the mitogen-activated protein kinase cascades, including ERK1/2 and p38 MAP kinase pathways (Howlett et al, 2002; Howlett, 2005) influencing a number of cellular functions from cell proliferation to apoptosis. Most importantly, CB1-R can effectively modulate a number of ion channels which play important role in the cannabinoid dependent presynaptic inhibition of neurotransmitter release. CB1-R activation results in the inhibiton of N-type (Mackie and Hille, 1992; Mackie et al, 1993), P/Q-type (Mackie et al, 1995; Twitchell et al, 1997), L-type (Gebremedhin et al, 1999) and T-type (Chemin et al, 2001) Ca^{2+} channels, whereas CB1-R stimulation activates inwardly rectifying potassium channels (GIRKs; Mackie at al, 1995) and increases voltage-dependent A-type outward K^+ currents (Deadwyler et al, 1995).

In addition, CB1-R activation is also coupled to PLC activation via $G_{i/o}$ proteins, thus it may increase IP_3 levels, thereby inducing Ca^{2+} release from intracellular Ca^{2+} stores (Sugiura et al, 1997; Venance et al, 1997; Netzeband et al, 1999).

CB1-R activation may also lead to cAMP accumulation, indicating that under certain conditions, CB1-R may be coupled to G_s (Glass and Felder, 1997; Abadji et al, 1999). Moreover, there is experimental evidence that in cell lines expressing CB1-R, application of cannabinoid ligands induced Ca^{2+} transients in a G_q protein dependent manner (Lauckner et al, 2005).

2.3.2. CB2 receptor

The cannabinoid receptor 2 (CB2-R) was first identified in HL60 cells (Munro et al, 1993), and somewhat later cloned from mouse and rat (Shire et al, 1996; Griffin et al, 2000; Brown et al, 2002). Similarly to CB1-R, CB2-R is another G-protein coupled receptor which acts via $G_{i/o}$ proteins and inhibits adenylyl cyclase (Bayewitch et al, 1995), activates the p83 and p42/44

MAPK pathways (Herrera et al, 2005), and increases ceramide production (Herrera et al, 2006). There are, however, major differences between the functional properties of CB1-R and CB2-R. 2-AG acts as high efficacy full agonist at both classical cannabinoid receptors, but anandamide proved to be a weak partial agonist at CB2-R (Lynn and Herkenham, 1994; Showalter et al, 1996; Sugiura et al, 2000; Shoemaker et al, 2005), and CB2-R is not involved in the modulation of either Ca^{2+} or K^{+} channels (Felder et al, 1995).

CB2-R is generally considered to be the peripheral cannabinoid receptor, since it is strongly expressed by immune cells and tissues (Munro et al, 1993). In contrast, the expression of CB2-R in the central nervous system is so weak that in most of the cases it is below the level of detection (Munro et al, 1993; Beltramo et al, 2006). Although experimental evidences indicate that CB2-R is expressed in the brainstem (Van Sickle et al, 2005), cerebellum (Ashton et al, 2006) and hippocampus (Onaivi et al, 2006), in most of the studies CB2-Rs were expressed by microglial cells at various levels of the central nervous system (Carlisle et al, 2002; Walter et al, 2003; Beltramo et al, 2006) including the spinal cord (Zhang et al, 2003).

2.4. **Degradation of endocannabinoids** (Fig. 5)

The magnitude and duration of cannabinoid signaling depends mainly on the balance between the biosynthesis and degradation of the endocannabinoid ligands. Similarly to their biogenesis, there are several metabolic pathways along which anandamide and 2-AG can be broken down. In addition to the primary degradative routes which are catalyzed by hydrolytic enzymes, several oxidative catabolic pathways have also been described.

2.4.1. Hydrolytic degradation of endocannabinoids

2.4.1.1. Degradation of anandamide (Fig. 5a)

Anandamide and other members of the NAE family are ethanolamide derivatives, therefore their hydrolysis is catalyzed by enzymes belonging to the amidase signature family. The most important and extensively characterized NAE degrading enzyme is fatty acid amide

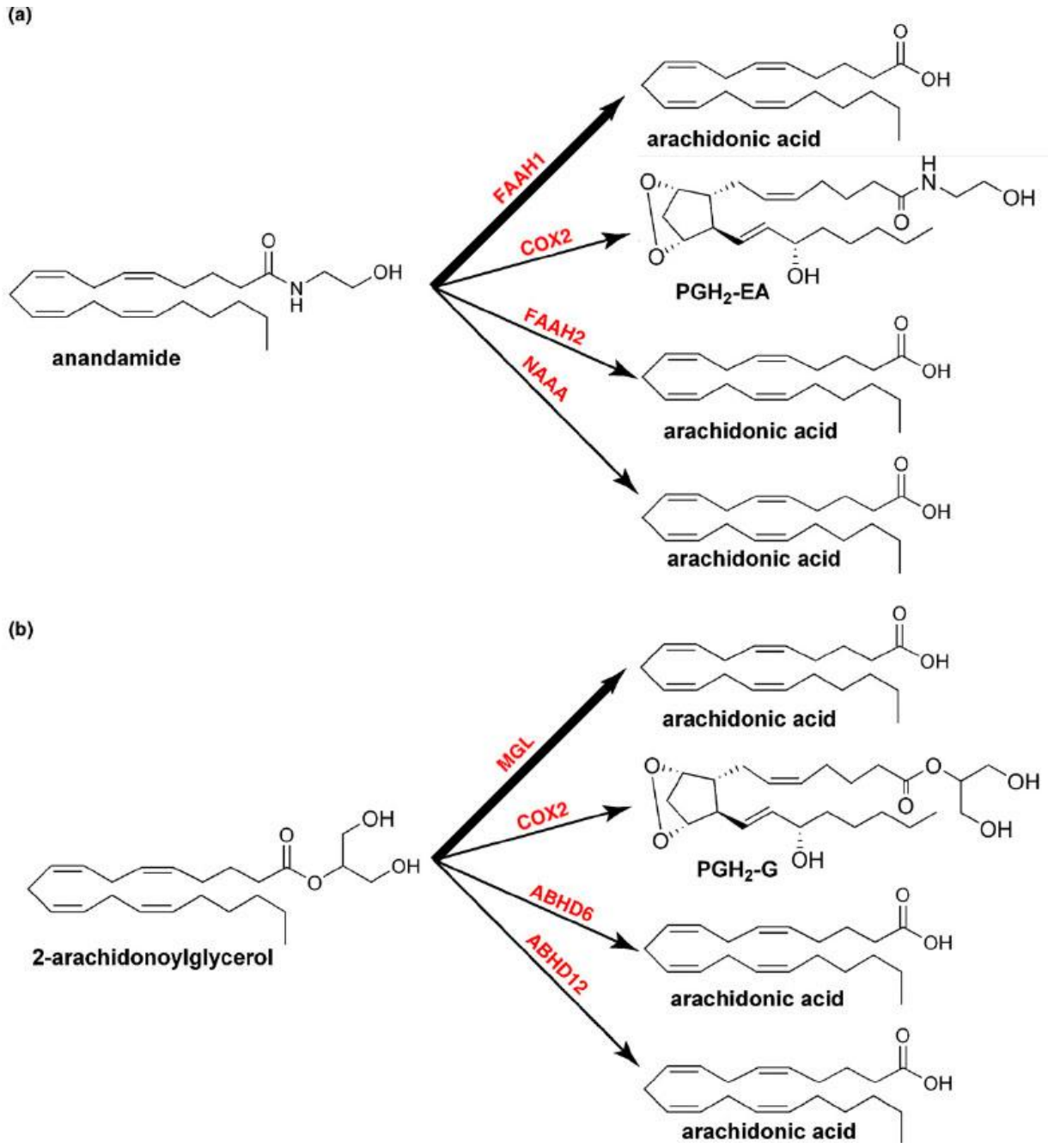

Fig. 5. Schematic illustration of the catabolic pathways involved in endocannabinoid degradation. Anandamide (a) and 2-AG (b) can be inactivated through multiple mechanisms including hydrolytic and oxidativ enzymatic pathways (Muccioli, 2010, modified).

hydrolase-1 (FAAH-1), which was first cloned and identified from rat liver (Cravatt et al, 1996). Genetical invalidation of FAAH-1 results in 15-fold greater anandamide levels in the brain when compared to that of wild-type mice (Cravatt et al, 2001), suggesting its primary role in the termination of anadamide-mediated signaling. FAAH-1 is widely expressed not only in the brain, but also in most peripheral tissues, and is localized mainly to intracellular membrane compatments (Giang and Cravatt, 1997; Yazulla et al, 1999; Bisogno et al, 1997; Maccarrone et al, 2001; Gulyás et al, 2004).

Importantly, anandamide degradation is described as a two-step process: anandamide has to be internalized first to reach the intracellular membrane compartments, where the inactivation step by FAAH-1is carried out (McKinney and Cravatt, 2005). Although the carrier-mediated facilitated diffusion had long been identified (Piomelli et al, 1999), the molecular identity of anandamide membrane transporter remained mysterious for years (Hillard and Jarrahian, 2003; Glaser et al, 2003). Recently, a FAAH-1 splice variant was identified, which lacks amidase activity but binds anandamide with high affinity. This FAAH-1 variant facilitates anandamide transport into cells, hence it was named FAAH-like anadamide transporter (FLAT; Fu et al, 2012).

Anandamide can be degraded by two additional hydrolytic enzymes. Fatty acid amide hydrolase-2 (FAAH-2) has been identified in human, but not in rodent tissues. It is involved in the degradation of NAEs primarily in peripheral tissues, but not in the central nervous system (Wei et al, 2006), similarly to N-acylethanolamine-hydrolyzing acid amidase (NAAA), which is predominantly expressed by immune cells (Tsuboi et al, 2007).

2.4.1.2. Degradation of 2-AG (Fig. 5b)

Inactivation of 2-AG is controlled by three serine hydrolases containing an α/β hydrolase domain, which together hydrolyze 99% of 2-AG into arachidonic acid and glycerol (Blankman et al, 2007).

The major and first characterized 2-AG inactivation pathway is catalyzed by monoacylglycerol lipase (MGL), which was first isolated from rat adipose tissue (Tornqvist and Belfrage, 1976), then from other tissues including human (Karlsson et al, 2001) and rat brain

(Dinh et al, 2002). In the central nervous system, approximately 85% of 2-AG is hydrolyzed by MGL (Blankman et al, 2007), thus it is thought to be the key enzyme determining the duration of 2-AG mediated cannabinoid signaling (Makara et al, 2005). Enzymatic activity of MGL is almost equivalent in cytosolic fraction and in membrane preparations, indicating that MGL is not an integral membrane protein, but can also be associated to membrane compartments (Sakurada and Noma, 1981; Bisogno et al, 1997; Goparaju et al, 1999).

The level of 2-AG is further controlled by two additional serine hydrolases. Predominantly expressed by neurons, α/β hydrolase domain 6 (ABHD6) is localized postsynaptically at the site of production of 2-AG, where its major function is the prevention of activity-dependent accumulation of 2-AG (Marrs et al, 2010), whereas α/β hydrolase domain 12 (ABHD12) is a microglia-specific 2-AG degrading enzyme (Blankman et al, 2007).

2.4.2. Oxidative degradation of endocannabinoids

Although anandamide and 2-AG are primarily inactivated by hydrolytic pathways, the degradation of endogenous cannabinoid ligands may also be catalyzed by oxidative enzymes such as cyclooxygenase-2 (COX-2; Woodward et al, 2008), lypoxygenase-12 (LOX-12) and 15 (LOX-15; Edgemond et al, 1998; Veldhuis et al, 2003). Interestingly, some of the metabolites, which are produced upon anandamide and 2-AG oxidation can also activate CB1-R, CB2-R, and TRPV1 (Craib et al, 2001; Kozak et al, 2002).

2.5. Roles of the endocannabinoid system in the retrograde modulation of synaptic transmission

It is generally accepted that endogenous cannabinoids are among the most ubiquitous neuromodulator compounds, acting as a retrograde signaling system in most of the brain areas. Although the depolarization induced suppression of synaptic transmission was described earlier (Llano et al, 1991; Pitler and Alger, 1992), it was demonstrated only in 2001 by three independent groups, that the endocannabinoid system plays critical role in the induction of this phenomenon. The cannabinoid induced short term synaptic plasticity at inhibitory and excitatory synapses was termed to depolarization induced suppression of inhibition (DSI; Wilson and

Nicoll, 2001; Ohno-Shosaku et al, 2001) and excitation (DSE; Kreitzer és Regehr, 2001), respectively.

2.5.1. Endocannabinoid-mediated short term depression

Endocannabinoid-mediated short term depression (eCB-STD) is generally described as an endocannabinoid evoked decrease of the amplitude of postsynaptic potentials with a relatively fast (several tens of seconds) recovery after the expression of the maximum effect. e-CB-STD can be induced through several, partly independent mechanisms.

Upon excitatory synaptic transmission, the postsynaptic depolarization activates voltage-gated Ca^{2+} channels (Pitler and Alger, 1992), probably postsynaptic N-type Ca^{2+} channels, which leads to the increase in the intracellular Ca^{2+} concentration (Llano et al, 1991; Lenz et al, 1998). Based on the most accepted model, the evoked Ca^{2+} transient alone induces endocannabinoid biosynthesis by activating DGL-α, resulting in 2-AG mobilization from postsynaptic neurons (Kano et al, 2009). Although the participation of DGL-α in the iniciation of eCB-STD seemed to be controversial based on pharmacological studies (Hashimotodani et al, 2008; Uchigashima et al, 2007; Min et al 2010; Safo and Regehr, 2005), genetic invalidation of DGL-α provided unequivocal evidence for the primary role of this enzyme in the Ca^{2+}-dependent 2-AG release (Gao et al, 2010; Tanimura et al, 2010). It is not yet understood how the released 2-AG moves across the synaptic cleft, but it has been demonstrated, that due to its lipophilic nature, 2-AG incorporates into the cell membrane of the presynaptic neuron, and reaches the perisynaptically localized CB1-Rs by fast lateral diffusion (Fig. 6; Makriyannis et al, 2005).

It is of note that the released 2-AG may diffuse passively up to 20 μm from the release site (Wilson and Nicoll, 2001), thus it may act on CB1-Rs in this range expressed by additional excitatory or inhibitory neurons or even by glial cells. The activation of CB1-Rs induces the aforementioned signal transduction pathways involving the β/γ subunits of G-proteins (Turu and Hunyadi, 2010), most importantly the inhibition of presynaptic voltage-gated Ca^{2+} channels and activation of K^+ channels, resulting in DSI or DSE, i.e. temporary suppression of neurotransmitter release from the presynaptic axon terminal (Wilson and Nicoll, 2001; Ohno-Shosaku et al, 2001; Kreitzer és Regehr, 2001). It is important to note, however, that Ca^{2+} influx can be evoked by stimulation of postsynaptic NMDA receptors which directly triggers

endocannabinoid biosynthesis without involving voltage-gated Ca^{2+} channels, resulting in an additional form of cannabinoid-dependent STD, termed NMDAR-driven eCB-STD (Ohno-Shosaku et al, 2007).

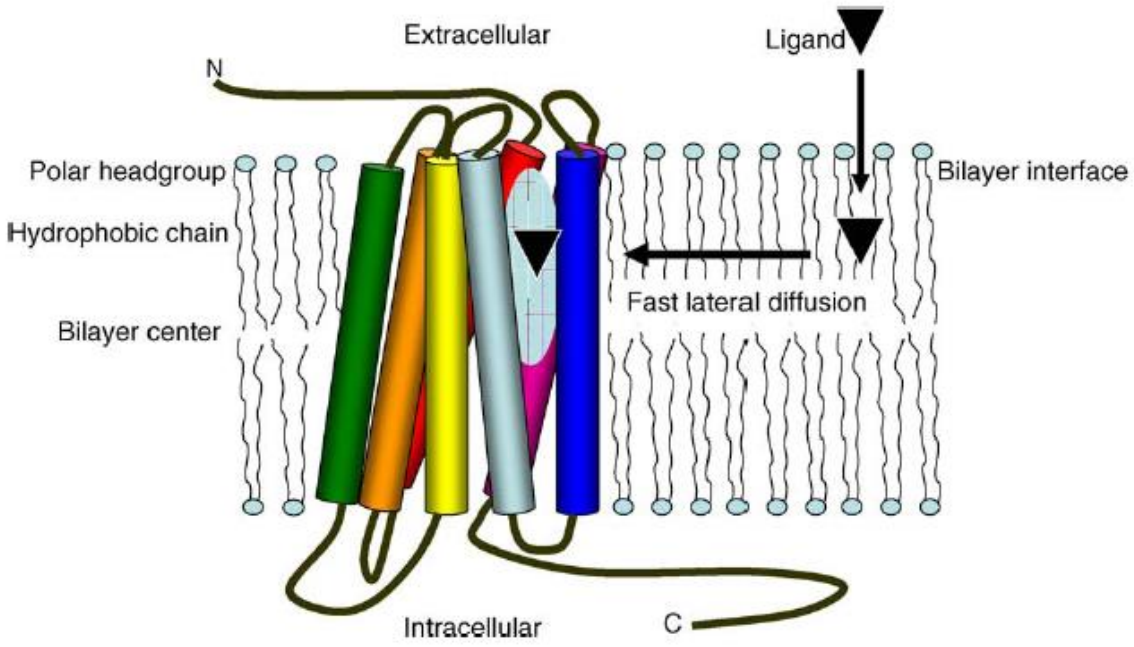

Fig. 6. Incorporation of a lipophilic ligand, such as anandamide or 2-AG, in the lipid bilayer and diffusion to its receptor binding site (Makriyannis et al, 2005)

Endocannabinoid-mediated STD can also be induced in a Ca^{2+}-independent manner, through stimulation of $G_{q/11}$ coupled receptors, including group I mGluRs (Maejima et al, 2001), M_1/M_3 muscarinic receptors (Fukudome et al, 2004), 5-HT_2 serotonin receptors (Best and Regehr, 2008) and many more. All of these receptors activate PLCβ through $G_{q/11}$ protein, indicating that 2-AG is produced by sequential enzymatic steps involving PLCβ and DGL-α. Indeed, various PLCβ knockout mice do not exhibit this form of eCB-STD, indicating that receptor-driven endocannabinoid release is strongly PLCβ-dependent (Hashimotodani et al, 2005; Maejima et al, 2005).

It has also been demonstrated, that the Ca^{2+}-dependent, depolarization-induced and Ca^{2+}-independent, G-protein induced processes can be activated simultaneously resulting in the

facilitation of 2-AG production (Ohno-Shosaku et al, 2002). In this Ca^{2+}-assisted, receptor-driven endocannabinoid release, the seemingly independent processes finally converge on the 2-AG biosynthetic pathway, which may play crucial role in the integration of postsynaptic events (Brenowitz and Regehr, 2005). PLCβ1 in the hippocampus and PLCβ4 in the cerebellum were proposed to coordinate this mechanism as coincidence detector of postsynaptic Ca^{2+} influxes and G-protein signaling (Hashimotodani et al, 2005, Maejima et al, 2005).

2.5.2. Endocannabinoid-mediated long term depression

It is generally accepted, that the molecular mechanisms inducing eCB-STD through the stimulation of endocannabinoid release, particularly the Ca^{2+}-assisted receptor driven form may also evoke long term synaptic depression (eCB-LTD, Fig. 7). As a widely expressed phenomenon in the central nervous system, eCB-LTD was demonstrated from the spinal cord to the cerebral cortex (Gerdeman et al, 2002; Robbe et al, 2002; Chevaleyre and Castillo, 2003; Sjöstrom et al, 2003; Kato et al, 2012). eCB-LTD is defined as the endocannabinoid-mediated modulation of the synaptic inputs by postsynaptic activity-dependent mechnisms over longer period of time (several tens of minutes; Gerdeman et al, 2002).

It has been demonstrated, that the extended duration of CB1-R activity is maintained by downstream signaling pathways different from those mediating eCB-STD. In the induction of eCB-LTD at both excitatory and inhibitory synapses, the α subunit of G protein plays pivotal role by inhibiting the cAMP/PKA pathway. Reduction of PKA activity leads to the dephosphorylation of the active zone protein RIM1α resulting in the depression of neurotransmitter release (Chevaleyre et al, 2007). Inhibition of cAMP/PKA signalization may also lead to LTD by reducing Ca^{2+} influx through voltage-gated Ca^{2+} channels (Mato et al, 2008).

2.5.3. Role of anandamide in the endocannabinoid-mediated modulation of synaptic transmission

According to the endocannabinoid-mediated synaptic plasticity paradigms, 2-AG release is necessary for the activation of the presynaptically located CB1-Rs, suggesting its pivotal role in triggering STD and/or LTD. Indeed, the endocannabinoid-dependent suppression of

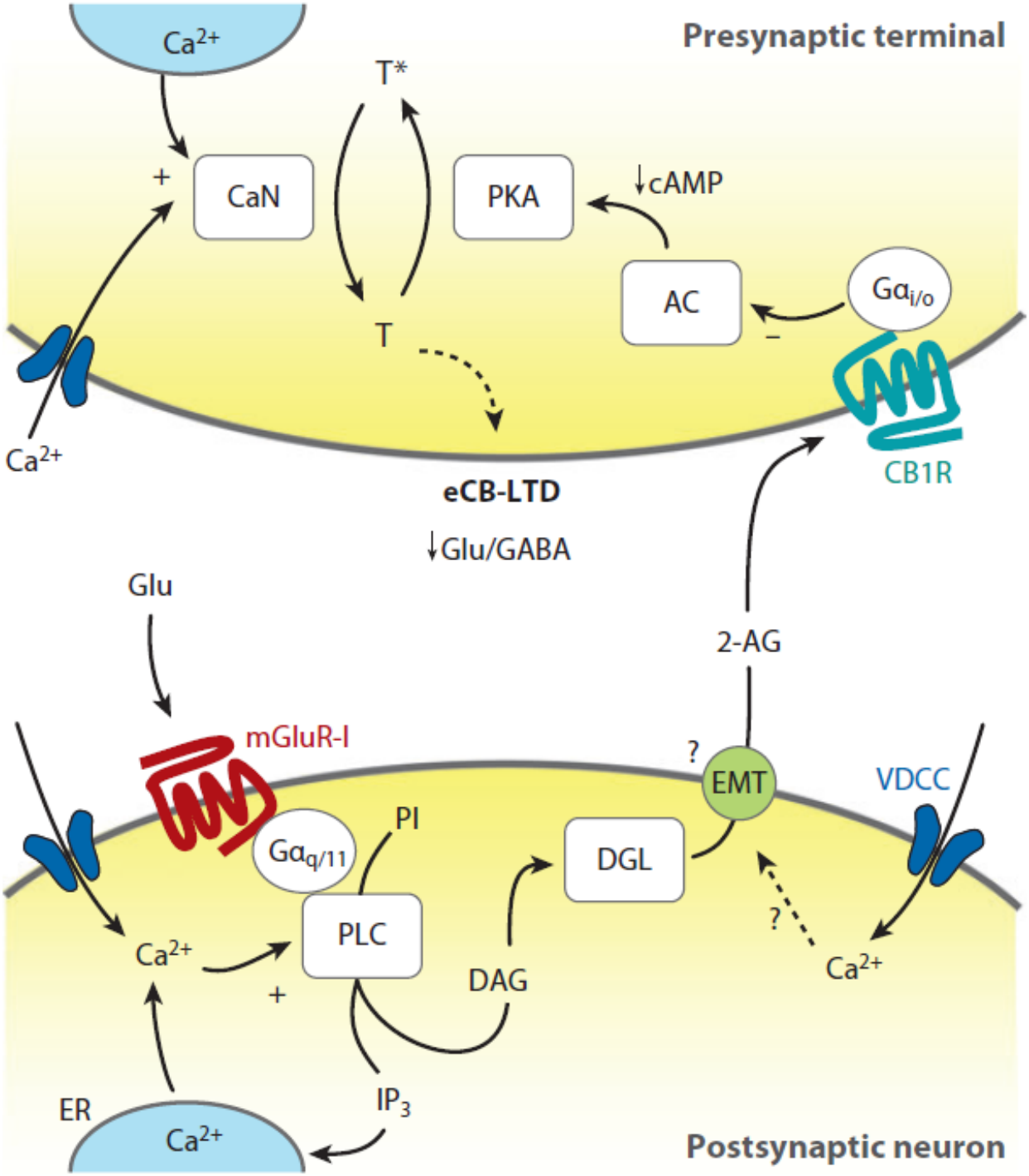

Fig. 7. Schematic representation of the endocannabinoid-dependent long-term depression (eCB-LTD) induction mechanism. Note that postsynaptic processes include common steps to induce both eCB-STD and eCB-LTD (Heifets and Castillo, 2009)

neurotransmitter release cannot be observed in DGL-α knockout mice (Gao et al, 2010; Tanimura et al, 2010) suggesting that 2-AG is the primary endocannabinoid ligand utilized in retrograde signalization, and the role of anandamide in the suppression of synaptic transmission cannot be very prominent. However, it has been demonstrated that anadamide mediates some forms of the endocannabinoid-dependent neural plasticity (Ade and Lovinger, 2007; Azad et al, 2004).

The crucial role of anandamide has been demonstrated in the control of depression (Gobbi et al, 2005) and anxiety (Kathuria et al, 2003), and in the regulation of nociceptive processing (Calignano et al, 1998; Hohmann et al, 2005; Long et al, 2009; Schlosburg et al, 2010). Moreover, it has also been shown that anandamide maintains constitutive CB1-R activation, and the induced tonic inhibitory actions mediated by CB1-Rs influence synaptic homeostasis, i.e. the general activities of neuronal network (Kim and Alger, 2010).

These findings suggest a seemingly clear functional segregation between the endocannabinoid-induced plasticity phenomena mediated by phasic 2-AG or tonic anandamide release. However, it was found that in DGL-α knockout mice, in addition to 2-AG, anandamide levels were also dropped by 50% (Gao et al, 2010; Tanimura et al, 2010), indicating an unexpected and unexplained interference between 2-AG and anadamide biosythesis.

3. MAJOR AIMS

Although a great body of literature suggests the functional importance of cannabinoid mechanisms in the modulation of spinal pain processing, the molecular architecture of the endocannabinoid signaling machinery in the spinal dorsal horn is significantly less well studied than that of the cerebral cortex or hippocampal formation. The objective of this study was to provide a detailed molecular anatomical description of key elements of the endocannabinoid system in the supeficial dorsal horn of the rodent's spinal cord.

Therefore, the major aims of our studies were the followings:

- to describe the cellular distribution and subcellular localization of CB1-Rs in the superficial spinal dorsal horn
- to provide an accurate description of cellular expression and ultrastructural localization of DGL-α and NAPE-PLD in laminae I-II of the spinal cord
- to investigate the expression of molecular elements of the endocannabinoid signaling apparatus by glial cells in the superficial spinal dorsal horn.

4. MATERIALS AND METHODS

4.1. Animals and preparation of tissue sections

Experiments were carried out on 17 adult rats (Wistar-Kyoto, 250‑300 g, Gödöllő, Hungary) and four wild-type, two CB1-R knockout and one NAPE-PLD knockout mice. All animal study protocols were approved by the Animal Care and Protection Committee at the University of Debrecen, and were in accordance with the European Community Council Directives and the rules of the Indiana University Institutional Animal Care and Use Committee. Fourteen animals were deeply anesthetized with sodium pentobarbital (50 mg/kg, i.p.) and transcardially perfused with Tyrode's solution (oxygenated with a mixture of 95% O_2, 5% CO_2), followed by a fixative containing either

(1) 4% paraformaldehyde (three adult rats and all mice; for peroxidase based single and fluorescent double immunostaining),

(2) 4% paraformaldehyde and 0.1% glutaraldehyde (three adult rats; for preembedding immunostaining for electronmicroscopy in case of DGL-α or NAPE-PLD localization studies) or

(3) 2.5% paraformaldehyde and 0.5% glutaraldehyde (for peroxidase- and nanogold-based immunohistochemistry for electron microscopy in case of CB1-R localization studies)

dissolved in 0.1 M phosphate buffer (PB, pH 7.4).). In three additional animals 2 weeks prior to the transcardial perfusion, the lumbar spinal cord was exposed by laminectomy and the L2‑S1 spinal dorsal roots were cut unilaterally under deep sodium pentobarbital anesthesia.

After the transcardial fixation, the L3-L5 lumbar segments of the spinal cord were removed, postfixed in their original fixative for 1 to 4 hours, and immersed into 10% and 20% sucrose dissolved in 0.1 M PB until they sank. In order to enhance reagent penetration the removed spinal cord was freeze-thawed in liquid nitrogen. Fifty-micrometer thick transverse sections were cut on a vibratome, and the sections were extensively washed in 0.1 M PB.

4.2. Immunohistochemistry

4.2.1. Single immunostaining

A single immunostaining protocol was performed to study the laminar distribution of CB1-R, DGL-α and NAPE-PLD. Free-floating sections were first incubated in

- rabbit anti-CB1-R antibody (diluted 1 : 5000; Cayman Chemical, Ann Arbor, MI, USA),

- rabbit anti-DGL-α (1:1,000, termed "INT" in Katona et al., 2006; a kind gift of Ken Mackie, Indiana University, USA) or

-guinea pig anti-NAPE-PLD antibody (diluted 1:200; Frontier Science Co., Ishikari, Hokkaido, Japan)

for 48 h at 4 °C, and then were transferred into biotinylated goat anti-rabbit IgG or goat anti-guinea pig IgG (diluted 1:200; Vector Labs., Burlingame, CA) for 12 h at 4 °C. Thereafter, the sections were treated with an avidin biotinylated horseradish peroxidase complex (diluted 1:100, Vector Labs., Burlingame, CA) for 5 h at room temperature, and the immunoreaction was completed with a 3,3'-diaminobenzidin (Sigma, St. Louis, MO) chromogen reaction. Before the antibody treatments the sections were kept in 10% normal goat serum (Vector Labs., Burlingame, CA) for 50 min. Antibodies were diluted in 10 mM Tris-phosphate-buffered isotonic saline (TPBS, pH 7.4) to which 1% normal goat serum (Vector Labs., Burlingame, CA) was added. Sections were mounted on glass slides, dehydrated and covered with Permount neutral medium.

4.2.2. Double immunostaining

Double-immunostaining protocols were performed to study the co-localization of CB1-R , DGL-α and NAPE-PLD immunoreactivity with various markers of nociceptive primary afferents, axon terminals of putative glutamatergic and GABAergic spinal neurons, astrocytes, and microglial cells. Free-floating sections were first incubated with a mixture of antibodies that contained rabbit anti-CB1-R (diluted 1 : 5000, Cayman Chemical), rabbit anti- DGL-α (1:1,000, termed "INT" in Katona et al., 2006) or guinea pig anti-NAPE-PLD antibody (diluted 1:200; Frontier Science Co., Ishikari, Hokkaido, Japan) and one of the following antibodies:

(1) guinea pig anti-calcitonin gene-related peptide (CGRP) (diluted 1:2,000; Peninsula Labs, San Carlos, CA),

(2) rabbit anti-calcitonin gene-related peptide (CGRP) (diluted 1:10,000; Millipore, Temecula, CA),

(3) biotinylated isolectin B4 (IB4) (1:2,000; Invitrogen, Eugene, OR),

(4) guinea pig anti-vesicular glutamate transporter 2 (VGLUT2) (diluted 1:2,000; Millipore, Temecula CA),

(5) mouse anti-vesicular glutamate transporter 2 (VGLUT2) (diluted 1:10,000; Millipore, Temecula, CA),

(6) a mixture of mouse anti-glutamic acid decarboxylase 65 and mouse anti-glutamic acid decarboxylase 67 (GAD65 and GAD67) (diluted 1:1,000; Millipore, Temecula, CA),

(7) mouse anti-glial fibrillary acidic protein (GFAP) (diluted 1:1,000; Millipore, Temecula, CA) and

(8) mouse anti-CD11b (diluted 1 : 500; AbD Serotec, Oxford, UK).

The sections were incubated in the primary antibody solutions for 2 days at 4 °C and were transferred for an overnight treatment into the appropriate mixtures of secondary antibodies that were selected from the following:

(1) goat anti-rabbit IgG conjugated with Alexa Fluor 555 (diluted 1:1,000; Invitrogen, Eugene, OR),

(2) goat anti-guinea pig IgG conjugated with Alexa Fluor 488 (diluted 1:1,000; Invitrogen, Eugene, OR),

(3) goat anti-mouse IgG conjugated with Alexa Fluor 488 (diluted 1:1,000; Invitrogen, Eugene, OR),

(4) goat anti-guinea pig IgG conjugated with Alexa Fluor 555 (diluted 1:1,000; Invitrogen, Eugene, OR),

(5) goat anti-rabbit IgG conjugated with Alexa Fluor 488 (diluted 1:1,000; Invitrogen, Eugene, OR) and

(6) streptavidin conjugated with Alexa Fluor 488 (diluted 1:1,000; Eugene, OR).

Before the antibody treatments the sections were kept in 10% normal goat serum (Vector Labs., Burlingame, California, USA) for 50 min. Antibodies were diluted in 10 mM TPBS (pH 7.4) to which 1% normal goat serum (Vector Labs., Burlingame, CA) was added. Sections were mounted on glass slides and covered with Vectashield (Vector Labs, Burlingame, CA).

4.2.3. Confocal microscopy and analysis

Series of 1 μm thick optical sections with 0.3 μm separation in the z-axis were scanned with an Olympus FV1000 confocal microscope. Scanning was carried out using a 60x oil-immersion lens (NA: 1.4). The confocal settings (laser power, confocal aperture, and gain) were identical for all sections, and care was taken to ensure that no pixels corresponding to puncta immunostained for each marker applied for the visualization of nociceptive primary afferents, axon terminals of glutamatergic and GABAergic spinal neurons, astrocytes and microglial cells were saturated. The scanned images were processed by Adobe Photoshop CS5 software. By filtering the background staining out with a high-pass intensity filter, threshold values were set for both CB1-R and the other markers.

The co-localization of CB1-R, DGL-α and NAPE-PLD with the investigated markers was quantitatively analyzed in the double-stained sections. A 10x10 standard square grid in which the edge-length of the unit square was 4 μm (the whole grid was 40 μm x 40 μm in size) was placed onto the regions of confocal images corresponding to laminae I–II of the superficial spinal dorsal horn. The proper placement of the grid was based on the following criteria: (a) the border between the dorsal column and the dorsal horn was easily identified on the basis of the intensity of immunostaining. (b) The border between laminae II and III was approximated on the basis of previous ultrastructural observations (McClung and Castro, 1978; McNeill et al., 1988; Molander et al., 1984). Thus, immunoreactivities and co-localizations were investigated in the most superficial 150 μm thick zone of the dorsal horn that had earlier been identified as a layer of the gray matter corresponding to laminae I and II in the L3-L5 segments of the spinal dorsal horn. Profiles that showed immunoreactivity for CB1-R, DGL-α or NAPE-PLD over the edges of the

standard grid were counted in the medial and lateral compartments of laminae I and II. The selected profiles were then examined whether they were also immunoreactive for the axonal or glial markers.

Since the CB1-R, DGL-α and NAPE-PLD antibodies utilized in the present study were raised against the intracellular domain of the enzyme, to define the colocalization values we counted only those CB1-R, DGL-α or NAPE-PLD immunolabeled puncta that were located within the confines of the areas immunostained for the marker.

The co-localization for all investigated markers was analyzed in three animals. The quantitative measurement was carried out in three sections that were randomly selected from each animal. Thus, the calculation of quantitative figures, mean values and standard error of means (SEM), was based on the investigation of nine sections.

The numbers of CB1-R- and VGLUT2-immunoreactive puncta in laminae I and IIi at the level of L4 spinal segment were quantitatively analysed in control animals and in animals with dorsal rhizotomy. A 10 x 10 standard square grid with an edge-length of 4 μm was put onto confocal images obtained from 1-μm-thick single optical sections. CB1-R- and VGLUT2-immunoreactive puncta over the edges of the standard grid were counted in the medial and lateral compartments of laminae I and IIi. The quantitative measurement was carried out in three control animals and in three animals with dorsal rhizotomy. Three randomly selected confocal sections were analysed from each animal. Thus the calculation of quantitative figures was based on the investigation of nine sections. From quantitative data obtained in the nine sections mean values and standard error of the means (SEM) were calculated. Data obtained from control animals and from animals with dorsal rhizotomy were compared. Statistical differences between experimental groups were determined using a one-way Anova test. Probabilities (P) of <0.05 were considered to be statistically significant.

4.2.4. Preembedding immunostaining with diaminobenzidine chromogen reaction for electron microscopy

A preembedding immunostaining similar to the single immunostaining protocol described above was performed to study the cellular distribution of DGL-α and NAPE-PLD at the ultrastructural level. Following extensive washes in 0.1 M PB (pH 7.4) and a treatment with 1%

sodium borohydride for 30 min, free-floating sections from animals fixed with 4% paraformaldehyde and 0.1% glutaraldehyde were first incubated with rabbit anti-DGL-α (1:1,000, termed "INT" in Katona et al., 2006) or guinea pig anti-NAPE-PLD antibody (diluted 1:200; Frontier Institute Co., Ishikari, Hokkaido, Japan) for 48 h at 4 °C, than were transferred into biotinylated goat anti-rabbit IgG or goat anti-guinea pig IgG (diluted 1:200; Vector Labs., Burlingame, CA) for 12 h at 4 °C. Thereafter, the sections were treated with an avidin biotinylated horseradish peroxidase complex (diluted 1:100; Vector Labs., Burlingame, CA) for 5 h at room temperature, and the immunoreaction was completed with a 3,3'-diaminobenzidine (Sigma, St. Louis, MO) chromogen reaction. Before the antibody treatments the sections were kept in 10% normal goat serum (Vector Labs., Burlingame, CA) for 50 min. Antibodies were diluted in 10 mM Tris-phosphate-buffered isotonic saline (TPBS, pH 7.4).

Immunostained sections were treated with 0.5% osmium tetroxide for 45 min, then dehydrated and flat-embedded into Durcupan ACM resin (Sigma, St. Louis, MO) on glass slides. Selected sections were re-embedded, ultrathin sections were cut and collected on Formvar-coated single-slot nickel grids, and counterstained with uranyl acetate and lead citrate.

4.2.5. Preembedding nanogold immunostaining for electron microscopy

A preembedding nanogold immunohistochemical protocol was performed to study the cellular distribution of CB1-R, DGL-α and NAPE-PLD with high resolution. Following extensive washes in 0.1 M PB (pH 7.4) and treatment with 1% sodium borohydride for 30 min, free-floating sections from animals fixed with 2.5% paraformaldehyde and 0.5% glutaraldehyde were incubated in rabbit anti-CB1-R antibody (1 : 2500, Cayman Chemical), whereas sections from rats perfused with 4% paraformaldehyde and 0.1% glutaraldehyde were treated with rabbit anti-DGL-α (1:1,000, termed "INT" in Katona et al., 2006) or guinea pig anti-NAPE-PLD antibody (diluted 1:200; Frontier Institute Co., Ishikari, Hokkaido, Japan) for 48 h at 4 °C. The sections were then transferred into a solution of goat anti-rabbit or goat anti-guinea pig IgG conjugated to 1-nm gold particles (1 : 100, Aurion,Wageningen, The Netherlands) for 12 h at 4 °C.

After repeated washing in 0.01 M Tris-buffered isotonic saline (TBS, pH 7.4), the sections were postfixed for 10 min in 2.5% glutaraldehyde and washed again in 0.01 M TBS and 0.1 M PB. The gold labeling was intensified with a silver enhancement reagent (Aurion R-GENT, Wageningen, The Netherlands). Sections were treated with 1% osmium tetroxide for 45 min, then

dehydrated and flat-embedded into Durcupan ACM resin (Sigma, St. Louis, MO) on glass slides. Selected sections were re-embedded, ultrathin sections were cut and collected on Formvar-coated single-slot nickel grids, and counterstained with uranyl acetate and lead citrate.

4.2.6. Controls

To test the specificity of the antibody raised against CB1-R, free-floating sections obtained from CB1-R knock-out (Ledent et al., 1999) and wild-type mice were immunostained according to the single immunostaining protocol described above. Sections of CB1-R knockout mice were negative for CB1-R, whereas wild-type mice showed a characteristic immunostaining identical to that observed in rats (Fig. 8).

To exclude false negative staining for CB1-R the double immunolabeling for CB1-R and CGRP was repeated using the anti-CB1-R antibody, which was originally diluted at 1:5000, at a dilution of 1:1000. The co-localization of CB1-R with CGRP was quantitatively analysed as described above. Levels of co-localization found with the lower and higher anti-CB1-R dilutions were compared. The two sets of co-localization values did not show any significant differences.

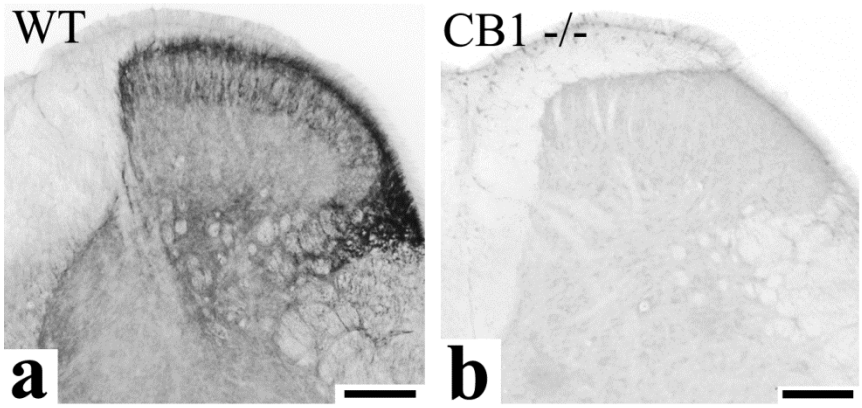

Fig. 8. Specificity of the anti-CB1-R antibody. Photo-micrographs showing immunoreactivity for CB1-R in wild-type (a) and knock-out (b) mice. CB1-R immunostaining can be observed in the dorsal horn of the wild type mouse, while the immunoreactivity is completely abolished from the dorsal horn of the CB1-R knock-out animal. Scale bars: 100 μm

The specificity of the primary antibody against DGLα has previously been extensively characterized (Katona et al., 2006). Brain sections were incubated simultaneously with the

antibody used in this study and with another antibody raised against a different epitope of the DGL-α protein (termed L26 in Katona et al., 2006). The two antibodies revealed identical immunostaining patterns (Katona et al., 2006). More recently, brain sections obtained from DGL-α knock-out mice (Tanimura et al., 2010) were immunostained for DGL-α with the antibody used in this study. No immunostaining was observed in these sections (Ludányi et al., 2011).

Unfortunately we were not able to obtain tissue samples from DGL-α knock-out mice. For this reason, to control the specificity of our antibody against DGL-α spinal cord sections were double-immunostained with the antibody used in this study (epitope: 790-908 aa; termed INT in Katona et al., 2006) and with another antibody raised against a different epitope of the DGLα protein (epitope: 1001-1042 aa) that we purchased from the Frontier Institute Co. (Ishikari, Hokkaido, Japan). The two antibodies revealed identical immunostaining patterns (Fig. 9).

The specificity of the primary antibody against NAPE-PLD has also been extensively tested earlier (Nyilas et al., 2008). Sections from the brain of NAPE-PLD knock-out mice (Leung et al., 2006) were negative for NAPE-PLD, whereas wild-type mice showed a characteristic immunostaining identical to that observed in rats (Nyilas et al., 2008).

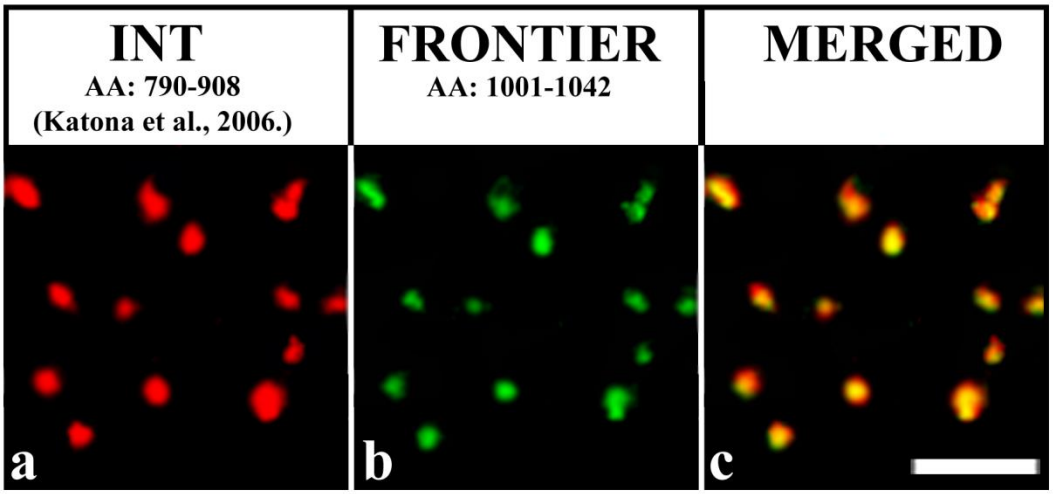

Fig. 9. Specificity of the anti-DGL-α antibody. Micrographs of a single 1µm thick laser scanning confocal optical section which was double-immunostained with the antibody used in this study (INT; red; a) and with another antibody raised against a different epitope of the DGL-α protein (FRONTIER; green; b). Mixed colors (yellow) on the superimposed image (c) indicate that the two antibodies revealed identical immunostaining patterns. Scale bar: 1 µm

The specificity of the primary antibody against NAPE-PLD has also been extensively tested earlier (Nyilas et al., 2008). Sections from the brain of NAPE-PLD knock-out mice (Leung

et al., 2006) were negative for NAPE-PLD, whereas wild-type mice showed a characteristic immunostaining identical to that observed in rats (Nyilas et al., 2008). Since the control experiments described earlier were performed in higher brain areas we have repeated these experiments in spinal cord samples. Sections from the spinal cord of NAPE-PLD knock-out mice (generated by Richard Palmiter and Serge Luquet; Liu et al., 2008) were negative for NAPE-PLD, whereas wild-type littermates showed a characteristic immunostaining identical to that observed in rats (Figs. 10).

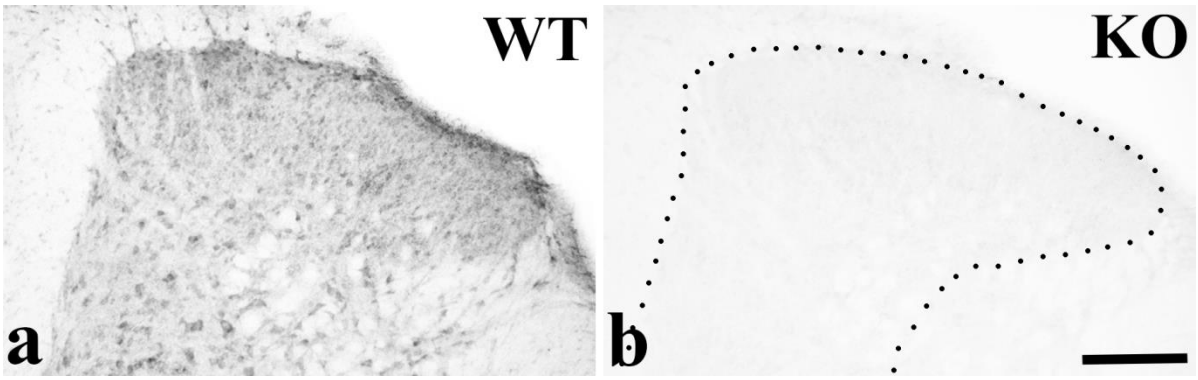

Fig.10. Specificity of the anti-NAPE-PLD antibody. Photomicrographs show immunoreactivity for NAPE-PLD in wild type (a) and NAPE-PLD knock out (b) mice. NAPE-PLD immunostaining can be observed in the dorsal horn of the wild-type mouse, while the immunoreactivity is completely absent from the dorsal horn of the NAPE-PLD knock out mouse. Scale bar: 100 µm

To obtain a more global view about the specificity of the anti-CB1, anti-DGL-α and anti-NAPE-PLD antibodies a Western-blot analysis was performed (Fig. 11.). While the rats were deeply anesthetized with sodium pentobarbital (50 mg/kg, i.p.), the spinal dorsal horn at the level of L3-L5 lumbar segments were dissected. The dorsal horn was sonicated in 20 mM Tris lysis buffer (pH 7.4) containing the following protease inhibitors (mM): EDTA (4.0), EGTA (2.5), PMSF (0.002) benzamidine (0.013), pepstatine A (0.004), soybean trypsine inhibitor (0.001), leupeptine (0.001) and aprotinin (0.001). After removing cell debris from the sonicated samples with centrifugation (1500 g for 10 minutes at 4^{o}C), the supernatant was centrifuged again (12,000 g for 20 minutes at 4^{o}C). The pellet was re-suspended in lysis buffer containing 1% Triton X-100 and 0.1% SDS, and the samples were run on 10% SDS-polyacrylamide gels according to the method of Laemmli (1970). The separated proteins were electrophoretically

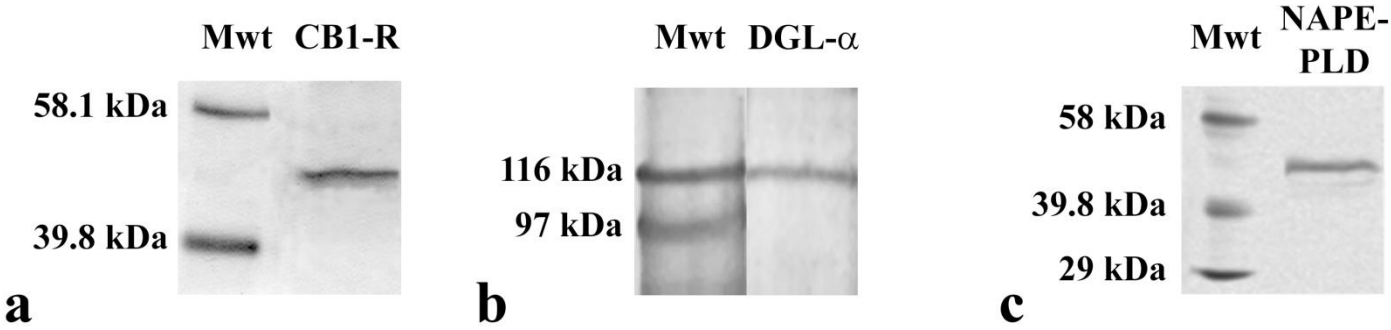

Fig. 11. Western blot analysis of the anti-CB1-R, anti-DGL-α and anti-NAPE-PLD antibodies. The single immunoreactive bands on the Western blots indicate that the antibodies detect proteins with a molecular mass of ~53 kDa, ~115 kDa and ~46 kDa which correspond to the molecular mass of CB1-R (a), DGL-α (b) and NAPE-PLD (c), respectively.

transferred onto PVDF membranes (Millipore, Billerica, MA, USA), and the membranes were immunostained according to the single immunostaining protocol described above. The immunostaining revealed only one immunoreactive band at molecular weight of 53 kDa for CB1-R (Fig. 11a), 115 kDa for DGL-α (Fig. 11b) and 46 kDa for NAPE-PLD (Fig. 11c) corresponding to the molecular weight of CB1-R (Song & Howlet, 1995; Grimsey et al., 2008) and the enzymes (Bisogno et al., 2003; Okamoto et al., 2004).

Since in our experiments IB4 was used as specific marker of non-peptidergic primary afferent terminals, we have to add, that in some of the earlier reports, IB4-binding to astrocytes and microglial cells has been demonstrated (Runyan et al., 2007; Streit, 1990; Villeda et al., 2006). In contrast to these reports, we have never seen IB4-binding on glial cells in the present study (Fig. 12).

To test the specificity of the immunostaining protocol, free-floating sections were incubated according to the single immunostaining protocol described above with primary antibodies omitted or replaced with 1% normal goat serum. No immunostaining was observed in these sections.

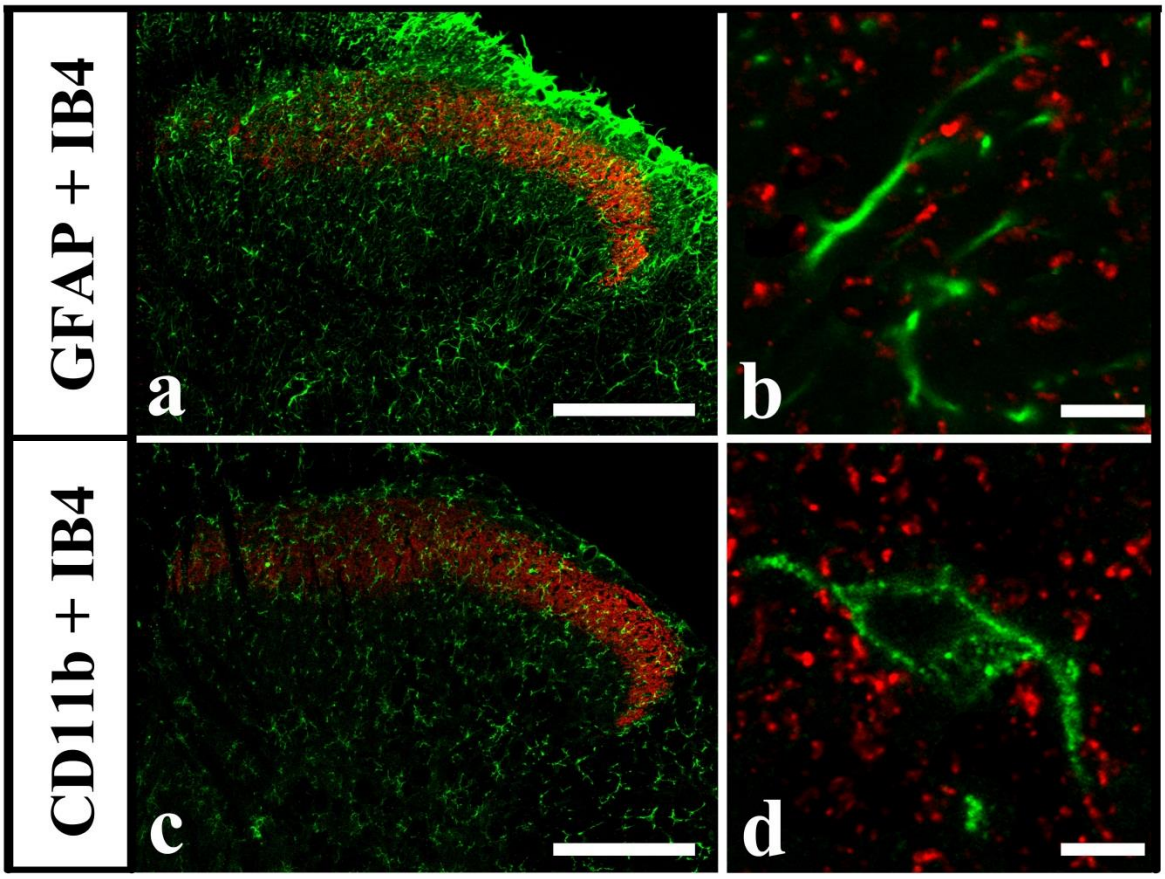

Fig. 12. Lack of co-localization between IB4-binding and immunostaining for glial markers. Micrographs of single laser scanning confocal optical sections illustrating IB4-binding (red) and immunostaining of markers that are specific for astrocytes (GFAP, green; a, b) and microglial cells (CD11b, green; c, d) in the superficial spinal dorsal horn with low (a, c) and high (b, d) magnification. Note that mixed colors (yellow) that may indicate double labeled structures are not observed on the superimposed images obtained with high magnification. Scale bar: 200 µm (a, c), 5 µm (b, d)

5. RESULTS

5.1. Distribution of CB1-R immunoreactivity in the superficial spinal dorsal horn

Peroxidase-based single immunostaining revealed an abundant immunoreactivity for CB1-R in the lumbar spinal cord of rats that was mostly confined to a twin band corresponding to lamina I and the inner portion of lamina II (lamina IIi) (Fig. 13). The two heavily stained bands were separated by a narrow zone corresponding to the outer portion of lamina II (lamina IIo), where only a sparse immunostaining was observed (Fig. 13). Immunostained elements appeared exclusively as punctuate profiles in both the densely and the sparsely stained zones (Fig. 13).

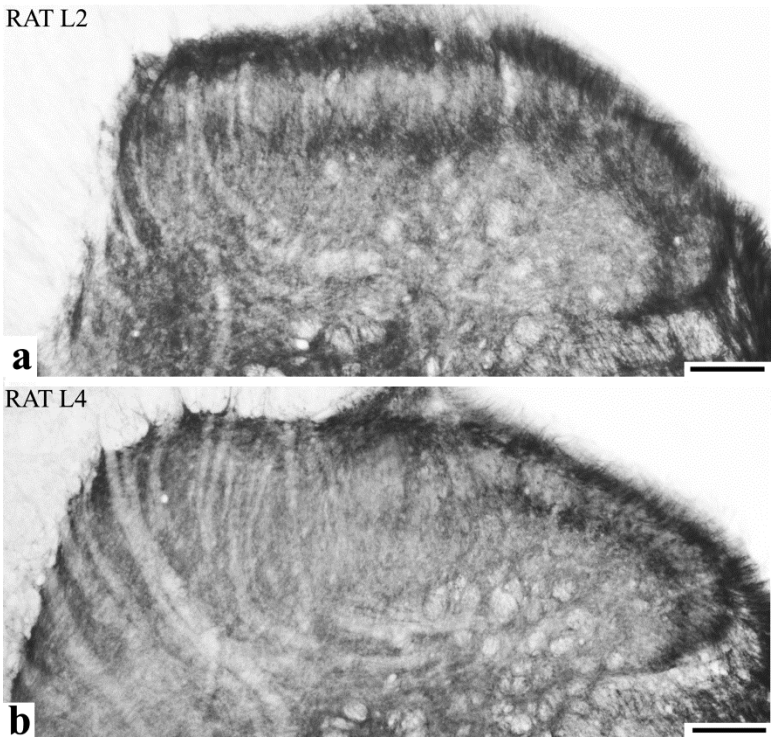

Fig. 13. Photomicrographs showing immuno-reactivity for CB1-R in the dorsal horn of rat at the spinal segmental levels of L2 (a) and L4 (b). Strong CB1-R immunoreactivity was found in laminae I and IIi of the spinal dorsal horn, while lamina IIo showed only a very faint labeling. Note that the immonolabeling in the medial aspect of lamina IIi at the level of L4 is much weaker than at the level of L2. Scale bars: 100 μm.

Somatic or dendritic immunostaining was never observed in laminae I and II. This pattern of immunostaining was characteristic of laminae I and II throughout the rostro-caudal extent of the

lumbar spinal cord with the exception of segment L4 and the adjacent territories of segments L3 and L5. At this level lamina IIi showed an intense immunostaining only in the lateral aspect of the dorsal horn, whereas the staining intensity in the medial aspect of lamina IIi was similar to that observed in lamina IIo (Fig. 13b). At his level of the spinal cord, the medial aspect of the dorsal horn receives high number of primary afferent inputs from the plantar surface of the hind paw, which makes the inner portion of lamina II less compact (Molander & Grant, 1985, 1986), thus the density of CB1-R immunoreactivity appears to be decreased. Otherwise, the distribution of immunoreactivity for CB1-R at the level of the L4 spinal segment was similar to that in other segments of the lumbar spinal cord.

5.2. Co-localization of CB1-R immunoreactivity with axonal and glial markers

Because of the importance of paw-innervating segments of the spinal cord in pain processing, studies concerning the axonal and glial localization of CB1 receptors were focused on the medial and lateral aspects of the L4 segment.

5.2.1. Co-localization of CB1-R immunoreactivity with markers of nociceptive primary afferents

There is general agreement that synaptic transmission from a population of the nociceptive primary afferents is mediated only by glutamate, whereas others, in addition to glutamate also release neuropeptides (Willis & Coggeshall, 2004). Most of the peptidergic nociceptive primary afferents express CGRP, whereas the cell-coat of the non-peptidergic axon terminals contains a polysaccharide that selectively binds the lectin isolated from Bandeiraea simplicifolia, IB4 (Willis & Coggeshall, 2004). Thus, to study the expression of CB1-Rs on central axon terminals of peptidergic and non-peptidergic nociceptive primary afferents we investigated the co-localization of CB1-Rs with CGRP immunoreactivity and IB4 binding. In agreement with previous studies, we observed a strong immunostaining for CGRP in laminae I–IIo (Traub et al., 1989; Nasu, 1999).

Investigating the co-localization between CB1-R and CGRP immunoreactivity, we found that 16.74 ± 1.55 and 18.15 ± 0.84% (when the CB1-R antibody was diluted 1 : 5000), and 17.62 ± 0.77 and 17.49 ± 0.87% (when the CB1-R antibody was diluted 1 : 1000) of CB1-R-immunoreactive puncta were also stained for CGRP, whereas 46.36 ± 2.54 and 49.10 ± 0.80% (when the CB1-R antibody was diluted 1 : 5000), and 44.35 ± 2.31 and 47.51 ± 0.68% (when the CB1-R antibody was diluted 1 : 1000) of CGRP-immunoreactive axon terminals proved to be immunoreactive also for CB1-R in the medial and lateral aspects of the dorsal horn, respectively (Fig. 14a-c and Fig. 15).

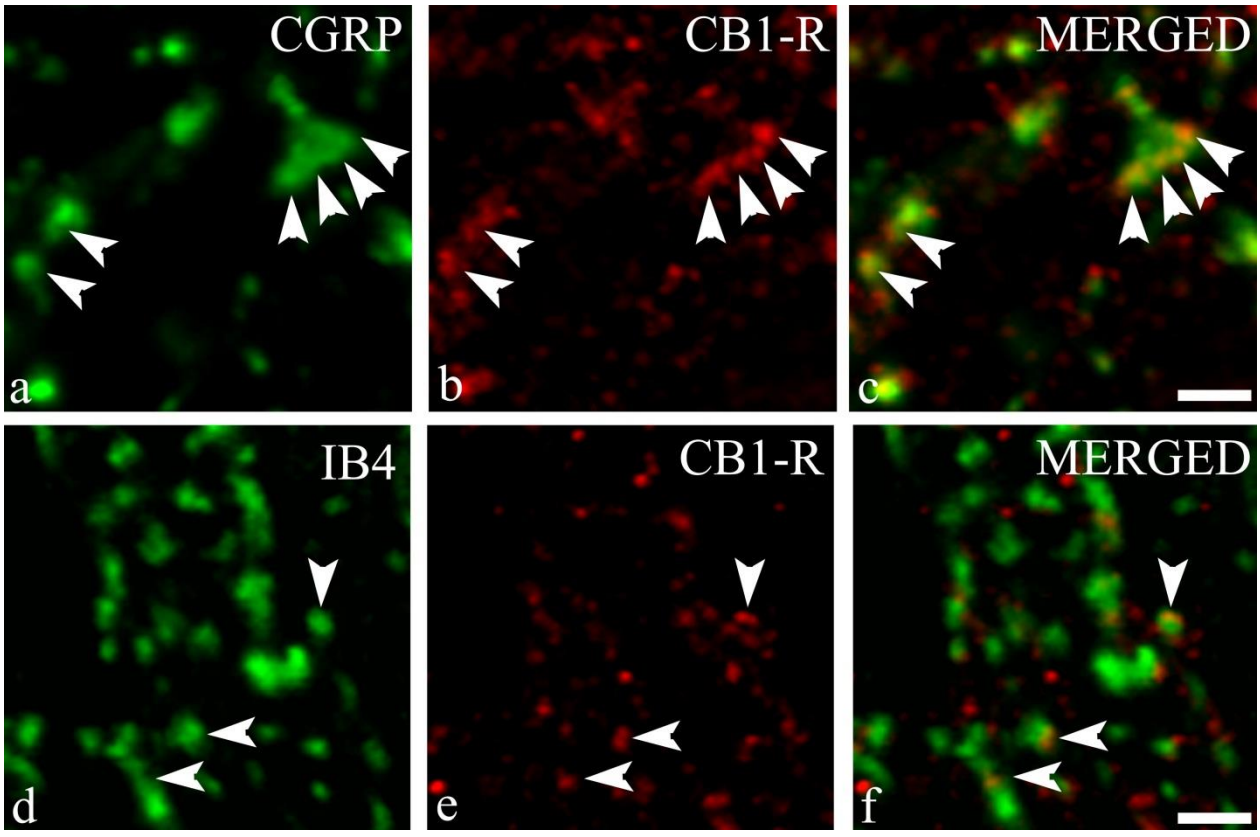

Fig. 14. Micrographs of single 1-μm-thick laser scanning confocal optical sections illustrating the co-localization between immunolabeling for CB1-R (red; b, e) and immunoreactivity for markers that are specific for axon terminals of peptidergic (CGRP, green; a) and non-peptidergic (IB4 binding, green; d) nociceptive primary afferents in the superficial spinal dorsal horn. Mixed colors (yellow) on the superimposed images (c, f) indicate double labeled structures. Double stained varicosities are marked with arrows. Note that CB1-R immunoreactivity can be observed in axon terminals of both peptidergic and non-peptidergic nociceptive primary afferents. Scale bars: 2 μm.

As has been reported previously, IB4 binding labeled a large number of axon terminals in lamina IIi (Guo et al., 1999). Although the intensity of CB1-R immunostaining was strikingly different in the medial and lateral aspects of lamina IIi (Fig. 13b), the co-localization between CB1-R immunoreactivity and IB4 binding was surprisingly similar in the medial and lateral

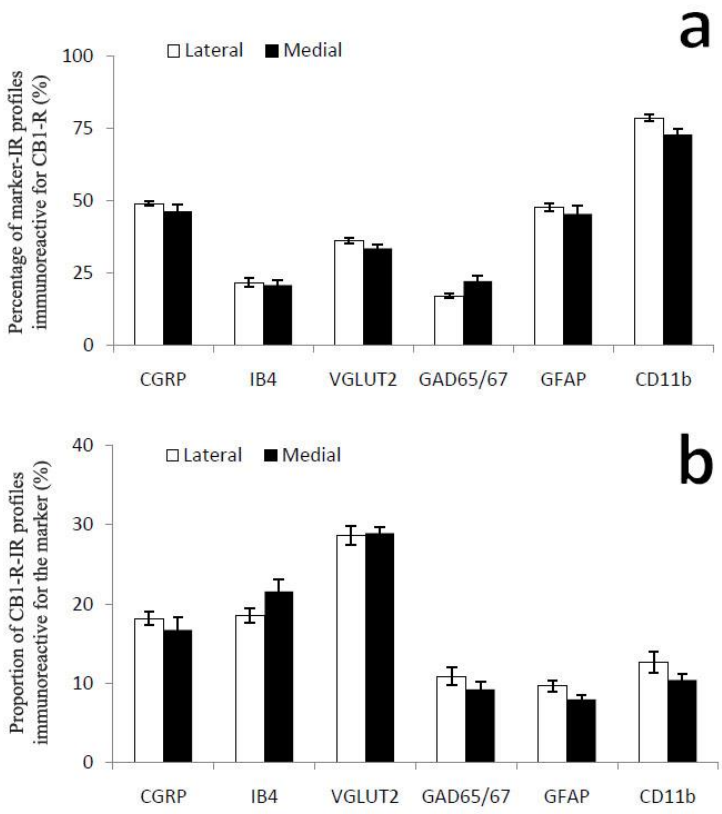

Fig. 15. Histograms showing the degree of co-localization between immunoreactivity for CB1-R and selected axonal and glial markers in laminae I–II of the spinal dorsal horn. (a) Percentage of profiles immunoreactive for the applied axonal and glial markers that were found to be labeled also for CB1-R in the lateral and medial aspects of laminae I–II. (b) Percentage of profiles immunoreactive for CB1-R that were found to be labeled also for the applied axonal and glial markers in the lateral and medial aspects of laminae I–II. Data are shown as mean ± SEM.

compartments: 21.56 ± 1.48 and 18.55 ± 0.92% of CB1-R-immunoreactive puncta were also positive for IB4 binding, whereas 20.94 ± 1.72 and 21.66 ± 1.56% axon terminals that were positive for IB4 binding proved to be immunoreactive also for CB1-R in the medial and lateral aspects of the dorsal horn, respectively (Fig. 14d-f and Fig. 15).

5.2.2. Co-localization of CB1-R immunoreactivity with markers of axon terminals of glutamatergic and GABAergic spinal neurons

Much experimental evidence in recent years suggests that VGLUT2 can be used as a marker for axon terminals of intrinsic spinal neurons (Li et al., 2003; Oliveira et al., 2003; Todd et al., 2003). However, it is also accepted that GABAergic neurons synthesize GABA with the aid of GAD (Martin et al., 2000). All GABAergic neurons in the spinal cord are thought to contain both isoforms of GAD (GAD65 and GAD67; Mackie et al., 2003; Tran et al., 2003), although the relative amounts of the two enzymes vary widely, with some cells expressing predominantly GAD65 and others mainly GAD67 (Soghomonian & Martin, 1998; Mackie et al., 2003). Therefore, to study the expression of CB1-Rs on central axon terminals of glutamatergic and GABAergic spinal neurons we investigated the co-localization between CB1-R and VGLUT2 as well as GAD65/67 immunoreactivities.

Confirming results of previous studies (Li et al., 2003; Oliveira et al., 2003; Todd et al., 2003), VGLUT2-immunoreactive axon terminals were homogeneously distributed in laminae I–II. Despite the contrasting distribution of CB1-R immunoreactivity in the medial and lateral aspects of lamina I–II, the co-localization between CB1-R and VGLUT2 immunoreactivity was very similar throughout the entire medio-lateral extent of the superficial spinal dorsal horn. It was found that 28.93 ± 0.70 and 28.71 ± 1.19% of CB1-R-immunoreactive puncta were also immunostained for VGLUT2, whereas 33.60 ± 1.34 and 36.28 ± 0.96% axon terminals that were positive for VGLUT2 were also immunoreactive for CB1-R in the medial and lateral aspects of the dorsal horn, respectively (Fig. 15 and Fig. 16 a-c).

Dorsal rhizotomy at the level of spinal segments L2–S1 caused a slight reduction in the number of VGLUT2-immunoreactive puncta in the superficial dorsal horn of the L4 spinal segment. Counting VGLUT2 immunoreactive puncta along the edges of a standard square grid, on average there were 44.6 ± 2.2 and 42.1 ± 1.7 puncta per grid in laminae I and IIi of control animals, respectively. In animals with dorsal rhizotomy, these values were 41.5 ± 1.5 and 39.7 ± 1.0 in laminae I and IIi, respectively. Thus, the loss of primary afferents terminating in the superficial spinal dorsal horn resulted in a noticeable but non-significant 8.52% ($P = 0.3645$) and 5.73% ($P = 0.3600$) decrease in the total numbers of VGLUT2-immunoreactive puncta in laminae I and IIi, respectively. The loss of VGLUT2-immunoreactive primary afferents did not cause any substantial change in the co-localization of CB1-R and VGLUT2 immunoreactivities either. In

animals with dorsal rhizotomy, 26.94 ± 0.41 and 25.49 ± 0.76% of CB1-R-immunoreactive puncta were also immunostained for VGLUT2, whereas 36.40 ± 1.21 and 35.50 ± 1.63% axon terminals that were positive for VGLUT2 were also immunoreactive for CB1-R in the medial and lateral aspects of the dorsal horn, respectively.

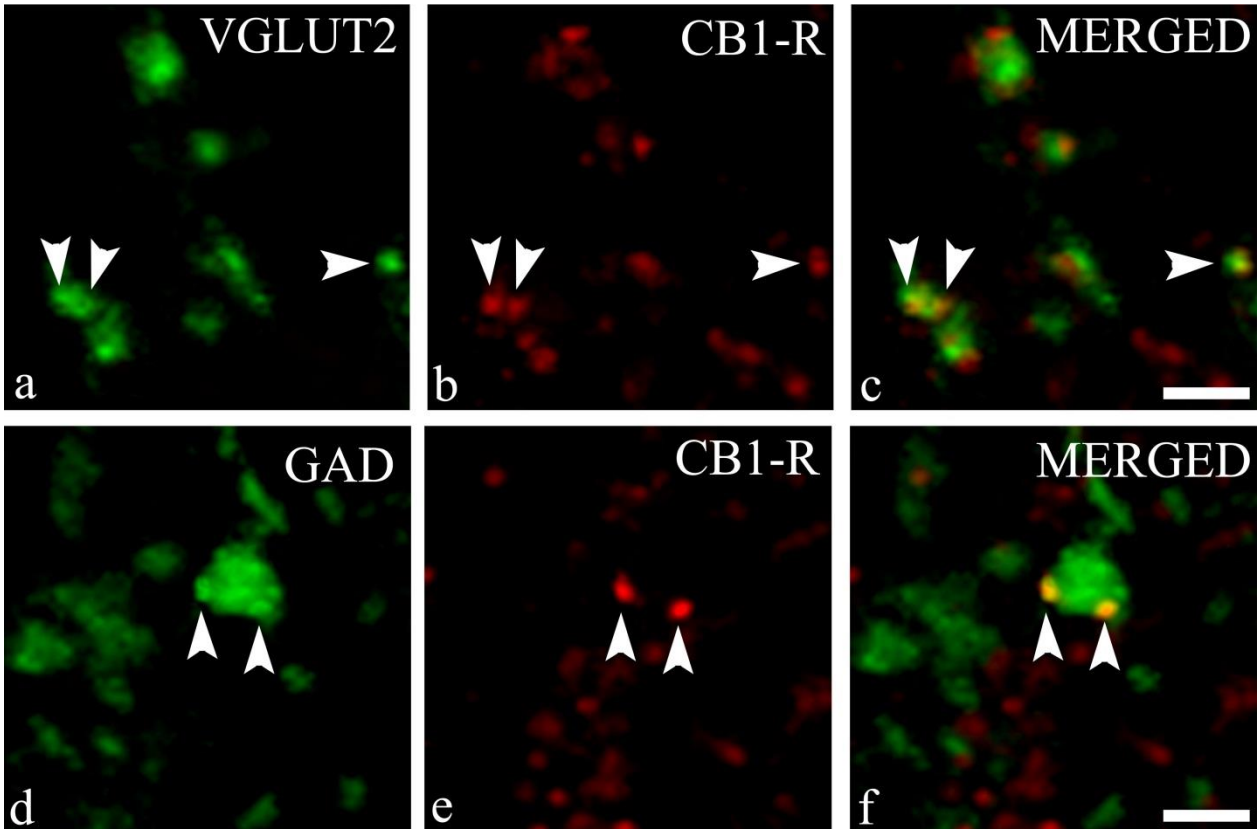

Fig. 12. Micrographs of single 1-μm-thick laser scanning confocal optical sections illustrating the co-localization between immunolabeling for CB1-R (red; b, e) and immunoreactivity for markers that are specific for excitatory (VGLUT2, green; a) and inhibitory (GAD65⁄67, green; d) axon terminals of intrinsic neurons in the superficial spinal dorsal horn. Mixed colors (yellow) on the superimposed images (c, f) indicate double labeled structures. Double stained varicosities are marked with arrows. Note that CB1-R immunoreactivity can be observed in both putative glutamatergic and GABAergic axon terminals. Scale bars: 2 μm.

Statistical differences between the corresponding co-localization values of control animals and animals with dorsal rhizotomy were all non-significant; P-values were 0.50, 0.13, 0.25 and 0.78, respectively.

Similar to earlier reports (Feldblum et al., 1995; Mackie et al., 2003), GAD65⁄67-immunoreactive axon terminals showed a dense and homogeneous distribution in the superficial spinal dorsal horn. Investigating the co-localization between CB1-R and GAD65⁄67

immunoreactivity, we found that 9.22 ± 1.01 and 10.88 ± 1.08% of CB1-R immunoreactive puncta were also stained for GAD65/67, whereas 22.22 ± 1.79 and 17.2 ± 0.89% of GAD65/67-immunoreactive axon terminals proved to be immunoreactive also for CB1-R in the medial and lateral aspects of the dorsal horn, respectively (Fig. 15 and Fig. 16 d-f).

5.2.3. Co-localization of CB1-R immunoreactivity with markers of astrocytes and microglial cells

A great deal of experimental evidence has accumulated in recent years suggesting the existence of a bidirectional communication between glial cells and neurons (Araque et al., 2001; Volterra & Bezzi, 2002; Nedergaard et al., 2003; Haydon & Carmignoto, 2006; Suter et al., 2007; Zhang et al., 2008). It has also been demonstrated that CB1-Rs are expressed by microglial cells in the cerebral cortex (Cabral & Marciano-Cabral, 2005), and also by astrocytes in the hippocampus (Navarrete & Araque, 2008), caudate putamen nucleus (Rodriguez et al., 2001) and dorsal horn of the spinal cord (Salio et al., 2002). Navarrete & Araque (2008) provided direct experimental evidence that CB1-Rs on astrocytes can be activated by endocannabinoids released by neurons, and also demonstrated that due to the activation of their CB1-Rs astrocytes release glutamate which activates NMDA receptors in neurons. Thus, because of its potential importance in pain processing we investigated the localization of CB1-Rs on astrocytes and microglial cells by using GFAP and CD11b as markers for astrocytes and microglial cells, respectively.

We obtained strong immunolabeling in the superficial spinal dorsal horn for both markers that was identical to that reported earlier (Garrison et al., 1991; Eriksson et al., 1993; Molander et al., 1997). Investigating the co-localization between CB1-R and GFAP immunoreactivity, we found that 7.98 ± 0.57 and 9.66 ± 0.71% of CB1-R immunoreactive puncta were also stained for GFAP, whereas 45.61 ± 2.66 and 47.87 ± 1.42% of GFAP-immunoreactive profiles proved to be immunoreactive also for CB1-R in the medial and lateral aspects of the dorsal horn, respectively (Fig. 15. and Fig. 17a-c). In addition to GFAP, we revealed a substantial co-localization between CB1-R and CD11b immunoreactivities. Our co-localization figures showed that 10.42 ± 0.78 and 12.66 ± 1.27% of CB1-R-immunoreactive puncta were also stained for CD11b, whereas 70.27 ± 0.64 and 78.79 ± 1.23% of CD11b-immunoreactive profiles proved to be immunoreactive also for CB1-R in the medial and lateral aspects of the dorsal horn, respectively (Fig. 15. and Fig. 17d-e).

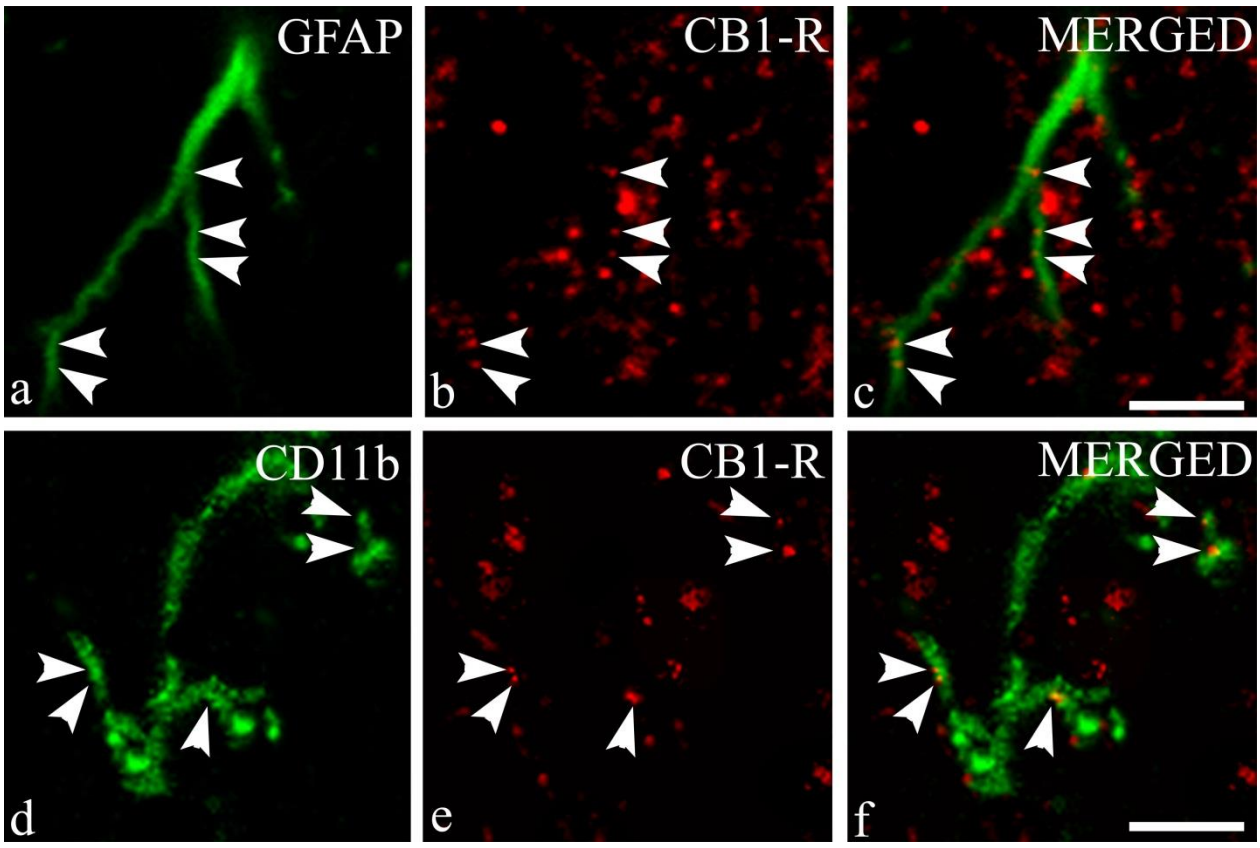

Fig. 17. Micrographs of single 1-μm-thick laser scanning confocal optical sections illustrating the co localization between immunolabeling for CB1-R (red; b, e) and immunoreactivity for markers that are specific for astrocytes (GFAP, green; a) and microglial cells (CD11b, green; d) in the superficial spinal dorsal horn. Mixed colors (yellow) on the superimposed images (c, f) indicate double labeled structures. Double-stained varicosities are marked with arrows. Note that CB1-R immunoreactivity can be observed both in astrocytes and microglial cells. Scale bars: 5 μm.

5.3. Distribution of CB1-receptors on the cell membrane of presynaptic axon terminals and glial processes

After revealing extensive co-localization between CB1-Rs and various axonal and glial markers, we intended to define the subcellular localization of CB1-receptors both in axon terminals and in glial profiles. Ultrathin sections immunostained according to the pre-embedding nanogold protocol for CB1-R were investigated at the ultrastructural level. Silver particles labeling CB1-Rs were recovered exclusively in axonal and glial-like profiles (Fig. 18). No

detectable staining was observed in dendrites or cell bodies of neurons. Immunoreactive axon terminals established both asymmetric (Fig. 18a-d) and symmetric (Fig. 18e) synaptic contacts.

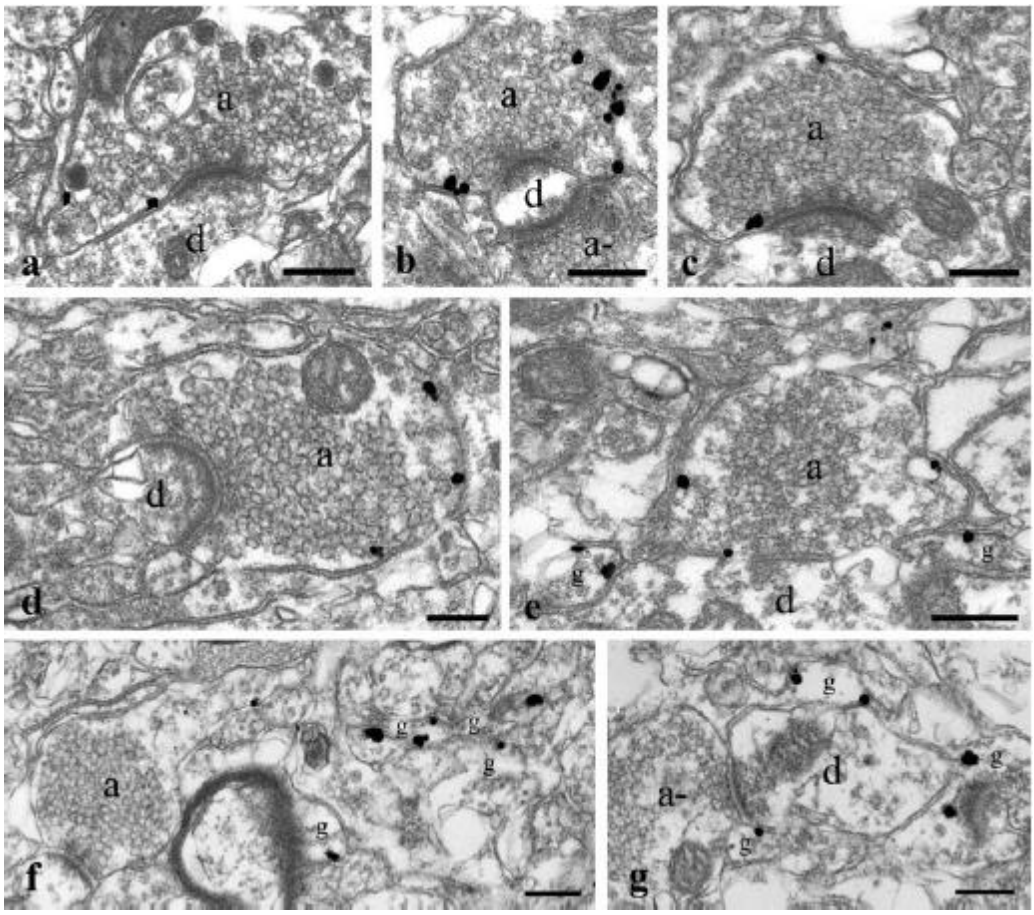

Fig. 18. Electron micrographs showing the distribution of CB1-R on axon terminals establishing asymmetric (a–d) and symmetric (e) synaptic contacts with postsynaptic dendrites in laminae I–II of the spinal dorsal horn. The axon terminal in insert a contains dense core synaptic vesicles. Silver particles labeling CB1-Rs are aligned along the surface membrane of axon terminals. Some of the particles are in close vicinity to synapses, and many others are located distant from the synaptic appositions. In addition to axon terminals, glial profiles in panels e, f and g also show positive immunolabeling for CB1-R. Note that all dendrites are negative for CB1-Rs. a, axon terminal immunoreactive for CB1-R; a-, axon terminal not labeled for CB1-R; d, postsynaptic dendrite; g, glial profile. Scale bars: 0.2 μm.

Immunoreactive axon terminals forming asymmetric and symmetric synaptic contacts contained spheroid and pleomorphic synaptic vesicles (Fig. 18), respectively, but dense core vesicles were also revealed in some of the terminals with asymmetric synaptic apposition (Fig. 18a). Immunolabeled glial-like processes were frequently seen (Fig 18e–g). In many cases, immunostained glial-like processes were revealed in close vicinity to synaptic contacts between

immunoreactive axon terminals and postsynaptic dendrites (Fig. 18e and g). Regardless of whether the labeled profile was an axon terminal or glial-like profile, immunogold particles were revealed exclusively in close association with the plasma membrane (Fig. 18). The membrane-associated silver particles were found at the protoplasmic face of the plasma membrane, in agreement with the intracellular location of the epitope recognized by the antibody. The silver precipitates attached to the plasma membrane were distributed on extra-synaptic membrane compartments both close to and far from the synaptic apposition (Fig.18). None of them was recovered within the synaptic apposition.

5.4. Distribution of DGL-α and NAPE-PLD immunoreactivity in the superficial spinal dorsal horn

To elucidate the distribution of the DGL-α protein in laminae I–II of the spinal dorsal horn, immunostaining for DGL-α with an antibody directed against a long internal segment of the enzyme (residues 790–908) (Katona et al., 2006) was carried out in the rat lumbar spinal cord. Both peroxidase-based and fluorescence single immunostaining revealed an abundant immunoreactivity for DGL-α throughout the superficial spinal dorsal horn. Lamina II appeared as a heavily stained band on the cross-section of the spinal cord, whereas lamina I and the deeper laminae of the dorsal horn were more sparsely stained (Fig. 19a, b). Immunostained elements appeared as punctate profiles both in the densely and sparsely stained zones (Fig. 19a, b). Besides the characteristic punctate labeling, larger immunoreactive spots resembling somata of neurons or glial cells were also scattered both in the gray and white matters (Fig. 19a, b).

To reveal immunonoreactivity for NAPE-PLD, sections of the lumbar spinal cord were reacted with a highly specific anti-NAPE-PLD antibody raised against the N-terminal 41 amino acids of the enzyme (Nyilas et al., 2008). Here, we observed a punctate immunostaining for NAPE-PLD, the density of which was more or less homogeneous throughout the entire cross-sectional area of the dorsal horn including laminae I and II (Fig. 19c, d). Similarly to DGL-α, larger NAPE-PLD immunoreactive spots resembling somata of neurons or glial cells were also observed (Fig. 19c, d).

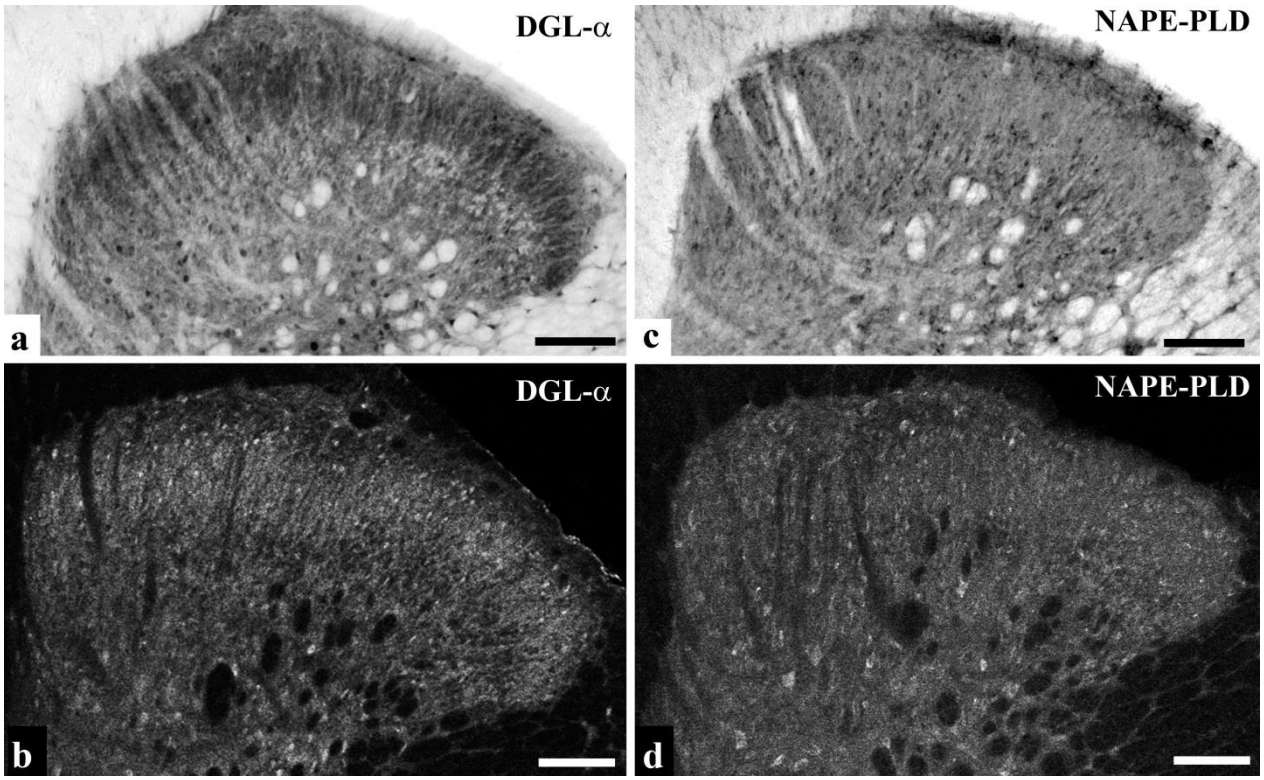

Fig. 19. The distribution of DGL-α and NAPE-PLD immunoreactivity in the spinal dorsal horn. a and b, Photomicrographs showing immunoreactivity for DGL-α in the spinal dorsal horn of rats following immunoperoxidase (a) and immunofluorescence (b) staining. We observed an abundant punctuate immunoreactivity for DGL-α. Lamina II of the superficial spinal dorsal horn appeared as a heavily stained band, whereas lamina I was more sparsely stained. Besides the characteristic punctuate labeling, larger immunoreactive spots resembling somata of neurons or glial cells were also scattered throughout both the gray and white matters. c and d, Photomicrographs showing immunoreactivity for NAPE-PLD in the dorsal horn of rat's spinal cord following immuno-peroxidase (c) and immunofluorescence (d) staining. Generally, we observed a homogeneous punctuate immunostaining for NAPE-PLD, but larger NAPE-PLD immunoreactive spots resembling somata of neurons or glial cells were also seen both in the gray and white matters. Note that the immunoperoxidase and immunofluorescent stainings show very similar patterns of immunoreactivity. Scale bar: 100 μm.

5.5. Co-localization of DGL-α and NAPE-PLD immunoreactivity with axonal and glial markers

Because of the importance of paw-innervating segments of the spinal cord in pain processing, studies concerning the axonal and glial localization of CB1 receptors were focused on the medial and lateral aspects of the L4 segment.

5.5.1. Co-localization of DGL-α and NAPE-PLD immunoreactivity with markers of nociceptive primary afferents

As described earlier, most of the peptidergic nociceptive primary afferents express CGRP, whereas the cell membrane of the nonpeptidergic axon terminals binds IB4 (Ribeiro da Silva and De Korninck, 2009; Willis and Coggeshall, 2004). Thus, to study the expression of DGL-α and NAPE-PLD on central axon terminals of peptidergic and nonpeptidergic nociceptive primary afferents we investigated the co-localization of the enzymes with CGRP immunoreactivity and IB4-binding.

Investigating the co-localization between DGL-α and CGRP immunoreactivity, we collected 703 and 1,224 profiles immunostained for CGRP and DGL-α, respectively, and found that only 1.96±0.78% of DGL-α immunoreactive puncta were also stained for CGRP, whereas 3.41±1.11% of CGRP immunoreactive axon terminals proved to be immunoreactive also for DGL-α in laminae I–II of the dorsal horn (Figs. 20a and 21a). The co-localization values for NAPE-PLD were even lower. Following a careful analysis of 760 and 1,304 profiles immunostained for CGRP and NAPE-PLD, respectively, we found that 1.69±0.91% of NAPE-PLD immunoreactive puncta were also stained for CGRP, whereas 1.97±0.76% of CGRP immunoreactive axon terminals proved to be immunoreactive also for NAPE-PLD in the superficial spinal dorsal horn (Fig. 20b and Fig. 21).

As it has been reported earlier, IB4-binding labeled a large number of axon terminals in lamina IIi (Guo et al., 1999) (Fig. 20c-d). Despite the strong immunostaining and the substantial spatial overlap between the investigated profiles, the co-localization between axon terminals labeled with IB4-binding and puncta immunoreactive for DGL-α or NAPE-PLD was very low. After the investigation of 660 IB4-binding and 1,490 DGL-α immunostained profiles, it was found that 2.48±0.99% of DGL-α immunoreactive puncta were also positive for IB4-binding, whereas 1.06±0.79% of axon terminals that were positive for IB4-binding proved to be immunoreactive also for DGL-α (Fig. 20c and Fig. 21). The co-localization values for NAPE-PLD were very similar. From 737 IB4-binding and 1,355 NAPE-PLD immunostained profiles 1.92±0.88% of NAPE-PLD immunoreactive puncta were also positive for IB4-binding, and 2.43±0.91% of axon terminals that were positive for IB4-binding proved to be immunoreactive also for NAPE-PLD in the superficial spinal dorsal horn (Fig. 20d and Fig. 21).

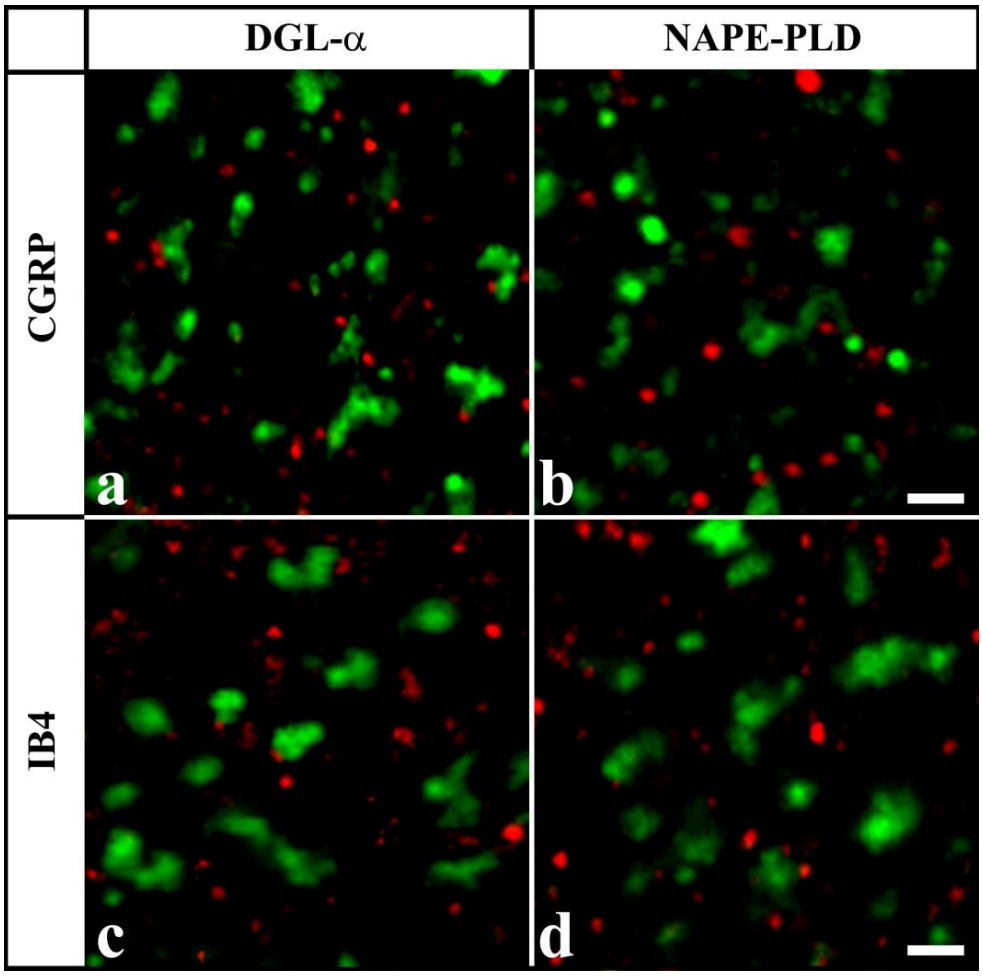

Fig. 20. Co-localization of DGL-α and NAPE-PLD with axonal markers. Micrographs of single 1 μm thick laser scanning confocal optical sections assessing co-localization between immunolabeling for DGL-α (red; a, c) or NAPE-PLD (red; b, d) and immunoreactivity for markers that are specific for axon terminals of specific populations of peptidergic (CGRP, green; a, b) and nonpeptidergic (IB4-binding, green; c, d) nociceptive primary afferents. Note that mixed colors (yellow) that may indicate double labeled structures are not observed on the superimposed images. Scale bar: 2 μm.

5.5.2. Co-localization of DGL-α and NAPE-PLD immunoreactivity with markers of axon terminals of putative glutamatergic and GABAergic spinal neurons

As mentioned above, VGLUT2 can be used as a marker for axon terminals of intrinsic spinal neurons, whereas GABAergic neurons in the spinal cord contain both isoforms of GAD (GAD65 and GAD67) (Mackie et al., 2003; Tran et al., 2003). Therefore, to study the expression of DGL-α and NAPE-PLD on central axon terminals of putative glutamatergic and GABAergic

spinal neurons we investigated co-localization between the enzymes and VGLUT2 as well as GAD65/67 immunoreactivities.

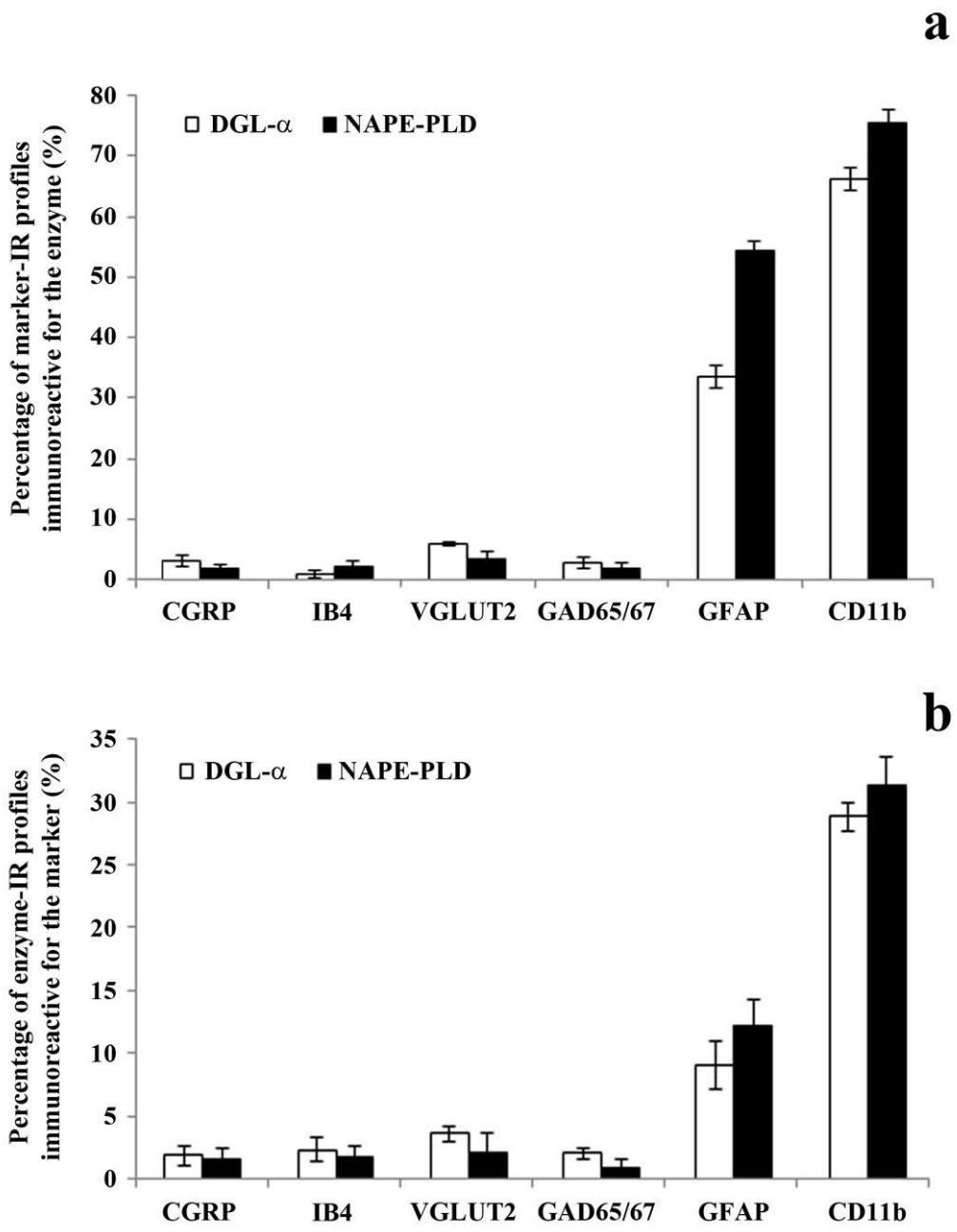

Fig. 21. The degree of co-localization of DGL-α and NAPE-PLD with axonal and glial markers. Histograms showing the degree of co-localization between immunoreactivity for DGL-α or NAPE-PLD and selected axonal and glial markers in laminae I-II of the spinal dorsal horn. a, Percentage of profiles immunoreactive for the applied axonal and glial markers that were found to be labeled also for DGL-α or NAPE-PLD. b, Percentage of profiles immunoreactive for DGL-α or NAPE-PLD that were found to be labeled also for the applied axonal and glial markers.
Data are shown as mean ± SEM.

The co-localization values between the investigated enzymes and VGLUT2 immunoreactivity were slightly higher than were found for the co-localization with axon terminals of nociceptive primary afferents, but were still very low. Evaluating 725 and 1,508 profiles immunostained for VGLUT2 and DGL-α, respectively, we found that 3.78±0.59% of DGL-α immunoreactive puncta were also immunostained for VGLUT2, whereas 6.76±0.47% of

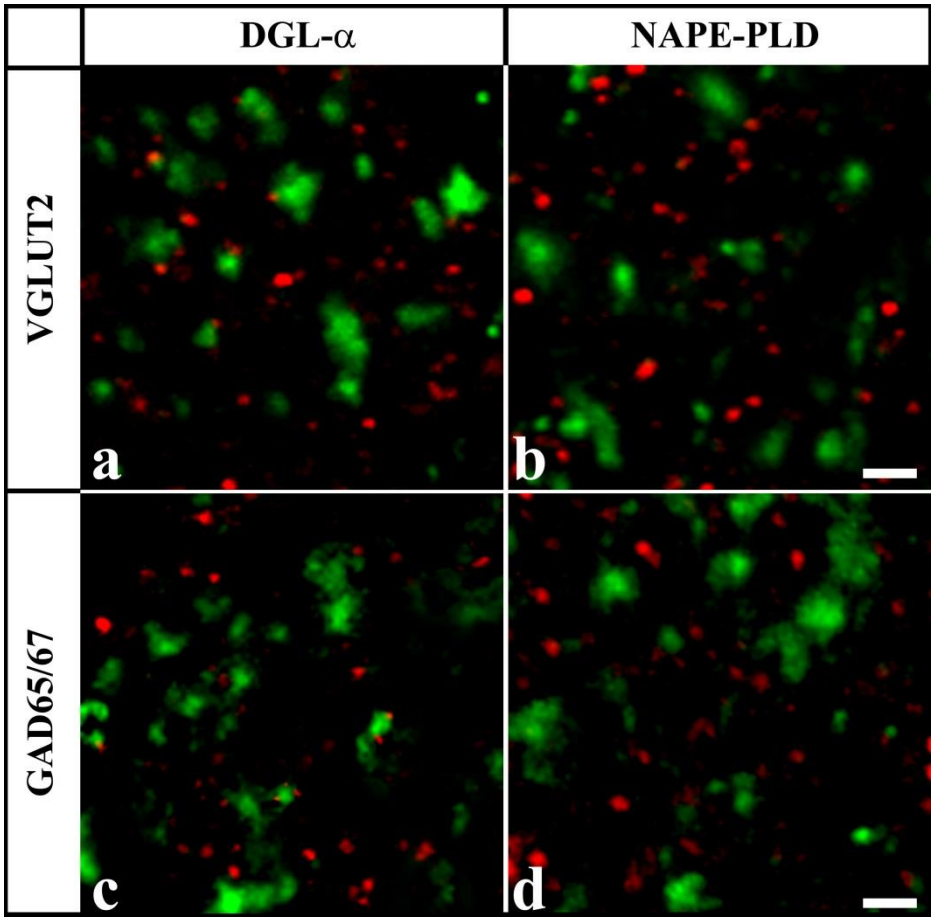

Fig.22. Co-localization of DGL-α and NAPE-PLD with axonal markers. Micrographs of single 1 μm thick laser scanning confocal optical sections assessing co-localization between immunolabeling for DGL-α (red; a, c, e) or NAPE-PLD (red; b, d) and immunoreactivity for markers that are specific for axon terminals of putative excitatory (VGLUT2, green; a, b) and inhibitory (GAD65/67, green; c, d) intrinsic neurons in the superficial spinal dorsal horn. Note that mixed colors (yellow) that may indicate double labeled structures are not observed on the superimposed images. Scale bar: 2 μm.

axon terminals that were positive for VGLUT2 were also immunoreactive for DGL-α (Fig. 21 and Fig. 22). The colocalization values for NAPE-PLD were even lower. In this case, after the

investigation of 681 and 1,526 profiles immunostained for VGLUT2 and NAPE-PLD, respectively, it was revealed that 2.23±1.67% of NAPE-PLD immunoreactive puncta were also stained for VGLUT2, whereas 3.96±1.31% of VGLUT2 immunoreactive axon terminals proved to be immunoreactive also for NAPE-PLD (Fig. 21 and Fig. 22).

Investigating the co-localization between DGL-α and GAD65/67 immunoreactivity, we collected 641 and 1,388 profiles immunstained for GAD65/67 and DGL-α, respectively, and found that 2.16±043% of DGL-α immunoreactive puncta were also stained for GAD65/67, whereas 3.12±0.93% of GAD65/67 immunoreactive axon terminals proved to be immunoreactive also for DGL-α (Fig. 21 and Fig. 22). The co-localization values for NAPE-PLD were approximately similar. From 707 and 1,431 puncta immunostained for GAD65/67 and NAPE-PLD, respectively, 0.91±0.7% of NAPE-PLD immunoreactive puncta were also positive for GAD65/67, and 2.11±1.06% of axon terminals that were immunostained for GAD65/67 turned out also to be immunoreactive for NAPE-PLD in laminae I–II (Fig. 21 and Fig. 22).

5.5.3. Co-localization of DGL-α and NAPE-PLD immunoreactivity with markers of astrocytes and microglial cells

Production and inactivation of endocannabinoids, anandamide and 2-AG, by cultured astrocytes and microglial cells have also been shown in many studies (Carrier et al., 2004; Marsicano et al., 2003; Walter and Stella, 2003, 2004; Walter et al., 2002, 2003, 2004). Thus, because of the potential importance of endogenous cannabinoids in spinal pain processing we investigated the localization of DGL-α and NAPE-PLD on astrocytes and microglial cells by using GFAP and CD11b as markers for astrocytes and microglial cells, respectively.

Investigating the co-localization between DGL-α and GFAP immunoreactivity, we collected 216 and 1,321 profiles immunoreactive for GFAP and DGL-α, respectively, and found that 9.39±1.96% of DGL-α immunoreactive puncta also stained for GFAP, whereas 33.33±2.06% of GFAP immunoreactive profiles proved to be immunoreactive also for DGL-α (Fig. 21 and Fig. 23 a-c). In addition to GFAP, we revealed a substantial co-localization between DGL-α and CD11b immunoreactivity. For the microglial marker, after the investigation of 207 and 1,297 profiles immunstained for CD11b and DGL-α, respectively, the co-localization analysis showed that 29.53±1.19% of DGL-α immunoreactive puncta were also stained for

CD11b, whereas 67.15±2.21% of CD11b immunoreactive profiles were also immunoreactive for DGL-α (Fig. 21 and Fig. 23 d-f).

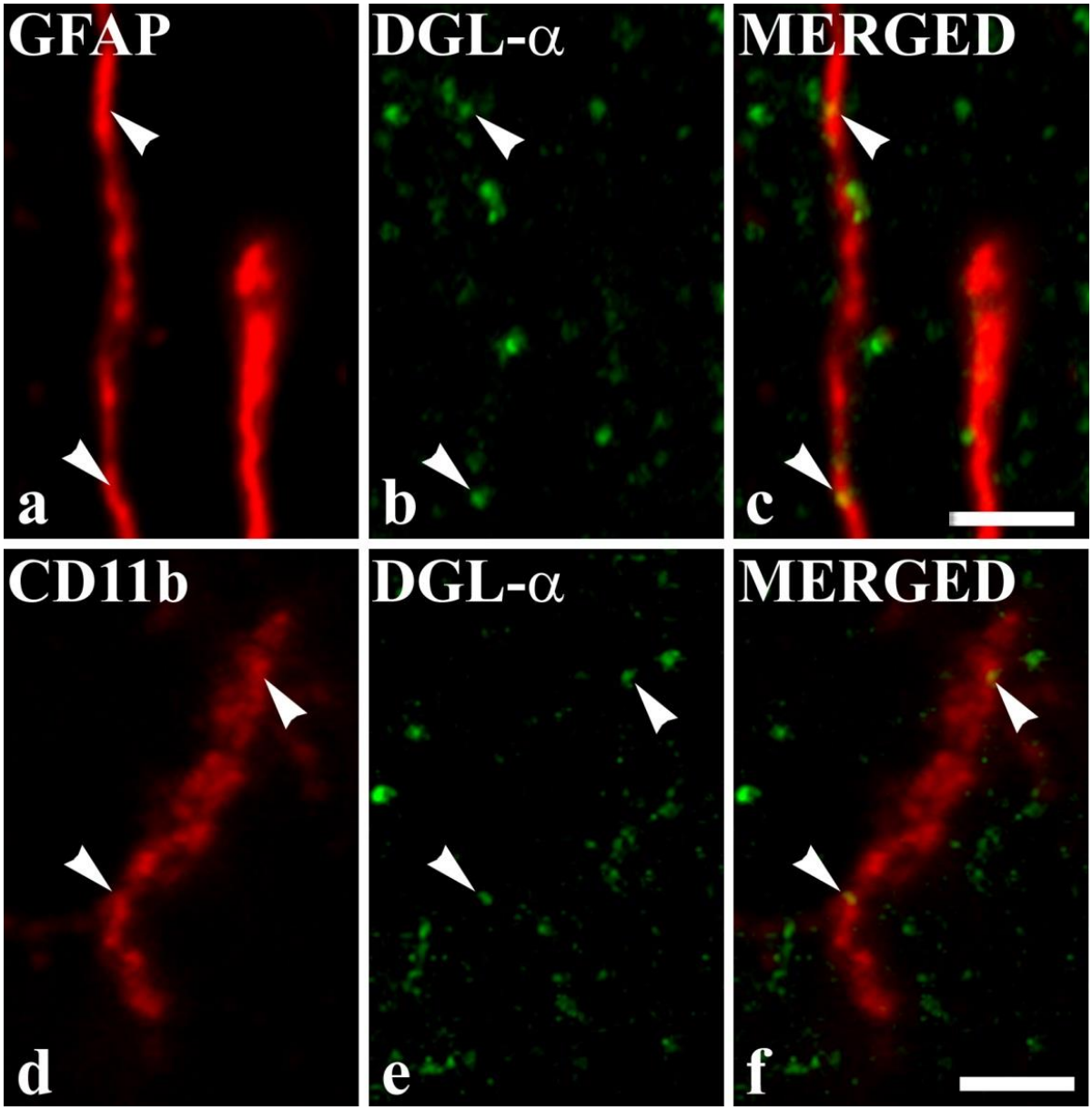

Fig. 23. Co-localization of DGL-α with glial markers. Micrographs of single 1.6 μm thick laser scanning confocal optical section (compressed images of three consecutive 1 μm thick optical sections with 0.3μm separation in the z-axis) illustrating the co-localization between immunolabeling for DGL-α (green; b, e) and immunoreactivity for a marker which is specific for astrocytes (GFAP, red; a); and microglial cells (CD11b, red; d) in the superficial spinal dorsal horn. Mixed colors (yellow) on the superimposed image (c, f) indicate double labeled spots within the illustrated glial processes. Puncta immunoreactive for DGL-α which are also stained for the glial marker are marked with arrowheads. Scale bar: 2 μm.

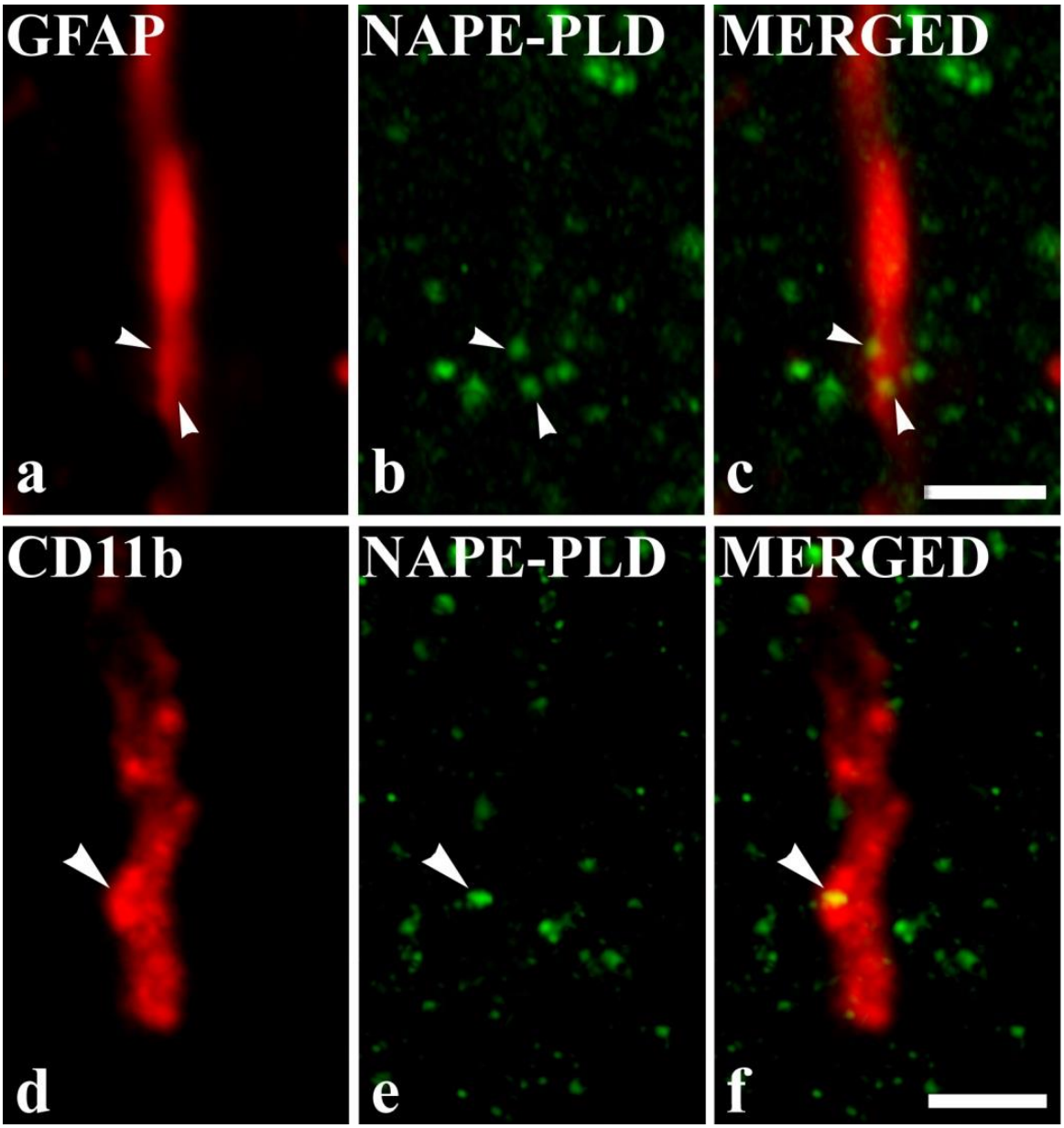

Fig. 24. Co-localization of NAPE-PLD with glial markers. Micrographs of single 1.6 μm thick laser scanning confocal optical section (compressed images of three consecutive 1 μm thick optical sections with 0.3 μm separation in the z-axis) illustrating the co-localization between immunolabeling for NAPE-PLD (green; b, e) and immunoreactivity for a marker which is specific for astrocytes (GFAP, red; a); and microglial cells (CD11b, red; d) in the superficial spinal dorsal horn. Mixed colors (yellow) on the superimposed image (c, f) indicate double labeled spots within the illustrated glial processes. Puncta immunoreactive for NAPE-PLD which are also stained for the glial marker are marked with arrowheads. Scale bar: 2 μm.

The co-localization values between NAPE-PLD and the glial markers were very similar to the figures that we obtained for the co-localization between DGL-α and the same glial markers.

However, there was a tendency for NAPE-PLD to have a slightly higher expression on glial cells than DGL-α. We collected 241 and 1,406 profiles immunoreactive for GFAP and NAPE-PLD, respectively, and found that 12.52±2.15% of NAPE-PLD immunoreactive puncta were also stained for GFAP, whereas 54.77±1.98% of GFAP immunoreactive profiles were also immunoreactive for NAPE-PLD in the superficial spinal dorsal horn (Fig. 21 and Fig. 24 g–i). In addition, we investigated 223 and 1,501 profiles immunoreactive for CD11b and NAPE-PLD, respectively, and observed that 32.11±2.30% of NAPE-PLD immunoreactive puncta were also stained for CD11b, whereas 75.34±2.60% of CD11b immunoreactive profiles were immunoreactive for NAPE-PLD (Fig. 21 and Fig. 24 j–l).

In order to substantiate the glial localization of the enzymes, in addition to the X-Y dimensions the confocal optical sections were also investigated in the X-Z and Y-Z projections. The X-Z and Y-Z images were drawn through the point of co-localization between the two markers, and the two orthogonal views were investigated for overlap. An example of this type of investigation is demonstrated on Fig. 25, where the X-Z and Y-Z projections of confocal images shown in Fig. 24c are illustrated.

5.6. Ultrastructural localization of DGL-α and NAPE-PLD immunoreactivity

Ultrathin sections immunostained for DGL-α and NAPE-PLD were investigated at the ultrastructural level. After finding a minimal overlap between immunolabeling for DGL-α and NAPE-PLD with various axonal markers and an extensive co-localization between DGL-α and NAPE-PLD with markers for astrocytes and microglial cells in double immunostained sections, we defined the subcellular localization of DGL-α and NAPE-PLD both in axon terminals and glial profiles. Furthermore, since we recovered only approximately half of the DGL-α and NAPE-PLD immunoreactive puncta on axon terminals and glial cells in the co-localization studies, an extensive search for DGL-α and NAPE-PLD immunolabeling in the somatodendritic compartment of neurons was also carried out.

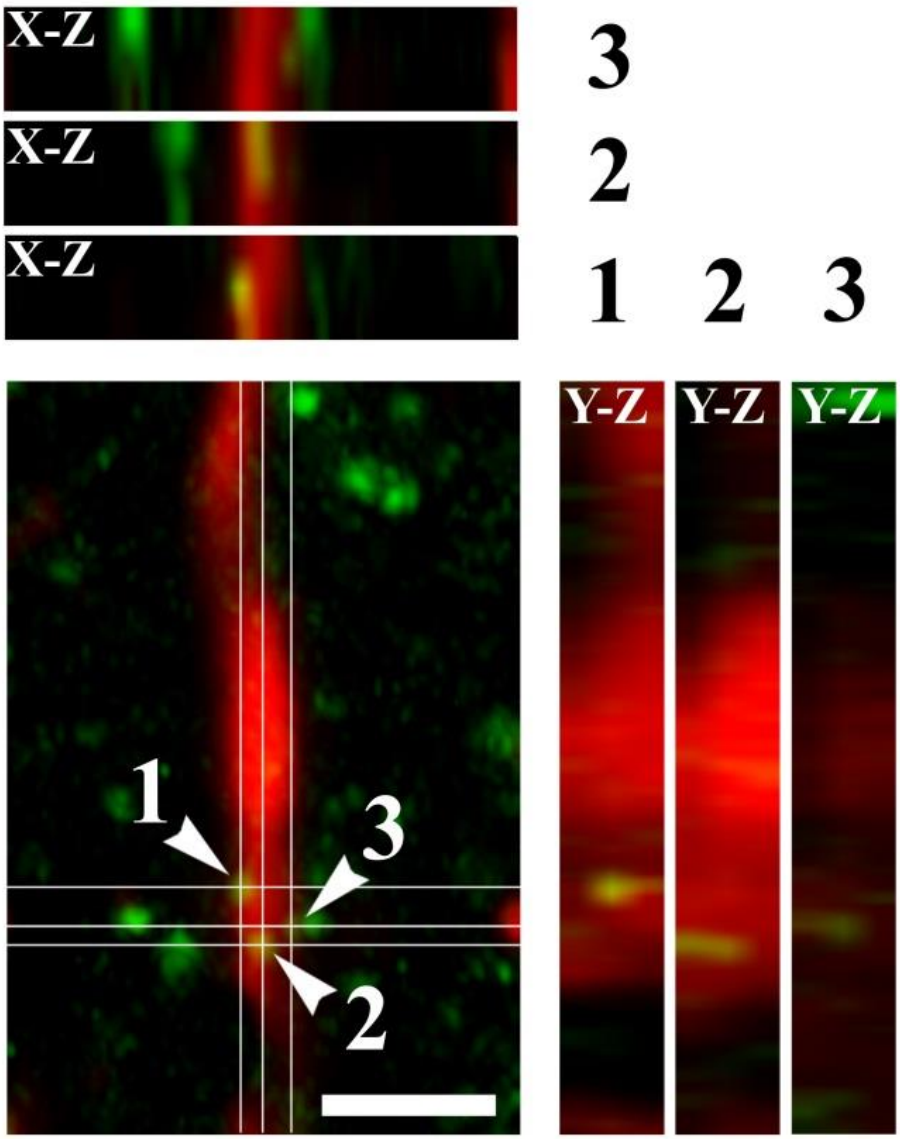

Fig.25. Co-localization between NAPE-PLD and GFAP illustrated in *x-y*, *x-z*, and *y-z* projections of confocal optical sections. Micrographs of a single 1.6 μm thick laser scanning confocal optical section, shown also in Fig. 24c, illustrating *x-y*, *x-z*, and *y-z* projections of the optical section double immunostained for GFAP (red) and NAPE-PLD (green). The points of co-localization between the two markers are at the crossing point of two lines indicating the planes through which orthogonal views of *x-z* and *y-z* projections were drawn. The *x-z* and *y-z* images of puncta 1, 2, 3 on insert a are identified by the serial numbers of the puncta beside and above the *x-z* and *y-z* projections, respectively. b, A part of a (without the lines indicating the planes of the orthogonal views) at the site of the NAPE-PLD immunoreactive puncta. According to the orthogonal images, as it is indicated by the mixed color (yellow), NAPE-PLD immunostained puncta 1 and 2 are within the confines of the GFAP immunoreactive profile [see the mixed color (yellow) on all the three projections]. However, in case of immunoreactive punctum 3, although there appears to be some overlap between the two markers indicated by the mixed color (yellow) on the *x-y* and *x-z* projections, the green color on the *y-z* projectional image clearly shows that the NAPE-PLD immunoreactive punctum is not within but adjacent to the GFAP immunoreactive profile.

In agreement with the results obtained from the co-localization studies, peroxidase reaction precipitates and silver intensified nanogold particles labeling DGL-α and NAPE-PLD were recovered primarily in dendrites (Fig.26 a–c and f–h; Fig. 27 a, b, d) and glial processes (Fig. 26 a, b, e and Fig. 27 e, f), and were found only occasionally in axon terminals (Fig. 26 d).

Regardless of whether the labeled profile was a dendrite, glia-like process or an axon terminal, immunolabeling was revealed exclusively in close association to the plasma membrane (Fig.27 and Fig. 28). The membrane-associated immunoprecipitates and nanogold particles were found at the cytoplasmic face of the plasma membrane (Fig. 26 and Fig. 28), in agreement with the intracellular location of the epitopes recognized by the antibodies. In dendrites, the end product of the immunoperoxidase and nanogold staining for DGL-α was observed at membrane compartments where the dendrites received synaptic contacts from axon terminals with different morphology (Fig. 26 a–c and f–h), including boutons representing the central element of synaptic glomeruli (Fig. 26 c).

Regardless of the morphology of the presynaptic axon, immunolabeling for DGL-α was always observed adjacent or in close vicinity to synaptic apposition. In case of the nanogold staining, silver intensified gold particles were found in perisynaptic position at asymmetric synaptic contacts (Fig. 26 f–h). In the case of the immunoperoxidase staining, the immunoprecipitate also covered a part of the postsynaptic membrane (Fig. 26 a,b).

Similar to DGL-α, immunolabeling for NAPE-PLD in dendrites also appeared as small immunoprecipitates associated with the inner surface of the cell membrane (Fig. 27 a,b,d). However, these immunolabeled membrane compartments were never observed in close vicinity to synaptic appositions (Fig. 27 a,b,d), although this finding may be limited by the fact that we investigated single and not serial ultrathin sections. In axon terminals, labeling was only occasionally found for either DGL-α or NAPE-PLD (Fig. 26 d and Fig. 27 c). In some cases the labeled membrane segments were adjacent to synaptic contacts (Fig. 26 d), in other cases there was no sign of synaptic specialization in the vicinity of the labeled membrane compartments (Fig. 27). We have to add, however, that we studied single and not serial ultrathin sections, thus the accurate relationship between the sites of labeling and synapses formed by the labeled axon terminal can not be definitively determined from our observations.

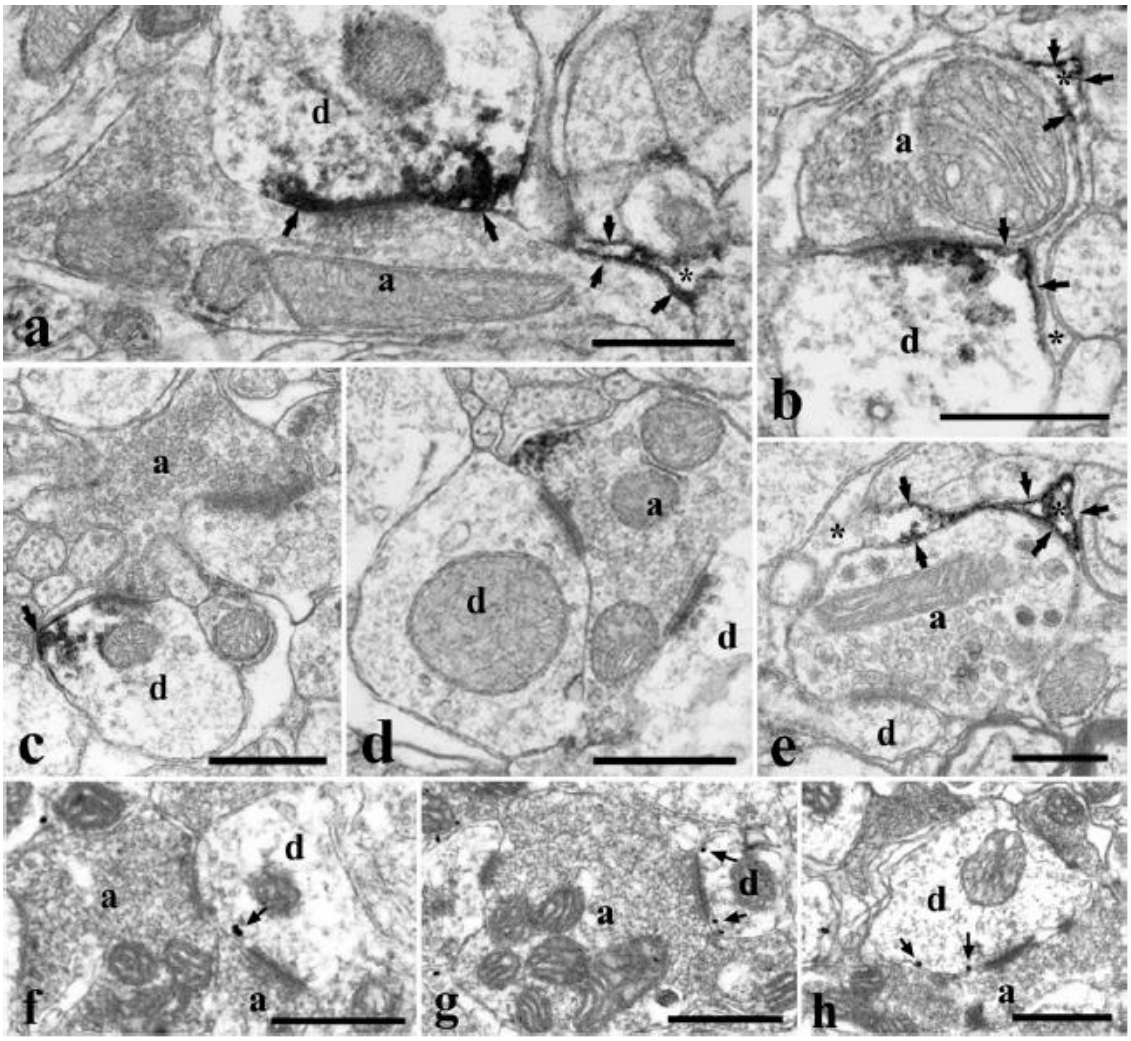

Fig. 26. Ultrastructural localization of DGL-α immunoreactivity in neurons and glial cells. Electron micrographs of preembedding immunoperoxidase (a–e) and nanogold (f–h) stained sections showing the distribution of DGL-α on postsynaptic dendrites (a–c, f–h) establishing synaptic contacts with axon terminals, in an axon terminal (d) and in glial profiles (a, b, e) in laminae I–II of the spinal dorsal horn. Immunoprecipitates and silver particles labeling DGL-α in dendrites and axon terminal aligned along the perisynaptic surface membrane. Immunoprecipitates labeling DGL-α in glial cells are also aligned along the surface membrane of glial processes. In some glial processes, the immunolabeled membrane compartments are in close vicinity to synapses (a, b). a: Axon terminal, d: postsynaptic dendrite, asterisk: glial profile. Arrows point at immunoperoxidase deposits and silver intensified nanogold particles. Bars: 0.5 μm.

In glia-like processes, the labeling was abundant for both DGL-α (Fig. 26 a, b, d) and NAPE-PLD (Fig. 27 e-f). Immunolabeled glia-like processes were frequently observed. It was a general finding that the membrane compartment immunureactive for DGL-α or NAPE-PLD was

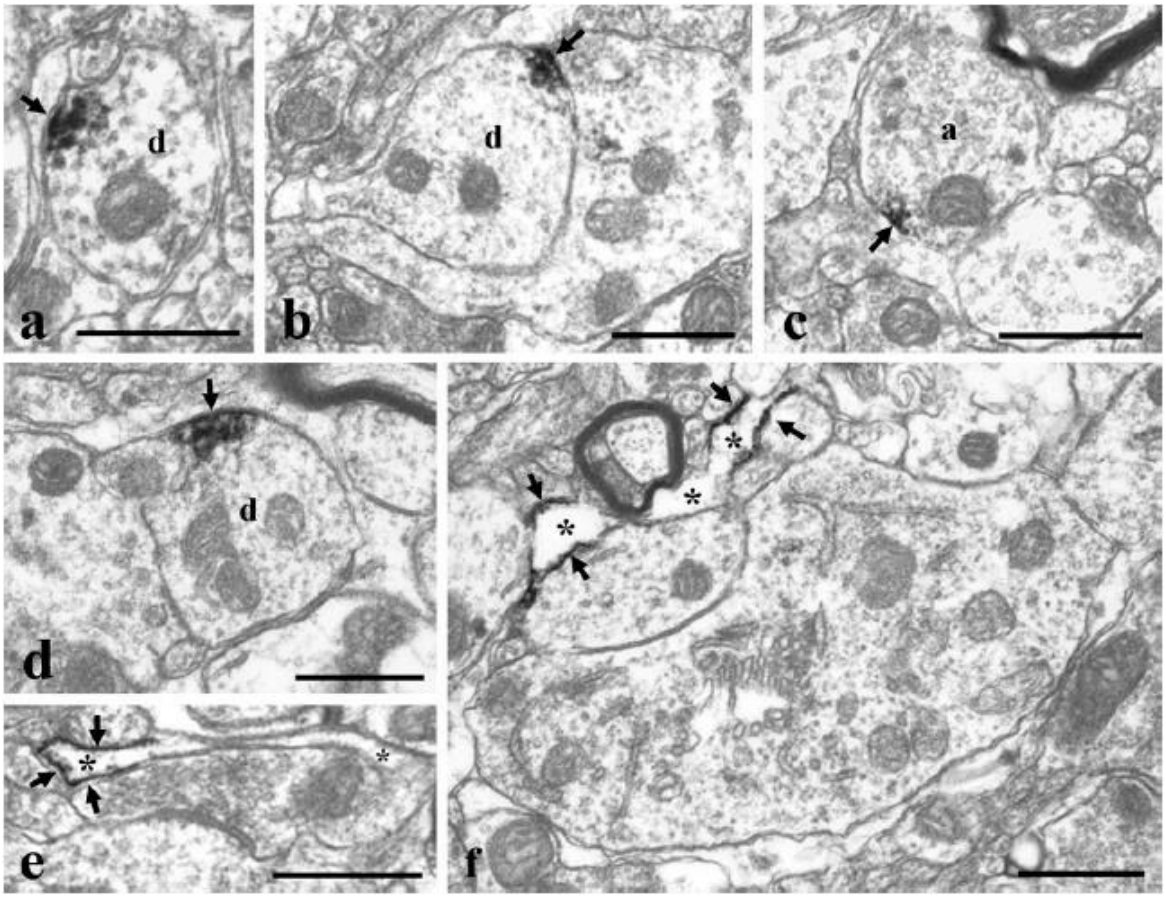

Fig. 27. Ultrastructural localization of NAPE-PLD immunoreactivity in neurons and glial cells. Electron micrographs of preembedding immunoperoxidase stained sections showing the distribution of NAPEPLD on dendrites (a, b, d), in an axon terminal (c) and in glial profiles (e, f) in laminae I–II of the spinal dorsal horn. Immunoprecipitates labeling NAPE-PLD in dendrites, axon terminal, and glial processes are aligned along the surface membrane. a: Axon terminal immunoreactive for NAPE-PLD, d: postsynaptic dendrite, asterisk: glial profile. Arrows point at immunoperoxidase deposits. Bars: 0.5 μm.

restricted only to a segment of the glial membrane, while the adjacent part of the glial profile was free of labeling (Fig. 27 b, e, f). In the case of DGL-α, immunostained glia-like processes were frequently revealed in close vicinity to synaptic contacts between axon terminals and postsynaptic dendrites immunoreactive for DGL-α (Fig. 26 a, b). In case of NAPE-PLD, however, dendritic segments immunoreactive for the enzyme were never observed in the vicinity of immunoreactive compartments of glia-like processes. Nevertheless, glia-like profiles immunostained for NAPE-PLD were sometimes revealed near to synapses (Fig. 27 e). Unfortunately, we were not able to define whether the detected immunoprecipitates were in astrocytes or microglial cells, since we cannot make any distinction between the profiles of these glial cells in the electron microscope.

6. DISCUSSION

Investigating the cellular distribution of CB1-Rs in laminae I–II of the rat spinal dorsal horn with immunocytochemical methods, we revealed CB1-R-immunoreactive puncta exclusively on axon terminals and glial cells. Studying the localization of CB1-R on different populations of axon terminals, we found that nearly half of the peptidergic and slightly more than 20% of the non-peptidergic nociceptive primary afferent terminals were positively stained for CB1-R. Besides axon terminals of primary afferents, more than one-third and approximately 20% of the axon terminals of putative glutamatergic and GABAergic spinal interneurons were also immunoreactive for CB1-R, respectively. In addition to axonal expression, we also revealed a strong CB1-R immunostaining on glial cells. Almost half of the astrocytic and nearly 80% of microglial profiles was immunolabelled for CB1-R.

We also investigated the distribution of DGL-α and NAPE-PLD, enzymes involved in synthesizing the endocannabinoid ligands 2-AG and anandamide, respectively, in the superficial spinal dorsal horn of rats. Postsynaptic dendrites displayed strong immunolabeling for both enzymes, but positive staining was revealed only occasionally in axon terminals. Immunolabeling for DGL-a in dendrites was always revealed at membrane compartments adjacent to synapses. Dendritic membrane segments immunolabeled for NAPE-PLD, however, were never found to be associated with synapses. In addition to dendritic expression, both enzymes showed a remarkably strong expression on astrocytes and microglial cells.

6.1. CB1 receptors on central axon terminals of nociceptive primary afferents

The localization of CB1-Rs in central and peripheral neurons that are implicated in nociceptive processing (Herkenham et al., 1991; Tsou et al., 1998) and the discovery of putative endogenous cannabinoids (Devane et al., 1992; Di Marzo et al., 1994; Mechoulam et al., 1995; Sugiura et al., 1995) suggested that an important function of the cannabinoid system is to modulate pain. It has been demonstrated that cannabinoids reduce behavioral responses to noxious stimuli (Buxbaum, 1972; Bloom et al., 1977; Moss & Johnson, 1980; Lichtman &

Martin, 1991; Fride & Mechoulam, 1993; Smith et al., 1994, 1998; Tsou et al., 1996; Richardson et al., 1997, 1998; Calignano et al., 1998). Furthermore, electrophysiological and neurochemical studies have provided convincing evidence that these anti-nociceptive actions are associated with cannabinoid-induced suppression of noxious stimulus-induced activity of neurons in the spinal cord (Hohmann et al., 1995, 1998, 1999; Meng et al., 1998; Strangman & Walker, 1999; Drew et al., 2000; Harris et al., 2000; Kelly & Chapman, 2001; Pertwee, 2001). The suppression proved to be mediated at least partly by the activation of presynaptic CB1-Rs expressed on central terminals of both C- and Aδ-type nociceptive primary afferents (Martin et al., 1996; Tsou et al., 1996; Morisset et al., 2001), thus decreasing the probability of glutamate release from nociceptive primary afferents (Luo et al., 2002; Wilson & Nicoll, 2002).

Although the presence of functional CB1-Rs on spinal axon terminals of nociceptive primary afferents is well established, how many of them express CB1-R is still a matter of debate. Farquhar-Smith et al. (2000) found that dorsal rhizotomy resulted in only a marked decrease in CB1-R immunoreactivity. In contrast, Hohmann & Herkenham (1999) found that dorsal rhizotomy induced a 50% loss in binding of cannabinoid agonists in laminae I–II. Physiological findings also indicate that a substantial proportion of nociceptive primary afferents respond to endogenous cannabinoid release in the spinal cord. C and Aδ fiber-evoked monosynaptic excitatory postsynaptic currents (EPSCs) can be depressed by CB1-R agonist in nearly one-third and two-thirds of spinal neurons, respectively (Luo et al., 2002).

Our present quantitative evaluation concerning the distribution of CB1-R-immunoreactive puncta in the superficial spinal dorsal horn has shed new light on this issue. On the one hand, we revealed that nearly half of the peptidergic and slightly more than one-fifth of the non-peptidergic nociceptive primary afferent axon terminals express CB1-Rs on their cell membrane. These values are in good agreement with earlier physiological observations and binding studies, but much higher than that suggested by Farquhar-Smith et al. (2000). Although we cannot fully explain the obvious difference between our and Farquhar-Smith's results, it is likely that the possible difference in the sensitivities of CB1-R antibodies utilized in the present and earlier studies may be responsible for the contrasting results. On the other hand, however, it is also essential to note that we were not able to detect CB1-Rs on at least half of the peptidergic and 80% of the nonpeptidergic axon terminals of nociceptive primary afferents, indicating that the magnitude of presynaptic cannabinoid modulation of different nociceptive inputs conducted by

different sets of nociceptive primary afferents may vary over a wide range, from very strong to none. What these types of nociceptive signals are, and what types are not controlled by presynaptic cannabinoid mechanisms will be the subjects of future studies.

6.2. CB1 receptors on axon terminals of spinal neurons

Similar to our present observations, autoradiographic studies in rats treated with neonatal capsaicin suggested that only 16% of spinal CB1-Rs are located on C-fiber afferent endings (Hohmann & Herkenham, 1998). Their anatomical study, in good agreement with our present results, suggested that a substantial proportion of CB1-Rs are likely to be expressed on intrinsic interneurons in the superficial spinal dorsal horn. Reinforcing this notion, expression of CB1-R mRNA (Mailleux & Vanderhaeghen, 1992; Hohmann, 2002) and immunoreactivity for CB1-R (Ong & Mackie, 1999; Ahluwalia et al., 2000; Salio et al., 2002) have been reported in all spinal laminae including the superficial spinal dorsal horn where functional studies demonstrated CB1-R-mediated presynaptic inhibition of both GABAergic (Jennings et al., 2001) and glutamatergic (Morisset & Urban, 2001) transmission.

Although the expression of functional CB1-Rs on spinal neurons is generally accepted, the distribution of CB1-Rs on the somatodendritic and axonal membrane compartments of spinal dorsal horn neurons is still far from completely known. In most morphological studies available, CB1-Rs were revealed within the somata and dendrites of spinal neurons (Ong & Mackie, 1999; Salio et al., 2002). In contrast, the application of endogenous cannabinoids onto spinal cord preparations has been shown to evoke responses that are likely to be mediated by presynaptic CB1-Rs (Jennings et al., 2001; Morisset & Urban, 2001). The present results strongly reinforce the findings obtained from physiological studies. Without obtaining any somato-dendritic staining, we encountered CB1-R-immunoreactive puncta on axon terminals of putative glutamatergic and GABAergic spinal interneurons in large numbers. However, similar to axon terminals of primary afferents only a proportion of axon terminals of intrinsic spinal neurons proved to be immunoreactive for CB1-Rs. We were not able to detect CB1-Rs in more than 60 and 80% of axon terminals of putative glutamatergic and GABAergic neurons, respectively, in laminae I–II of the spinal gray matter, indicating that a pre-synaptic cannabinoid mechanism may modulate only some of the excitatory and inhibitory interactions among spinal neurons. This conclusion appears to be well supported by the present results, although the proportion of CB1-R

expressing and non-expressing axon terminals of putative glutamatergic spinal neurons may have been slightly miscalculated as some of the VGLUT2-immunoreactive boutons may represent axon terminals of primary afferents (Li et al., 2003; Todd et al., 2003).

6.3. CB1 receptors on glial cells

It has recently become generally accepted that there are bidirectional communication pathways between glial cells and neurons in the central nervous system (Araque et al., 2001; Nedergaard et al., 2003; Haydon & Carmignoto, 2006). Endocannabinoid-mediated neuron–astrocyte as well as neuron–microglial cell signaling has been reported (Cabral & Marciano-Cabral, 2005; Navarrete & Araque, 2008). For instance, Navarrete & Araque (2008) demonstrated that hippocampal astrocytes express CB1-Rs, activation of which lead to phospholipase C-dependent Ca^{2+} mobilization from internal stores. The increased Ca^{2+} level stimulates glutamate release from the astrocytes that activates NMDA receptors in pyramidal neurons. CB1-Rs expressed by microglial cells in the cerebral cortex also appear to be functionally relevant. They have been implicated as linked to the modulation of chemokine and cytokine expression in the central nervous system (Cabral & Marciano-Cabral, 2005). In addition to telencephalic structures (Moldrich & Wenger, 2000; Rodriguez et al., 2001), the expression of CB1-Rs by astrocytes has also been demonstrated in the superficial spinal dorsal horn (Salio et al., 2002).

In agreement with previous studies, here we demonstrated that half of the astrocytic and 80% of microglial profiles express CB1-Rs in laminae I–II of the spinal dorsal horn. There is general agreement that glial cells in the spinal dorsal horn can powerfully control pain when they are activated to produce various pain mediators (Suter et al., 2007; Milligan & Watkins, 2009). Although the significance of glial CB1-Rs in spinal nociceptive information and pain processing is far from being understood, it is likely that, similar to their reported function in the hippocampus and cerebral cortex, they may modulate chemokine, cytokine or glutamate release, and might also be involved in other signaling mechanisms in the superficial spinal dorsal horn. Nevertheless, the fact that astrocytes and microglial cells express CB1-Rs in the superficial spinal dorsal horn must be considered when interpreting the cellular basis of the effects of cannabinoids on pain behavior.

6.4. DGL-α and NAPE-PLD in axon terminals

We found only occasional immunolabeling for DGL-α in axon terminals of multiple origins in the superficial spinal dorsal horn. This observation is in good agreement with the results of recent morphological studies confirming that DGL-α is primarily localized in postsynaptic dendrites that face CB1-R expressing terminals (Katona et al., 2006; Nyilas et al., 2009; Suarez et al., 2008; Yoshida et al., 2006).

Our present findings concerning the scanty appearance of NAPE-PLD in axon terminals, however, do not harmonize so well with earlier reports. Authors of some recent articles noted that in higher brain centers NAPE-PLD is concentrated presynaptically in several types of excitatory axon terminals, where it is localized predominantly on the intracellular membrane cisternae of axonal calcium stores (Egertova et al., 2008; Nyilas et al., 2008; Okamoto et al., 2007). The expression of NAPE-PLD in the cell bodies of primary sensory neurons within dorsal root ganglia (DRG) has also been reported (Nagy et al., 2009; van der Stelt et al., 2005). In contrast to this, we observed unexpectedly low levels of NAPE-PLD immunolabeling in axon terminals in the superficial spinal dorsal horn. This finding suggests that the NAPE-PLD protein is transported from the perikarya of DRG and spinal neurons to their spinal axon terminals in such a limited amount that it is below the threshold of immunocytochemical detection, indicating that the synthesis of anandamide (or other acyl amines) in axon terminals of the dorsal horn by NAPE-PLD may not be very prominent.

6.5. Differential distribution of DGL-α and NAPE-PLD in dendrites

There is general agreement in the literature that 2-AG is released from postsynaptic neurons in an activity dependent manner, travels retrogradely through the synaptic cleft, engages presynaptic CB1-Rs, which then suppress neurotransmitter release from glutamatergic axon terminals (Kreitzer and Regehr, 2001; Maejima et al., 2001; Ohno-Shosaku et al., 2001; Piomelli, 2003). Variations in this basic scheme accounts for numerous forms of short- and long-term synaptic plasticity and activity-dependent modifications of neuronal functions in the central nervous system (Chevaleyre et al., 2006; Marinelli et al., 2008; Wilson and Nicoll, 2001, 2002; Yoshida et al., 2006). Our present results concerning the perisynaptic dendritic distribution of DGL-α are fully consistent with these previous findings.

In contrast to the well-established distribution and functional properties of 2-AG-mediated retrograde signaling, the molecular architecture underlying the synthetic side of the anandamide-related endocannabinoid system remains largely unknown, although endogenous anandamide has often been implicated in various behaviors, such as emotion, learning, or pain (for review see Kano et al., 2009). In addition, even the sparsely available data addressing the organization of anandamide-related molecular machineries are controversial. As mentioned earlier, most authors have found that NAPE-PLD is concentrated presynaptically in several types of excitatory axon terminals (Egertova et al., 2008; Nyilas et al., 2008; Okamoto et al., 2007). Others, however, argue in favor of a somatodendritic localization of NAPE-PLD (Cristino et al., 2008). Our present findings clearly support the idea of dendritic localization of NAPE-PLD in the superficial spinal dorsal horn.

6.6. DGL-α and NAPE-PLD in glial cells

The expression of functional CB1-Rs by astrocytes and microglial cells has been reported (Navarrete and Araque, 2008; Rodriguez et al., 2001; Salio et al., 2002; Walter and Stella, 2003; Walter et al., 2002, 2003, 2004). It has also been demonstrated that astrocytes and microglial cells have the potential to produce 2-AG and anandamide and thus can communicate with neighboring neurons through endocannabinoid signaling (Ahluwalia et al., 2003; Carrier et al., 2004; Marsicano et al., 2003, Walter and Stella, 2003; Stella and Piomelli, 2001; Walter et al., 2002, 2003). Endocannabinoid mediated astrocyte-neuron as well as microglial cell-neuron signaling has indeed been reported (Cabral and Marciano-Cabral, 2005; Navarrete and Araque, 2008). Our present results demonstrating an abundant expression of DGL-α and NAPE-PLD in both astrocytes and microglial cells provide further evidence for possible communication pathways between glial cells and neurons, as well as between glial cells (Araque et al., 2001; Haydon and Camignoto, 2006; Nedergaard et al., 2003) in the spinal dorsal horn.

6.7. A proposed scheme for the endocannabinoid mechanisms in the superficial spinal dorsal horn

In the superficial spinal dorsal horn, the primary activation of neurons in laminae I–II arises from nociceptive primary afferents, which is necessary to induce the activity dependent endocannabinoid mobilization Spinal neurons activated by glutamatergic nociceptive primary afferent inputs may release 2-AG from perisynaptic and anandamide from extrasynaptic dendritic membrane compartments (Fig. 28).

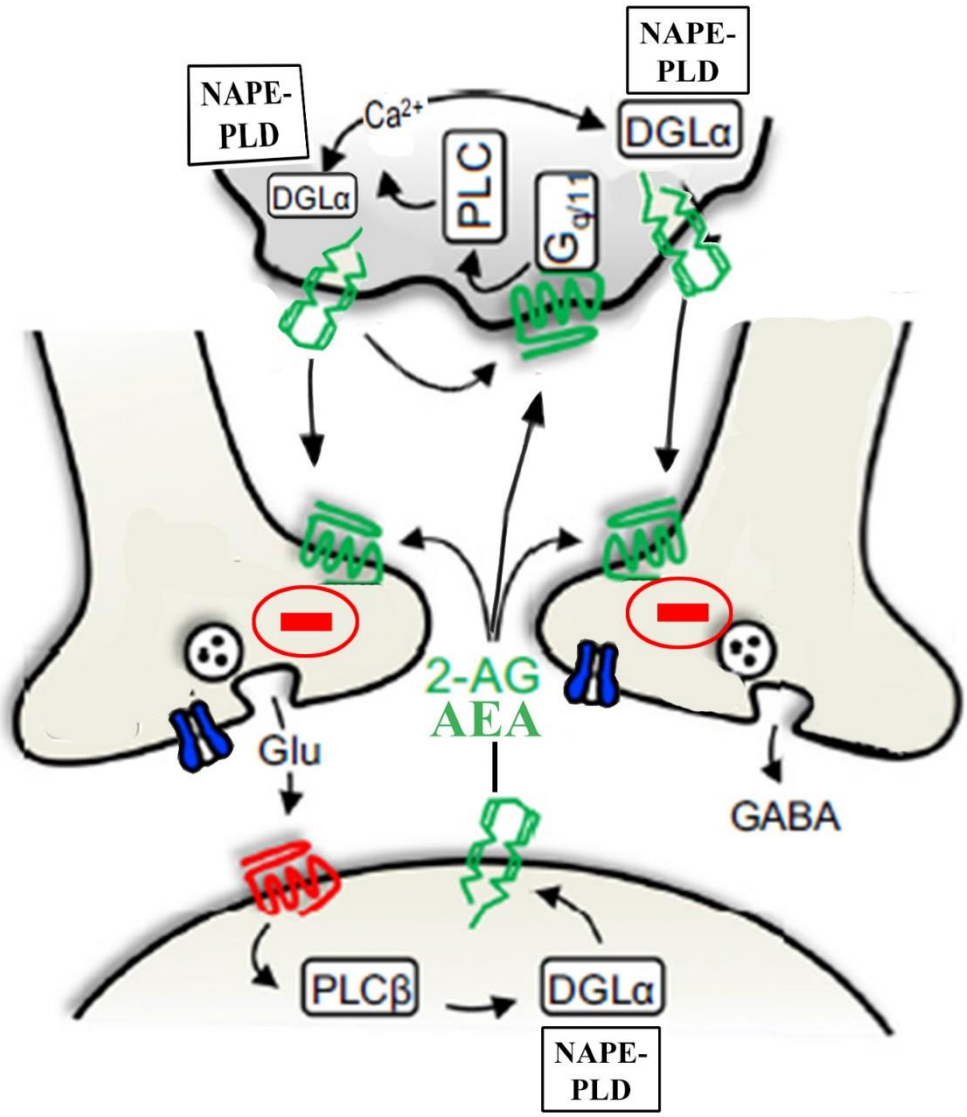

Fig. 28. Molecular organization of the endocannabinoid system in the spinal dorsal horn. Proposed scheme based on our results. (Castillo et al, 2013, modified)

The released endocannabinoids may diffuse out from their site of mobilization and activate CB1-Rs on axon terminals of primary afferents as well as spinal interneurons resulting in temporary impairment of neurotransmitter release from the CB1-R expressing axon terminals. The endocannabinoid-induced decrease in the probability of neurotransmission either from primary afferents or intrinsic spinal neurons may deeply influence the function of the spinal pain processing neural network.

In addition to neurons, astrocytes and microglial cells also express CB1-Rs, which may also be activated by the postsynaptically released endogenous cannabinoids resulting in phospholipase C-dependent Ca^{2+} mobilization from cytoplasmic stores (Beltramo and Piomelli, 2000; Dinh et al., 2002; Navarrete and Araque, 2008; Stella and Piomelli, 2001; Witting et al., 2004). In turn, the increased Ca^{2+} level may activate DGL-α and NAPE-PLD resulting in the release of 2-AG and anandamide from glial cells (Fig.28). The released endocannabinoids may diffuse out and, together with 2-AG and anandamide released by dendrites, may act on neural CB1-Rs affecting functional properties of spinal neurons remote from their site of release (Bisogno et al., 1999). Alternatively, $G_{q/11}$-linked GPCRs expressed on astrocytes and microglia may also drive glial endocannabinoid production.

Although the way how the glial endocannabinoid system contributes to nociceptive functions remains to be elucidated, the fact that astrocytes and microglial cells express functional CB1-Rs, DGL-a and NAPE-PLD must be considered in the interpretation of effects of cannabinoids on spinal pain processing; especially in chronic pain when the number and activity of microglial cells and astrocytes are substantially increased (Cao and Zhang, 2008; Graeber, 2010; Scholz and Woolf, 2007).

7. SUMMARY

A long line of experimental evidence indicates that endogenous cannabinoid mechanisms play important roles in nociceptive information processing in various areas of the nervous system including the spinal cord. In our experiments, using immunocytochemical methods at the light and electron microscopic levels, we investigated the cellular distribution of type-1 cannabinoid receptor (CB1-R), and the two major endocannabinoid-synthesizing enzymes, diacylglycerol lipase alpha (DGL-α) and N-acylphosphatidylethanolamine-specific phospholipase D (NAPE-PLD) in laminae I and II of the rodent spinal dorsal horn.

Axonal varicosities revealed a strong immunoreactivity for CB1-R, but no CB1-R expression was observed on dendrites and perikarya of neurons. Investigating the co-localization of CB1-R with markers of peptidergic and non-peptidergic primary afferents, and axon terminals of putative glutamatergic and GABAergic spinal neurons we found that nearly half of the peptidergic (immunoreactive for calcitonin gene-related peptide) and more than 20% of the non-peptidergic (binding isolectin B4) nociceptive primary afferents, more than one third and approximately 20% of the axon terminals of putative glutamatergic (immunoreactive for vesicular glutamate transporter 2) and GABAergic (immunoreactive for glutamic acid decarboxylase; GAD65 and ⁄ or GAD67) spinal interneurons, respectively, were positively stained for CB1-R. In addition to axon terminals, almost half of the astrocytic (immunoreactive for glial fibrillary acidic protein) and nearly 80% of microglial (immunoreactive for CD11b) profiles were also immunolabeled for CB1-R.

In contrast to the abundant axonal distribution of CB-Rs, immunoreactivities for DGL-α and NAPE-PLD were primarily associated with dendrites in the spinal dorsal horn, while axon terminals showed positive labeling only occasionally. However, the dendritic localization of DGL-α and NAPE-PLD showed a remarkably different distribution. DGL-α immunolabeling in dentrites was always revealed at membrane compartments in close vicinity to synapses. In contrast to this, dendritic NAPE-PLD labeling was never observed in association with synaptic contacts. In addition to dendrites, a substantial proportion of astrocytic and microglial profiles were also immunolabeled for both DGL-α and NAPE-PLD. Glial processes immunostained for DGL-α were frequently found near to synapses in which the postsynaptic dendrite was immunoreactive for DGL-α, whereas NAPE-PLD immunoreactivity on glial profiles at the vicinity of synapses was only occasionally observed.

Our results suggest that both neurons and glial cells can synthesize and release 2-AG and anandamide in the superficial spinal dorsal horn. 2-AG can primarily be released by postsynaptic dendrites and glial processes adjacent to synapses, whereas anandamide can predominantly be released from nonsynaptic dendritic and glial compartments. The activity-dependent release of endogenous cannabinoids may activate a complex signaling mechanism in the pain processing spinal neural circuits into which both neurons and glial cells may contribute.

8. REFERENCES

Abadji, V., Lucas-Lenard, J.M., Chin, C., & Kendall, D.A. (1999) Involvement of the carboxyl terminus of the third intracellular loop of the cannabinoid CB1 receptor in constitutive activation of Gs. *Journal of neurochemistry*, **72**, 2032–2038.

Abood, M.E. & Martin, B.R. (1996) Molecular neurobiology of the cannabinoid receptor. *International review of neurobiology*, **39**, 197–221.

Adams, I.B. & Martin, B.R. (1996) Cannabis: pharmacology and toxicology in animals and humans. *Addiction (Abingdon, England)*, **91**, 1585–1614.

Ade, K.K. & Lovinger, D.M. (2007) Anandamide regulates postnatal development of long-term synaptic plasticity in the rat dorsolateral striatum. *The Journal of neuroscience : the official journal of the Society for Neuroscience*, **27**, 2403–2409.

Agarwal, N., Pacher, P., Tegeder, I., Amaya, F., Constantin, C.E., Brenner, G.J., Rubino, T., Michalski, C.W., Marsicano, G., Monory, K., Mackie, K., Marian, C., Batkai, S., Parolaro, D., Fischer, M.J., Reeh, P., Kunos, G., Kress, M., Lutz, B., Woolf, C.J., & Kuner, R. (2007) Cannabinoids mediate analgesia largely via peripheral type 1 cannabinoid receptors in nociceptors. *Nature neuroscience*, **10**, 870–879.

Ahluwalia, J., Urban, L., Bevan, S., & Nagy, I. (2003) Anandamide regulates neuropeptide release from capsaicin-sensitive primary sensory neurons by activating both the cannabinoid 1 receptor and the vanilloid receptor 1 in vitro. *European Journal of Neuroscience*, **17**, 2611–2618.

Ahluwalia, J., Urban, L., Capogna, M., Bevan, S., & Nagy, I. (2000) Cannabinoid 1 receptors are expressed in nociceptive primary sensory neurons. *Neuroscience*, **100**, 685–688.

Araque, A., Carmignoto, G., & Haydon, P.G. (2001) Dynamic signaling between astrocytes and neurons. *Annual review of physiology*, **63**, 795–813.

Ashton, J.C., Friberg, D., Darlington, C.L., & Smith, P.F. (2006) Expression of the cannabinoid CB2 receptor in the rat cerebellum: an immunohistochemical study. *Neuroscience letters*, **396**, 113–116.

Astarita, G., Ahmed, F., & Piomelli, D. (2008) Identification of biosynthetic precursors for the endocannabinoid anandamide in the rat brain. *Journal of lipid research*, **49**, 48–57.

Azad, S.C., Monory, K., Marsicano, G., Cravatt, B.F., Lutz, B., Zieglgänsberger, W., & Rammes, G. (2004) Circuitry for associative plasticity in the amygdala involves endocannabinoid signaling. *The Journal of neuroscience : the official journal of the Society for Neuroscience*, **24**, 9953–9961.

Battista, N., Di Tommaso, M., Bari, M., & Maccarrone, M. (2012) The endocannabinoid system: an overview. *Frontiers in behavioral neuroscience*, **6**, 9.

Bayewitch, M., Avidor-Reiss, T., Levy, R., Barg, J., Mechoulam, R., & Vogel, Z. (1995) The peripheral cannabinoid receptor: adenylate cyclase inhibition and G protein coupling. *FEBS letters*, **375**, 143–147.

Beltramo, M., Bernardini, N., Bertorelli, R., Campanella, M., Nicolussi, E., Fredduzzi, S., & Reggiani, A. (2006) CB2 receptor-mediated antihyperalgesia: possible direct involvement of neural mechanisms. *The European journal of neuroscience*, **23**, 1530–1538.

Beltramo, M. & Piomelli, D. (2000) Carrier-mediated transport and enzymatic hydrolysis of the endogenous cannabinoid 2-arachidonylglycerol. *Neuroreport*, **11**, 1231–1235.

Berridge, M.J., Lipp, P., & Bootman, M.D. (2000) The versatility and universality of calcium signalling. *Nature reviews. Molecular cell biology*, **1**, 11–21.

Best, A.R. & Regehr, W.G. (2008) Serotonin evokes endocannabinoid release and retrogradely suppresses excitatory synapses. *The Journal of neuroscience : the official journal of the Society for Neuroscience*, **28**, 6508–6515.

Bidaut-Russell, M. & Howlett, A.C. (1991) Cannabinoid receptor-regulated cyclic AMP accumulation in the rat striatum. *Journal of neurochemistry*, **57**, 1769–1773.

Bisogno, T., Berrendero, F., Ambrosino, G., Cebeira, M., Ramos, J.A., Fernandez-Ruiz, J.J., & Di Marzo, V. (1999) Brain regional distribution of endocannabinoids: implications for their biosynthesis and biological function. *Biochemical and biophysical research communications*, **256**, 377–380.

Bisogno, T., Howell, F., Williams, G., Minassi, A., Cascio, M.G., Ligresti, A., Matias, I., Schiano-Moriello, A., Paul, P., Williams, E.-J., Gangadharan, U., Hobbs, C., Di Marzo, V., & Doherty, P. (2003) Cloning of the first sn1-DAG lipases points to the spatial and temporal regulation of endocannabinoid signaling in the brain. *The Journal of cell biology*, **163**, 463–468.

Bisogno, T., Ligresti, A., & Di Marzo, V. (2005) The endocannabinoid signalling system: biochemical aspects. *Pharmacology, biochemistry, and behavior*, **81**, 224–238.

Bisogno, T., Maurelli, S., Melck, D., De Petrocellis, L., & Di Marzo, V. (1997) Biosynthesis, uptake, and degradation of anandamide and palmitoylethanolamide in leukocytes. *The Journal of biological chemistry*, **272**, 3315–3323.

Bisogno, T., Melck, D., Bobrov MYu, Gretskaya, N.M., Bezuglov, V. V, De Petrocellis, L., & Di Marzo, V. (2000) N-acyl-dopamines: novel synthetic CB(1) cannabinoid-receptor ligands and inhibitors of anandamide inactivation with cannabimimetic activity in vitro and in vivo. *The Biochemical journal*, **351 Pt 3**, 817–824.

Bisogno, T., Sepe, N., Melck, D., Maurelli, S., De Petrocellis, L., & Di Marzo, V. (1997) Biosynthesis, release and degradation of the novel endogenous cannabimimetic metabolite 2-arachidonoylglycerol in mouse neuroblastoma cells. *The Biochemical journal*, **322 (Pt 2**, 671–677.

Blankman, J.L., Simon, G.M., & Cravatt, B.F. (2007) A comprehensive profile of brain enzymes that hydrolyze the endocannabinoid 2-arachidonoylglycerol. *Chemistry & biology*, **14**, 1347–1356.

Bloom, A.S., Dewey, W.L., Harris, L.S., & Brosius, K.K. (1977) 9-nor-9beta-hydroxyhexahydrocannabinol, a cannabinoid with potent antinociceptive activity: comparisons with morphine. *The Journal of pharmacology and experimental therapeutics*, **200**, 263–270.

Brenowitz, S.D. & Regehr, W.G. (2005) Associative short-term synaptic plasticity mediated by endocannabinoids. *Neuron*, **45**, 419–431.

Brose, N., Betz, A., & Wegmeyer, H. (2004) Divergent and convergent signaling by the diacylglycerol second messenger pathway in mammals. *Current opinion in neurobiology*, **14**, 328–340.

Brown, S.M., Wager-Miller, J., & Mackie, K. (2002) Cloning and molecular characterization of the rat CB2 cannabinoid receptor. *Biochimica et biophysica acta*, **1576**, 255–264.

Buxbaum, D.M. (1972) Analgesic activity of 9 -tetrahydrocannabinol in the rat and mouse. *Psychopharmacologia*, **25**, 275–280.

Cabral, G. a & Marciano-Cabral, F. (2005) Cannabinoid receptors in microglia of the central nervous system: immune functional relevance. *Journal of leukocyte biology*, **78**, 1192–1197.

Calignano, A., La Rana, G., Giuffrida, A., & Piomelli, D. (1998) Control of pain initiation by endogenous cannabinoids. *Nature*, **394**, 277–281.

Cao, H. & Zhang, Y.-Q. (2008) Spinal glial activation contributes to pathological pain states. *Neuroscience and biobehavioral reviews*, **32**, 972–983.

Carlisle, S.J., Marciano-Cabral, F., Staab, A., Ludwick, C., & Cabral, G.A. (2002) Differential expression of the CB2 cannabinoid receptor by rodent macrophages and macrophage-like cells in relation to cell activation. *International immunopharmacology*, **2**, 69–82.

Carrier, E.J., Kearn, C.S., Barkmeier, A.J., Breese, N.M., Yang, W., Nithipatikom, K., Pfister, S.L., Campbell, W.B., & Hillard, C.J. (2004) Cultured rat microglial cells synthesize the endocannabinoid 2-arachidonylglycerol, which increases proliferation via a CB2 receptor-dependent mechanism. *Molecular pharmacology*, **65**, 999–1007.

Chávez, A.E., Chiu, C.Q., & Castillo, P.E. (2010) TRPV1 activation by endogenous anandamide triggers postsynaptic long-term depression in dentate gyrus. *Nature neuroscience*, **13**, 1511–1518.

Chemin, J., Monteil, A., Perez-Reyes, E., Nargeot, J., & Lory, P. (2001) Direct inhibition of T-type calcium channels by the endogenous cannabinoid anandamide. *The EMBO journal*, **20**, 7033–7040.

Chevaleyre, V. & Castillo, P.E. (2003) GABAergic Synapses : A Novel Role of Endocannabinoids in Regulating Excitability **38**, 461–472.

Chevaleyre, V., Heifets, B.D., Kaeser, P.S., Südhof, T.C., Purpura, D.P., & Castillo, P.E. (2007) Endocannabinoid-mediated long-term plasticity requires cAMP/PKA signaling and RIM1alpha. *Neuron*, **54**, 801–812.

Chevaleyre, V., Takahashi, K.A., & Castillo, P.E. (2006) Endocannabinoid-mediated synaptic plasticity in the CNS. *Annual review of neuroscience*, **29**, 37–76.

Craib, S.J., Ellington, H.C., Pertwee, R.G., & Ross, R.A. (2001) A possible role of lipoxygenase in the activation of vanilloid receptors by anandamide in the guinea-pig bronchus. *British journal of pharmacology*, **134**, 30–37.

Cravatt, B.F., Demarest, K., Patricelli, M.P., Bracey, M.H., Giang, D.K., Martin, B.R., & Lichtman, A.H. (2001) Supersensitivity to anandamide and enhanced endogenous cannabinoid signaling in mice lacking fatty acid amide hydrolase. *Proceedings of the National Academy of Sciences of the United States of America*, **98**, 9371–9376.

Cravatt, B.F., Giang, D.K., Mayfield, S.P., Boger, D.L., Lerner, R.A., & Gilula, N.B. (1996) Molecular characterization of an enzyme that degrades neuromodulatory fatty-acid amides. *Nature*, **384**, 83–87.

Cristino, L., Starowicz, K., De Petrocellis, L., Morishita, J., Ueda, N., Guglielmotti, V., & Di Marzo, V. (2008) Immunohistochemical localization of anabolic and catabolic enzymes for anandamide and other putative endovanilloids in the hippocampus and cerebellar cortex of the mouse brain. *Neuroscience*, **151**, 955–968.

De Petrocellis, L., Cascio, M.G., & Di Marzo, V. (2004) The endocannabinoid system: a general view and latest additions. *British journal of pharmacology*, **141**, 765–774.

Deadwyler, S.A., Hampson, R.E., Mu, J., Whyte, A., & Childers, S. (1995) Cannabinoids modulate voltage sensitive potassium A-current in hippocampal neurons via a cAMP-dependent process. *The Journal of pharmacology and experimental therapeutics*, **273**, 734–743.

Devane, W.A., Hanus, L., Breuer, A., Pertwee, R.G., Stevenson, L.A., Griffin, G., Gibson, D., Mandelbaum, A., Etinger, A., & Mechoulam, R. (1992) Isolation and structure of a brain

constituent that binds to the cannabinoid receptor. *Science (New York, N.Y.)*, **258**, 1946–1949.

Di Marzo, V., Breivogel, C.S., Tao, Q., Bridgen, D.T., Razdan, R.K., Zimmer, A.M., Zimmer, A., & Martin, B.R. (2000) Levels, metabolism, and pharmacological activity of anandamide in CB(1) cannabinoid receptor knockout mice: evidence for non-CB(1), non-CB(2) receptor-mediated actions of anandamide in mouse brain. *Journal of neurochemistry*, **75**, 2434–2444.

Di Marzo, V., De Petrocellis, L., Sepe, N., & Buono, A. (1996) Biosynthesis of anandamide and related acylethanolamides in mouse J774 macrophages and N18 neuroblastoma cells. *The Biochemical journal*, **316 (Pt 3**, 977–984.

Di Marzo, V., Fontana, A., Cadas, H., Schinelli, S., Cimino, G., Schwartz, J.C., & Piomelli, D. (1994) Formation and inactivation of endogenous cannabinoid anandamide in central neurons. *Nature*, **372**, 686–691.

Di Marzo, V., Melck, D., Bisogno, T., & De Petrocellis, L. (1998) Endocannabinoids: endogenous cannabinoid receptor ligands with neuromodulatory action. *Trends in neurosciences*, **21**, 521–528.

Dinh, T.P., Carpenter, D., Leslie, F.M., Freund, T.F., Katona, I., Sensi, S.L., Kathuria, S., & Piomelli, D. (2002) Brain monoglyceride lipase participating in endocannabinoid inactivation. *Proceedings of the National Academy of Sciences of the United States of America*, **99**, 10819–10824.

Drew, G.M., Mitchell, V.A., & Vaughan, C.W. (2008) Glutamate spillover modulates GABAergic synaptic transmission in the rat midbrain periaqueductal grey via metabotropic glutamate receptors and endocannabinoid signaling. *The Journal of neuroscience : the official journal of the Society for Neuroscience*, **28**, 808–815.

Drew, L.J., Harris, J., Millns, P.J., Kendall, D.A., & Chapman, V. (2000) Activation of spinal cannabinoid 1 receptors inhibits C-fibre driven hyperexcitable neuronal responses and increases [35S]GTPgammaS binding in the dorsal horn of the spinal cord of noninflamed and inflamed rats. *The European journal of neuroscience*, **12**, 2079–2086.

Edgemond, W.S., Hillard, C.J., Falck, J.R., Kearn, C.S., & Campbell, W.B. (1998) Human platelets and polymorphonuclear leukocytes synthesize oxygenated derivatives of arachidonylethanolamide (anandamide): their affinities for cannabinoid receptors and pathways of inactivation. *Molecular pharmacology*, **54**, 180–188.

Egertová, M., Cravatt, B.. F., & Elphick, M.. R. (2003) Comparative analysis of fatty acid amide hydrolase and cb(1) cannabinoid receptor expression in the mouse brain: evidence of a widespread role for fatty acid amide hydrolase in regulation of endocannabinoid signaling. *Neuroscience*, **119**, 481–496.

Egertová, M. & Elphick, M.R. (2000) Localisation of cannabinoid receptors in the rat brain using antibodies to the intracellular C-terminal tail of CB. *The Journal of comparative neurology*, **422**, 159–171.

Egertová, M., Simon, G.M., Cravatt, B.F., & Elphick, M.R. (2008) Localization of N-acyl phosphatidylethanolamine phospholipase D (NAPE-PLD) expression in mouse brain: A new perspective on N-acylethanolamines as neural signaling molecules. *The Journal of comparative neurology*, **506**, 604–615.

Elphick, M.R. & Egertová, M. (2001) The neurobiology and evolution of cannabinoid signalling. *Philosophical transactions of the Royal Society of London. Series B, Biological sciences*, **356**, 381–408.

Eriksson, N.P., Persson, J.K., Svensson, M., Arvidsson, J., Molander, C., & Aldskogius, H. (1993) A quantitative analysis of the microglial cell reaction in central primary sensory projection territories following peripheral nerve injury in the adult rat. *Experimental brain research. Experimentelle Hirnforschung. Expérimentation cérébrale*, **96**, 19–27.

Farooqui, A.A., Taylor, W.A., & Horrocks, L.A. (1986) Characterization and solubilization of membrane bound diacylglycerol lipases from bovine brain. *The International journal of biochemistry*, **18**, 991–997.

Farquhar-Smith, W.P., Egertová, M., Bradbury, E.J., McMahon, S.B., Rice, a S., & Elphick, M.R. (2000) Cannabinoid CB(1) receptor expression in rat spinal cord. *Molecular and cellular neurosciences*, **15**, 510–521.

Farquhar-smith, W.P., Egertova, M., Bradbury, E.J., Mcmahon, S.B., Rice, A.S.C., Elphick, M.R., & Expression, R. (2000) Cannabinoid CB 1 Receptor Expression in Rat Spinal Cord. *Molecular and Cellular Neuroscience*, **521**, 510 –521.

Feldblum, S., Dumoulin, A., Anoal, M., Sandillon, F., & Privat, A. (1995) Comparative distribution of GAD65 and GAD67 mRNAs and proteins in the rat spinal cord supports a differential regulation of these two glutamate decarboxylases in vivo. *Journal of neuroscience research*, **42**, 742–757.

Felder, C.C., Joyce, K.E., Briley, E.M., Mansouri, J., Mackie, K., Blond, O., Lai, Y., Ma, A.L., & Mitchell, R.L. (1995) Comparison of the pharmacology and signal transduction of the human cannabinoid CB1 and CB2 receptors. *Molecular pharmacology*, **48**, 443–450.

Felder, C.C., Nielsen, A., Briley, E.M., Palkovits, M., Priller, J., Axelrod, J., Nguyen, D.N., Richardson, J.M., Riggin, R.M., Koppel, G.A., Paul, S.M., & Becker, G.W. (1996) Isolation and measurement of the endogenous cannabinoid receptor agonist, anandamide, in brain and peripheral tissues of human and rat. *FEBS letters*, **393**, 231–235.

Foord, S.M., Bonner, T.I., Neubig, R.R., Rosser, E.M., Pin, J.-P., Davenport, A.P., Spedding, M., & Harmar, A.J. (2005) International Union of Pharmacology. XLVI. G protein-coupled receptor list. *Pharmacological reviews*, **57**, 279–288.

Fride, E. & Mechoulam, R. (1993) Pharmacological activity of the cannabinoid receptor agonist, anandamide, a brain constituent. *European journal of pharmacology*, **231**, 313–314.

Fu, J., Bottegoni, G., Sasso, O., Bertorelli, R., Rocchia, W., Masetti, M., Guijarro, A., Lodola, A., Armirotti, A., Garau, G., Bandiera, T., Reggiani, A., Mor, M., Cavalli, A., & Piomelli, D. (2012) A catalytically silent FAAH-1 variant drives anandamide transport in neurons. *Nature neuroscience*, **15**, 64–69.

Fukudome, Y., Ohno-Shosaku, T., Matsui, M., Omori, Y., Fukaya, M., Tsubokawa, H., Taketo, M.M., Watanabe, M., Manabe, T., & Kano, M. (2004) Two distinct classes of muscarinic action on hippocampal inhibitory synapses: M2-mediated direct suppression and M1/M3-mediated indirect suppression through endocannabinoid signalling. *The European journal of neuroscience*, **19**, 2682–2692.

Gao, Y., Vasilyev, D. V, Goncalves, M.B., Howell, F. V, Hobbs, C., Reisenberg, M., Shen, R., Zhang, M.-Y., Strassle, B.W., Lu, P., Mark, L., Piesla, M.J., Deng, K., Kouranova, E. V, Ring, R.H., Whiteside, G.T., Bates, B., Walsh, F.S., Williams, G., Pangalos, M.N., Samad, T. a, & Doherty, P. (2010) Loss of retrograde endocannabinoid signaling and reduced adult neurogenesis in diacylglycerol lipase knock-out mice. *The Journal of neuroscience : the official journal of the Society for Neuroscience*, **30**, 2017–2024.

Gaoni, Y., Mechoulam, R. (1964) Isolation, structure, and partial synthesis of an active constituent of hashish. *Journal of the American Chemical Society*, **86**, 1646–1647.

Garrison, C.J., Dougherty, P.M., Kajander, K.C., & Carlton, S.M. (1991) Staining of glial fibrillary acidic protein (GFAP) in lumbar spinal cord increases following a sciatic nerve constriction injury. *Brain research*, **565**, 1–7.

Gebremedhin, D., Lange, A.R., Campbell, W.B., Hillard, C.J., & Harder, D.R. (1999) Cannabinoid CB1 receptor of cat cerebral arterial muscle functions to inhibit L-type Ca2+ channel current. *The American journal of physiology*, **276**, H2085–93.

Gerdeman, G.L. & Lovinger, D.M. (2003) Emerging roles for endocannabinoids in long-term synaptic plasticity. *British journal of pharmacology*, **140**, 781–789.

Giang, D.K. & Cravatt, B.F. (1997) Molecular characterization of human and mouse fatty acid amide hydrolases. *Proceedings of the National Academy of Sciences of the United States of America*, **94**, 2238–2242.

Glass, M. & Felder, C.C. (1997) Concurrent stimulation of cannabinoid CB1 and dopamine D2 receptors augments cAMP accumulation in striatal neurons: evidence for a Gs linkage to the

CB1 receptor. *The Journal of neuroscience : the official journal of the Society for Neuroscience*, **17**, 5327–5333.

Gobbi, G., Bambico, F.R., Mangieri, R., Bortolato, M., Campolongo, P., Solinas, M., Cassano, T., Morgese, M.G., Debonnel, G., Duranti, A., Tontini, A., Tarzia, G., Mor, M., Trezza, V., Goldberg, S.R., Cuomo, V., & Piomelli, D. (2005) Antidepressant-like activity and modulation of brain monoaminergic transmission by blockade of anandamide hydrolysis. *Proceedings of the National Academy of Sciences of the United States of America*, **102**, 18620–18625.

Gómez-Ruiz, M., Hernández, M., de Miguel, R., & Ramos, JA. (2007) An overview on the biochemistry of the endocannabinoid system. *Molecular Neurobiology*, **36**, 3-14.

Goparaju, S.K., Ueda, N., Taniguchi, K., & Yamamoto, S. (1999) Enzymes of porcine brain hydrolyzing 2-arachidonoylglycerol, an endogenous ligand of cannabinoid receptors. *Biochemical pharmacology*, **57**, 417–423.

Goparaju, S.K., Ueda, N., Yamaguchi, H., & Yamamoto, S. (1998) Anandamide amidohydrolase reacting with 2-arachidonoylglycerol, another cannabinoid receptor ligand. *FEBS letters*, **422**, 69–73.

Graeber, M.B. (2010) Changing face of microglia. *Science (New York, N.Y.)*, **330**, 783–788.

Griffin, G., Tao, Q., & Abood, M.E. (2000) Cloning and pharmacological characterization of the rat CB(2) cannabinoid receptor. *The Journal of pharmacology and experimental therapeutics*, **292**, 886–894.

Grimsey, N.L., Goodfellow, C.E., Scotter, E.L., Dowie, M.J., Glass, M., & Graham, E.S. (2008) Specific detection of CB1 receptors; cannabinoid CB1 receptor antibodies are not all created equal! *Journal of neuroscience methods*, **171**, 78–86.

Grueter, B.A., Brasnjo, G., & Malenka, R.C. (2010) Postsynaptic TRPV1 triggers cell type-specific long-term depression in the nucleus accumbens. *Nature neuroscience*, **13**, 1519–1525.

Gulyas, A.I., Cravatt, B.F., Bracey, M.H., Dinh, T.P., Piomelli, D., Boscia, F., & Freund, T.F. (2004) Segregation of two endocannabinoid-hydrolyzing enzymes into pre- and postsynaptic compartments in the rat hippocampus, cerebellum and amygdala. *The European journal of neuroscience*, **20**, 441–458.

Guo, A., Vulchanova, L., Wang, J., Li, X., & Elde, R. (1999) Immunocytochemical localization of the vanilloid receptor 1 (VR1): relationship to neuropeptides, the P2X3 purinoceptor and IB4 binding sites. *The European journal of neuroscience*, **11**, 946–958.

Guo, Y., Wang, H., Okamoto, Y., Ueda, N., Kingsley, P.J., Marnett, L.J., Schmid, H.H.O., Das, S.K., & Dey, S.K. (2005) N-acylphosphatidylethanolamine-hydrolyzing phospholipase D is

an important determinant of uterine anandamide levels during implantation. *The Journal of biological chemistry*, **280**, 23429–23432.

Hanus, L., Abu-Lafi, S., Fride, E., Breuer, A., Vogel, Z., Shalev, D.E., Kustanovich, I., & Mechoulam, R. (2001) 2-arachidonyl glyceryl ether, an endogenous agonist of the cannabinoid CB1 receptor. *Proceedings of the National Academy of Sciences of the United States of America*, **98**, 3662–3665.

Harris, J., Drew, L.J., & Chapman, V. (2000) Spinal anandamide inhibits nociceptive transmission via cannabinoid receptor activation in vivo. *Neuroreport*, **11**, 2817–2819.

Hashimotodani, Y., Ohno-Shosaku, T., Maejima, T., Fukami, K., & Kano, M. (2008) Pharmacological evidence for the involvement of diacylglycerol lipase in depolarization-induced endocanabinoid release. *Neuropharmacology*, **54**, 58–67.

Hashimotodani, Y., Ohno-Shosaku, T., Tsubokawa, H., Ogata, H., Emoto, K., Maejima, T., Araishi, K., Shin, H.-S., & Kano, M. (2005) Phospholipase Cbeta serves as a coincidence detector through its Ca2+ dependency for triggering retrograde endocannabinoid signal. *Neuron*, **45**, 257–268.

Haydon, P.G. & Carmignoto, G. (2006) Astrocyte control of synaptic transmission and neurovascular coupling. *Physiological reviews*, **86**, 1009–1031.

Heifets, B.D. & Castillo, P.E. (2009) Endocannabinoid signaling and long-term synaptic plasticity. *Annual review of physiology*, **71**, 283–306.

Herkenham, M., Lynn, A.B., Johnson, M.R., Melvin, L.S., De Costa, B.R., & Rice, K.C. (1991) Characterization and localization of cannabinoid receptors in rat brain: a quantitative in vitro autoradiographic study. *The Journal of neuroscience : the official journal of the Society for Neuroscience*, **11**, 563–583.

Herkenham, M., Lynn, A.B., Little, M.D., Johnson, M.R., Melvin, L.S., De Costa, B.R., & Rice, K.C. (1990) Cannabinoid receptor localization in brain. *Proceedings of the National Academy of Sciences of the United States of America*, **87**, 1932–1936.

Herrera, B., Carracedo, A., Diez-Zaera, M., Gómez del Pulgar, T., Guzmán, M., & Velasco, G. (2006) The CB2 cannabinoid receptor signals apoptosis via ceramide-dependent activation of the mitochondrial intrinsic pathway. *Experimental cell research*, **312**, 2121–2131.

Herrera, B., Carracedo, A., Diez-Zaera, M., Guzmán, M., & Velasco, G. (2005) p38 MAPK is involved in CB2 receptor-induced apoptosis of human leukaemia cells. *FEBS letters*, **579**, 5084–5088.

Hillard, C.J., Wilkison, D.M., Edgemond, W.S., & Campbell, W.B. (1995) Characterization of the kinetics and distribution of N-arachidonylethanolamine (anandamide) hydrolysis by rat brain. *Biochimica et biophysica acta*, **1257**, 249–256.

Hohmann, A.G., Briley, E.M., & Herkenham, M. (1999) Pre- and postsynaptic distribution of cannabinoid and mu opioid receptors in rat spinal cord. *Brain research*, **822**, 17–25.

Hohmann, A.G. & Herkenham, M. (1998) Regulation of cannabinoid and mu opioid receptors in rat lumbar spinal cord following neonatal capsaicin treatment. *Neuroscience letters*, **252**, 13–16.

Hohmann, A.G. & Herkenham, M. (1999) Localization of central cannabinoid CB1 receptor messenger RNA in neuronal subpopulations of rat dorsal root ganglia: a double-label in situ hybridization study. *Neuroscience*, **90**, 923–931.

Hohmann, A.G., Martin, W.J., Tsou, K., & Walker, J.M. (1995) Inhibition of noxious stimulus-evoked activity of spinal cord dorsal horn neurons by the cannabinoid WIN 55,212-2. *Life sciences*, **56**, 2111–2118.

Hohmann, A.G. & Program, B. (2002) Spinal and peripheral mechanisms of cannabinoid antinociception: behavioral, neurophysiological and neuroanatomical perspectives. *Chemistry and physics of lipids*, **121**, 173–190.

Hohmann, A.G., Suplita, R.L., Bolton, N.M., Neely, M.H., Fegley, D., Mangieri, R., Krey, J.F., Walker, J.M., Holmes, P. V, Crystal, J.D., Duranti, A., Tontini, A., Mor, M., Tarzia, G., & Piomelli, D. (2005) An endocannabinoid mechanism for stress-induced analgesia. *Nature*, **435**, 1108–1112.

Hohmann, A.G., Tsou, K., & Walker, J.M. (1998) Cannabinoid modulation of wide dynamic range neurons in the lumbar dorsal horn of the rat by spinally administered WIN55,212-2. *Neuroscience letters*, **257**, 119–122.

Howlett, A.C. (1985) Cannabinoid inhibition of adenylate cyclase. Biochemistry of the response in neuroblastoma cell membranes. *Molecular pharmacology*, **27**, 429–436.

Howlett, A.C. (2002) The cannabinoid receptors. *Prostaglandins & other lipid mediators*, **68-69**, 619–631.

Howlett, A.C. (2005) Cannabinoid receptor signaling. *Handbook of experimental pharmacology*, 53–79.

Howlett, A.C. & Fleming, R.M. (1984) Cannabinoid inhibition of adenylate cyclase. Pharmacology of the response in neuroblastoma cell membranes. *Molecular pharmacology*, **26**, 532–538.

Howlett, A.C., Qualy, J.M., & Khachatrian, L.L. (1986) Involvement of Gi in the inhibition of adenylate cyclase by cannabimimetic drugs. *Molecular pharmacology*, **29**, 307–313.

Huang, S.M., Strangman, N.M., & Walker, J.M. (1999) Liquid chromatographic-mass spectrometric measurement of the endogenous cannabinoid 2-arachidonylglycerol in the

spinal cord and peripheral nervous system. *Zhongguo yao li xue bao = Acta pharmacologica Sinica*, **20**, 1098–1102.

Jennings, E.A., Vaughan, C.W., & Christie, M.J. (2001) Cannabinoid actions on rat superficial medullary dorsal horn neurons in vitro. *The Journal of physiology*, **534**, 805–812.

Jin, X.-H., Uyama, T., Wang, J., Okamoto, Y., Tonai, T., & Ueda, N. (2009) cDNA cloning and characterization of human and mouse Ca(2+)-independent phosphatidylethanolamine N-acyltransferases. *Biochimica et biophysica acta*, **1791**, 32–38.

Jung, K.-M., Astarita, G., Thongkham, D., & Piomelli, D. (2011) Diacylglycerol lipase-alpha and -beta control neurite outgrowth in neuro-2a cells through distinct molecular mechanisms. *Molecular pharmacology*, **80**, 60–67.

Kano, M., Ohno-shosaku, T., Hashimotodani, Y., & Uchigashima, M. (2009) Endocannabinoid-Mediated Control of Synaptic Transmission. *Physiological Reviews*, 309–380.

Karlsson, M., Reue, K., Xia, Y.R., Lusis, A.J., Langin, D., Tornqvist, H., & Holm, C. (2001) Exon-intron organization and chromosomal localization of the mouse monoglyceride lipase gene. *Gene*, **272**, 11–18.

Kathuria, S., Gaetani, S., Fegley, D., Valiño, F., Duranti, A., Tontini, A., Mor, M., Tarzia, G., La Rana, G., Calignano, A., Giustino, A., Tattoli, M., Palmery, M., Cuomo, V., & Piomelli, D. (2003) Modulation of anxiety through blockade of anandamide hydrolysis. *Nature medicine*, **9**, 76–81.

Kato, A., Punnakkal, P., Pernía-Andrade, A.J., Von Schoultz, C., Sharopov, S., Nyilas, R., Katona, I., & Zeilhofer, H.U. (2012) Endocannabinoid-dependent plasticity at spinal nociceptor synapses. *The Journal of physiology*, **590**, 4717–4733.

Katona, I., Urbán, G.M., Wallace, M., Ledent, C., Jung, K.-M., Piomelli, D., Mackie, K., & Freund, T.F. (2006) Molecular composition of the endocannabinoid system at glutamatergic synapses. *The Journal of neuroscience : the official journal of the Society for Neuroscience*, **26**, 5628–5637.

Kawamura, Y., Fukaya, M., Maejima, T., Yoshida, T., Miura, E., Watanabe, M., Ohno-Shosaku, T., & Kano, M. (2006) The CB1 cannabinoid receptor is the major cannabinoid receptor at excitatory presynaptic sites in the hippocampus and cerebellum. *The Journal of neuroscience : the official journal of the Society for Neuroscience*, **26**, 2991–3001.

Kelly, S. & Chapman, V. (2001) Selective cannabinoid CB1 receptor activation inhibits spinal nociceptive transmission in vivo. *Journal of neurophysiology*, **86**, 3061–3064.

Kim, J. & Alger, B.E. (2010) Reduction in endocannabinoid tone is a homeostatic mechanism for specific inhibitory synapses. *Nature neuroscience*, **13**, 592–600.

Kozak, K.R., Gupta, R.A., Moody, J.S., Ji, C., Boeglin, W.E., DuBois, R.N., Brash, A.R., & Marnett, L.J. (2002) 15-Lipoxygenase metabolism of 2-arachidonylglycerol. Generation of a peroxisome proliferator-activated receptor alpha agonist. *The Journal of biological chemistry*, **277**, 23278–23286.

Kreitzer, A.C. & Regehr, W.G. (2001) Retrograde inhibition of presynaptic calcium influx by endogenous cannabinoids at excitatory synapses onto Purkinje cells. *Neuron*, **29**, 717–727.

Laemmli, U.K. (1970) Cleavage of structural proteins during the assembly of the head of bacteriophage T4. *Nature*, **227**, 680–685.

Lauckner, J.E., Hille, B., & Mackie, K. (2005) The cannabinoid agonist WIN55,212-2 increases intracellular calcium via CB1 receptor coupling to Gq/11 G proteins. *Proceedings of the National Academy of Sciences of the United States of America*, **102**, 19144–19149.

Lauckner, J.E., Jensen, J.B., Chen, H.-Y., Lu, H.-C., Hille, B., & Mackie, K. (2008) GPR55 is a cannabinoid receptor that increases intracellular calcium and inhibits M current. *Proceedings of the National Academy of Sciences of the United States of America*, **105**, 2699–2704.

Ledent, C., Valverde, O., Cossu, G., Petitet, F., Aubert, J.F., Beslot, F., Böhme, G.A., Imperato, A., Pedrazzini, T., Roques, B.P., Vassart, G., Fratta, W., & Parmentier, M. (1999) Unresponsiveness to cannabinoids and reduced addictive effects of opiates in CB1 receptor knockout mice. *Science (New York, N.Y.)*, **283**, 401–404.

Lenz, R.A., Wagner, J.J., & Alger, B.E. (1998) N- and L-type calcium channel involvement in depolarization-induced suppression of inhibition in rat hippocampal CA1 cells. *The Journal of physiology*, **512 (Pt 1**, 61–73.

Leung, D., Saghatelian, A., Simon, G.M., & Cravatt, B.F. (2006) Inactivation of N-acyl phosphatidylethanolamine phospholipase D reveals multiple mechanisms for the biosynthesis of endocannabinoids. *Biochemistry*, **45**, 4720–4726.

Li, J.-L., Fujiyama, F., Kaneko, T., & Mizuno, N. (2003) Expression of vesicular glutamate transporters, VGluT1 and VGluT2, in axon terminals of nociceptive primary afferent fibers in the superficial layers of the medullary and spinal dorsal horns of the rat. *The Journal of comparative neurology*, **457**, 236–249.

Lichtman, A.H. & Martin, B.R. (1991) Spinal and supraspinal components of cannabinoid-induced antinociception. *The Journal of pharmacology and experimental therapeutics*, **258**, 517–523.

Liu, J., Wang, L., Harvey-White, J., Huang, B.X., Kim, H.-Y., Luquet, S., Palmiter, R.D., Krystal, G., Rai, R., Mahadevan, A., Razdan, R.K., & Kunos, G. (2008) Multiple pathways involved in the biosynthesis of anandamide. *Neuropharmacology*, **54**, 1–7.

Liu, J., Wang, L., Harvey-White, J., Osei-Hyiaman, D., Razdan, R., Gong, Q., Chan, A.C., Zhou, Z., Huang, B.X., Kim, H.-Y., & Kunos, G. (2006) A biosynthetic pathway for anandamide. *Proceedings of the National Academy of Sciences of the United States of America*, **103**, 13345–13350.

Llano, I., Leresche, N., & Marty, A. (1991) Calcium entry increases the sensitivity of cerebellar Purkinje cells to applied GABA and decreases inhibitory synaptic currents. *Neuron*, **6**, 565–574.

Long, J.Z., Nomura, D.K., Vann, R.E., Walentiny, D.M., Booker, L., Jin, X., Burston, J.J., Sim-Selley, L.J., Lichtman, A.H., Wiley, J.L., & Cravatt, B.F. (2009) Dual blockade of FAAH and MAGL identifies behavioral processes regulated by endocannabinoid crosstalk in vivo. *Proceedings of the National Academy of Sciences of the United States of America*, **106**, 20270–20275.

Luo, C., Kumamoto, E., Furue, H., Chen, J., & Yoshimura, M. (2002) Anandamide inhibits excitatory transmission to rat substantia gelatinosa neurones in a manner different from that of capsaicin. *Neuroscience letters*, **321**, 17–20.

Maccarrone, M., Attinà, M., Bari, M., Cartoni, A., Ledent, C., & Finazzi-Agrò, A. (2001) Anandamide degradation and N-acylethanolamines level in wild-type and CB1 cannabinoid receptor knockout mice of different ages. *Journal of neurochemistry*, **78**, 339–348.

Mackie, K., Devane, W.A., & Hille, B. (1993) Anandamide, an endogenous cannabinoid, inhibits calcium currents as a partial agonist in N18 neuroblastoma cells. *Molecular pharmacology*, **44**, 498–503.

Mackie, K. & Hille, B. (1992) Cannabinoids inhibit N-type calcium channels in neuroblastoma-glioma cells. *Proceedings of the National Academy of Sciences of the United States of America*, **89**, 3825–3829.

Mackie, K., Lai, Y., Westenbroek, R., & Mitchell, R. (1995) Cannabinoids activate an inwardly rectifying potassium conductance and inhibit Q-type calcium currents in AtT20 cells transfected with rat brain cannabinoid receptor. *The Journal of neuroscience : the official journal of the Society for Neuroscience*, **15**, 6552–6561.

Mackie, M., Hughes, D.I., Maxwell, D.J., Tillakaratne, N.J.K., & Todd, A.J. (2003) Distribution and colocalisation of glutamate decarboxylase isoforms in the rat spinal cord. *Neuroscience*, **119**, 461–472.

Maejima, T., Hashimoto, K., Yoshida, T., Aiba, a, Kano, M., & Hasimoto, K. (2001) Presynaptic inhibition caused by retrograde signal from metabotropic glutamate to cannabinoid receptors. *Neuron*, **31**, 463–475.

Maejima, T., Oka, S., Hashimotodani, Y., Ohno-shosaku, T., Aiba, A., Wu, D., Waku, K., Sugiura, T., & Kano, M. (2005) Synaptically driven endocannabinoid release requires Ca2+-

assisted metabotropic glutamate receptor subtype 1 to phospholipase Cbeta4 signaling cascade in the cerebellum. *The Journal of neuroscience : the official journal of the Society for Neuroscience*, **25**, 6826–6835.

Mailleux, P. & Vanderhaeghen, J.J. (1992) Distribution of neuronal cannabinoid receptor in the adult rat brain: a comparative receptor binding radioautography and in situ hybridization histochemistry. *Neuroscience*, **48**, 655–668.

Makara, J.K., Mor, M., Fegley, D., Szabó, S.I., Kathuria, S., Astarita, G., Duranti, A., Tontini, A., Tarzia, G., Rivara, S., Freund, T.F., & Piomelli, D. (2005) Selective inhibition of 2-AG hydrolysis enhances endocannabinoid signaling in hippocampus. *Nature neuroscience*, **8**, 1139–1141.

Makriyannis, A., Tian, X., & Guo, J. (2005) How lipophilic cannabinergic ligands reach their receptor sites. *Prostaglandins & other lipid mediators*, **77**, 210–218.

Marinelli, S., Pacioni, S., Bisogno, T., Di Marzo, V., Prince, D. a, Huguenard, J.R., & Bacci, A. (2008) The endocannabinoid 2-arachidonoylglycerol is responsible for the slow self-inhibition in neocortical interneurons. *The Journal of neuroscience : the official journal of the Society for Neuroscience*, **28**, 13532–13541.

Marrs, W.R., Blankman, J.L., Horne, E. a, Thomazeau, A., Lin, Y.H., Coy, J., Bodor, A.L., Muccioli, G.G., Hu, S.S.-J., Woodruff, G., Fung, S., Lafourcade, M., Alexander, J.P., Long, J.Z., Li, W., Xu, C., Möller, T., Mackie, K., Manzoni, O.J., Cravatt, B.F., & Stella, N. (2010) The serine hydrolase ABHD6 controls the accumulation and efficacy of 2-AG at cannabinoid receptors. *Nature neuroscience*, **13**, 951–957.

Marsicano, G., Goodenough, S., Monory, K., Hermann, H., Eder, M., Cannich, A., Azad, S.C., Cascio, M.G., Gutiérrez, S.O., Van der Stelt, M., López-Rodriguez, M.L., Casanova, E., Schütz, G., Zieglgänsberger, W., Di Marzo, V., Behl, C., & Lutz, B. (2003) CB1 cannabinoid receptors and on-demand defense against excitotoxicity. *Science (New York, N.Y.)*, **302**, 84–88.

Martin, D.L., Liu, H., Martin, S.B., & Wu, S.J. (n.d.) Structural features and regulatory properties of the brain glutamate decarboxylases. *Neurochemistry international*, **37**, 111–119.

Mato, S., Lafourcade, M., Robbe, D., Bakiri, Y., & Manzoni, O.J. (2008) Role of the cyclic-AMP/PKA cascade and of P/Q-type Ca++ channels in endocannabinoid-mediated long-term depression in the nucleus accumbens. *Neuropharmacology*, **54**, 87–94.

Matsuda, L.A., Lolait, S.J., Brownstein, M.J., Young, A.C., & Bonner, T.I. (1990) Structure of a cannabinoid receptor and functional expression of the cloned cDNA. *Nature*, **346**, 561–564.

Mátyás, F., Yanovsky, Y., Mackie, K., Kelsch, W., Misgeld, U., & Freund, T.F. (2006) Subcellular localization of type 1 cannabinoid receptors in the rat basal ganglia. *Neuroscience*, **137**, 337–361.

McClung, J.R. & Castro, A.J. (1978) Rexed's laminar scheme as it applies to the rat cervical spinal cord. *Experimental neurology*, **58**, 145–148.

McNeill, D.L., Coggeshall, R.E., & Carlton, S.M. (1988) A light and electron microscopic study of calcitonin gene-related peptide in the spinal cord of the rat. *Experimental neurology*, **99**, 699–708.

Mechoulam, R., Ben-Shabat, S., Hanus, L., Ligumsky, M., Kaminski, N.E., Schatz, A.R., Gopher, A., Almog, S., Martin, B.R., & Compton, D.R. (1995) Identification of an endogenous 2-monoglyceride, present in canine gut, that binds to cannabinoid receptors. *Biochemical pharmacology*, **50**, 83–90.

Melzack, R. & Wall, P.D. (1965) Pain mechanisms: a new theory. *Science (New York, N.Y.)*, **150**, 971–979.

Meng, I.D., Manning, B.H., Martin, W.J., & Fields, H.L. (1998) An analgesia circuit activated by cannabinoids. *Nature*, **395**, 381–383.

Merkel, O., Schmid, P.C., Paltauf, F., & Schmid, H.H.O. (2005) Presence and potential signaling function of N-acylethanolamines and their phospholipid precursors in the yeast Saccharomyces cerevisiae. *Biochimica et biophysica acta*, **1734**, 215–219.

Milligan, E.D. & Watkins, L.R. (2009) Pathological and protective roles of glia in chronic pain. *Nature reviews. Neuroscience*, **10**, 23–36.

Min, R., Testa-Silva, G., Heistek, T.S., Canto, C.B., Lodder, J.C., Bisogno, T., Di Marzo, V., Brussaard, A.B., Burnashev, N., & Mansvelder, H.D. (2010) Diacylglycerol lipase is not involved in depolarization-induced suppression of inhibition at unitary inhibitory connections in mouse hippocampus. *The Journal of neuroscience : the official journal of the Society for Neuroscience*, **30**, 2710–2715.

Molander, C. & Grant, G. (1985) Cutaneous projections from the rat hindlimb foot to the substantia gelatinosa of the spinal cord studied by transganglionic transport of WGA-HRP conjugate. *The Journal of comparative neurology*, **237**, 476–484.

Molander, C. & Grant, G. (1986) Laminar distribution and somatotopic organization of primary afferent fibers from hindlimb nerves in the dorsal horn. A study by transganglionic transport of horseradish peroxidase in the rat. *Neuroscience*, **19**, 297–312.

Molander, C., Hongpaisan, J., Svensson, M., & Aldskogius, H. (1997) Glial cell reactions in the spinal cord after sensory nerve stimulation are associated with axonal injury. *Brain research*, **747**, 122–129.

Molander, C., Xu, Q., & Grant, G. (1984) The cytoarchitectonic organization of the spinal cord in the rat. I. The lower thoracic and lumbosacral cord. *The Journal of comparative neurology*, **230**, 133–141.

Moldrich, G. & Wenger, T. (2000) Localization of the CB1 cannabinoid receptor in the rat brain. An immunohistochemical study. *Peptides*, **21**, 1735–1742.

Morishita, J., Okamoto, Y., Tsuboi, K., Ueno, M., Sakamoto, H., Maekawa, N., & Ueda, N. (2005) Regional distribution and age-dependent expression of N-acylphosphatidylethanolamine-hydrolyzing phospholipase D in rat brain. *Journal of neurochemistry*, **94**, 753–762.

Morisset, V. & Urban, L. (2001) Cannabinoid-induced presynaptic inhibition of glutamatergic EPSCs in substantia gelatinosa neurons of the rat spinal cord. *Journal of neurophysiology*, **86**, 40–48.

Moss, D.E. & Johnson, R.L. (1980) Tonic analgesic effects of delta 9-tetrahydrocannabinol as measured with the formalin test. *European journal of pharmacology*, **61**, 313–315.

Muccioli, G.G. (2010) Endocannabinoid biosynthesis and inactivation, from simple to complex. *Drug discovery today*, **15**, 474–483.

Munro, S., Thomas, K.L., & Abu-Shaar, M. (1993) Molecular characterization of a peripheral receptor for cannabinoids. *Nature*, **365**, 61–65.

Nagy, B., Fedonidis, C., Photiou, A., Wahba, J., Paule, C.C., Ma, D., Buluwela, L., & Nagy, I. (2009) Capsaicin-sensitive primary sensory neurons in the mouse express N-Acyl phosphatidylethanolamine phospholipase D. *Neuroscience*, **161**, 572–577.

Nasu, F. (1999) Analysis of calcitonin gene-related peptide (CGRP)-containing nerve fibres in the rat spinal cord using light and electron microscopy. *Journal of electron microscopy*, **48**, 267–275.

Navarrete, M. & Araque, A. (2008) Endocannabinoids mediate neuron-astrocyte communication. *Neuron*, **57**, 883–893.

Nedergaard, M., Ransom, B., & Goldman, S. a. (2003) New roles for astrocytes: redefining the functional architecture of the brain. *Trends in neurosciences*, **26**, 523–530.

Netzeband, J.G., Conroy, S.M., Parsons, K.L., & Gruol, D.L. (1999) Cannabinoids enhance NMDA-elicited Ca2+ signals in cerebellar granule neurons in culture. *The Journal of neuroscience : the official journal of the Society for Neuroscience*, **19**, 8765–8777.

Nyilas, R., Dudok, B., Urbán, G.M., Mackie, K., Watanabe, M., Cravatt, B.F., Freund, T.F., & Katona, I. (2008) Enzymatic machinery for endocannabinoid biosynthesis associated with calcium stores in glutamatergic axon terminals. *The Journal of neuroscience : the official journal of the Society for Neuroscience*, **28**, 1058–1063.

Nyilas, R., Gregg, L.C., Mackie, K., Watanabe, M., Zimmer, A., Hohmann, A.G., & Katona, I. (2009) Molecular architecture of endocannabinoid signaling at nociceptive synapses mediating analgesia. *The European journal of neuroscience*, **29**, 1964–1978.

Ohno-Shosaku, T., Hashimotodani, Y., Ano, M., Takeda, S., Tsubokawa, H., & Kano, M. (2007) Endocannabinoid signalling triggered by NMDA receptor-mediated calcium entry into rat hippocampal neurons. *The Journal of physiology*, **584**, 407–418.

Ohno-shosaku, T., Maejima, T., & Kano, M. (2001) Endogenous cannabinoids mediate retrograde signals from depolarized postsynaptic neurons to presynaptic terminals. *Neuron*, **29**, 729–738.

Ohno-Shosaku, T., Shosaku, J., Tsubokawa, H., & Kano, M. (2002) Cooperative endocannabinoid production by neuronal depolarization and group I metabotropic glutamate receptor activation. *The European journal of neuroscience*, **15**, 953–961.

Okamoto, Y., Morishita, J., Tsuboi, K., Tonai, T., Ueda, N., & Hospital, N.Z. (2004) Molecular characterization of a phospholipase D generating anandamide and its congeners. *The Journal of biological chemistry*, **279**, 5298–5305.

Okamoto, Y., Morishita, J., Wang, J., Schmid, P.C., Krebsbach, R.J., Schmid, H.H.O., & Ueda, N. (2005) Mammalian cells stably overexpressing N-acylphosphatidylethanolamine-hydrolysing phospholipase D exhibit significantly decreased levels of N-acylphosphatidylethanolamines. *The Biochemical journal*, **389**, 241–247.

Okamoto, Y., Tsuboi, K., & Ueda, N. (2009) Enzymatic formation of anandamide. *Vitamins and hormones*, **81**, 1–24.

Okamoto, Y., Wang, J., Morishita, J., & Ueda, N. (2007) Biosynthetic pathways of the endocannabinoid anandamide. *Chemistry & biodiversity*, **4**, 1842–1857.

Oliveira, A.L.R., Hydling, F., Olsson, E., Shi, T., Edwards, R.H., Fujiyama, F., Kaneko, T., Hökfelt, T., Cullheim, S., & Meister, B. (2003) Cellular localization of three vesicular glutamate transporter mRNAs and proteins in rat spinal cord and dorsal root ganglia. *Synapse (New York, N.Y.)*, **50**, 117–129.

Onaivi, E.S., Ishiguro, H., Gong, J.-P., Patel, S., Perchuk, A., Meozzi, P.A., Myers, L., Mora, Z., Tagliaferro, P., Gardner, E., Brusco, A., Akinshola, B.E., Liu, Q.-R., Hope, B., Iwasaki, S., Arinami, T., Teasenfitz, L., & Uhl, G.R. (2006) Discovery of the presence and functional expression of cannabinoid CB2 receptors in brain. *Annals of the New York Academy of Sciences*, **1074**, 514–536.

Ong, W.Y. & Mackie, K. (1999) A light and electron microscopic study of the CB1 cannabinoid receptor in the primate spinal cord. *Journal of neurocytology*, **28**, 39–45.

Pacher, P., Bátkai, S., & Kunos, G. (2006) The endocannabinoid system as an emerging target of pharmacotherapy. *Pharmacological reviews*, **58**, 389–462.

Pertwee, R.G. (2001) Cannabinoid receptors and pain. *Progress in neurobiology*, **63**, 569–611.

Pertwee, R.G. (2007) GPR55: a new member of the cannabinoid receptor clan? *British journal of pharmacology*, **152**, 984–986.

Pertwee, R.G., Howlett, A.C., Abood, M.E., Alexander, S.P.H., Di Marzo, V., Elphick, M.R., Greasley, P.J., Hansen, H.S., Kunos, G., Mackie, K., Mechoulam, R., & Ross, R.A. (2010) International Union of Basic and Clinical Pharmacology. LXXIX. Cannabinoid receptors and their ligands: beyond CB_1 and CB_2. *Pharmacological reviews*, **62**, 588–631.

Pinto, J.C., Potié, F., Rice, K.C., Boring, D., Johnson, M.R., Evans, D.M., Wilken, G.H., Cantrell, C.H., & Howlett, A.C. (1994) Cannabinoid receptor binding and agonist activity of amides and esters of arachidonic acid. *Molecular pharmacology*, **46**, 516–522.

Piomelli, D. (2003) The molecular logic of endocannabinoid signalling. *Nature reviews. Neuroscience*, **4**, 873–884.

Pitler, T.A. & Alger, B.E. (1992) Postsynaptic spike firing reduces synaptic GABAA responses in hippocampal pyramidal cells. *The Journal of neuroscience : the official journal of the Society for Neuroscience*, **12**, 4122–4132.

Porter, A.C., Sauer, J.-M., Knierman, M.D., Becker, G.W., Berna, M.J., Bao, J., Nomikos, G.G., Carter, P., Bymaster, F.P., Leese, A.B., & Felder, C.C. (2002) Characterization of a novel endocannabinoid, virodhamine, with antagonist activity at the CB1 receptor. *The Journal of pharmacology and experimental therapeutics*, **301**, 1020–1024.

Richardson, J.D., Aanonsen, L., & Hargreaves, K.M. (1998) Antihyperalgesic effects of spinal cannabinoids. *European journal of pharmacology*, **345**, 145–153.

Ribeiro da Silva A, De Korninck Y. 2009. Morphological and neuro- chemical organization of the spinal dorsal horn. In: Basbaum AI, Bushnell MC, editors *Science of pain*. Oxford: Elsevier. pp 279–310.

Robbe, D., Kopf, M., Remaury, A., Bockaert, J., & Manzoni, O.J. (2002) Endogenous cannabinoids mediate long-term synaptic depression in the nucleus accumbens. *Proceedings of the National Academy of Sciences of the United States of America*, **99**, 8384–8388.

Rodriguez, J.J., Mackie, K., & Pickel, V.M. (2001) Ultrastructural localization of the CB1 cannabinoid receptor in mu-opioid receptor patches of the rat Caudate putamen nucleus. *The Journal of neuroscience : the official journal of the Society for Neuroscience*, **21**, 823–833.

Runyan, S.A., Roy, R.R., Zhong, H., & Phelps, P.E. (2007) L1 cell adhesion molecule is not required for small-diameter primary afferent sprouting after deafferentation. *Neuroscience*, **150**, 959–969.

Safo, P.K. & Regehr, W.G. (2005) Endocannabinoids control the induction of cerebellar LTD. *Neuron*, **48**, 647–659.

Sakurada, T. & Noma, A. (1981) Subcellular localization and some properties of monoacylglycerol lipase in rat adipocytes. *Journal of biochemistry*, **90**, 1413–1419.

Salio, C., Cottone, E., Conrath, M., & Franzoni, M.F. (2002) CB1 cannabinoid receptors in amphibian spinal cord: relationships with some nociception markers. *Journal of chemical neuroanatomy*, **24**, 153–162.

Salio, C., Doly, S., Fischer, J., Franzoni, M.F., & Conrath, M. (2002) Neuronal and astrocytic localization of the cannabinoid receptor-1 in the dorsal horn of the rat spinal cord. *Neuroscience letters*, **329**, 13–16.

Salio, C., Fischer, J., Franzoni, M.F., & Conrath, M. (2002) Pre- and postsynaptic localizations of the CB1 cannabinoid receptor in the dorsal horn of the rat spinal cord. *Neuroscience*, **110**, 755–764.

Salio, C., Fischer, J., Franzoni, M.F., Mackie, K., Kaneko, T., & Conrath, M. (2001) CB1-cannabinoid and mu-opioid receptor co-localization on postsynaptic target in the rat dorsal horn. *Neuroreport*, **12**, 3689–3692.

Schlosburg, J.E., Blankman, J.L., Long, J.Z., Nomura, D.K., Pan, B., Kinsey, S.G., Nguyen, P.T., Ramesh, D., Booker, L., Burston, J.J., Thomas, E.A., Selley, D.E., Sim-Selley, L.J., Liu, Q., Lichtman, A.H., & Cravatt, B.F. (2010) Chronic monoacylglycerol lipase blockade causes functional antagonism of the endocannabinoid system. *Nature neuroscience*, **13**, 1113–1119.

Schmid, H.H.O., Schmid, P.C., & Berdyshev, E. V (2002) Cell signaling by endocannabinoids and their congeners: questions of selectivity and other challenges. *Chemistry and physics of lipids*, **121**, 111–134.

Scholz, J. & Woolf, C.J. (2007) The neuropathic pain triad: neurons, immune cells and glia. *Nature neuroscience*, **10**, 1361–1368.

Shire, D., Calandra, B., Rinaldi-Carmona, M., Oustric, D., Pessègue, B., Bonnin-Cabanne, O., Le Fur, G., Caput, D., & Ferrara, P. (1996) Molecular cloning, expression and function of the murine CB2 peripheral cannabinoid receptor. *Biochimica et biophysica acta*, **1307**, 132–136.

Simon, G.M. & Cravatt, B.F. (2006) Endocannabinoid biosynthesis proceeding through glycerophospho-N-acyl ethanolamine and a role for alpha/beta-hydrolase 4 in this pathway. *The Journal of biological chemistry*, **281**, 26465–26472.

Simon, G.M. & Cravatt, B.F. (2008) Anandamide biosynthesis catalyzed by the phosphodiesterase GDE1 and detection of glycerophospho-N-acyl ethanolamine precursors in mouse brain. *The Journal of biological chemistry*, **283**, 9341–9349.

Sjöström, P.J., Turrigiano, G.G., & Nelson, S.B. (2003) Neocortical LTD via coincident activation of presynaptic NMDA and cannabinoid receptors. *Neuron*, **39**, 641–654.

Smart, D., Gunthorpe, M.J., Jerman, J.C., Nasir, S., Gray, J., Muir, A.I., Chambers, J.K., Randall, A.D., & Davis, J.B. (2000) The endogenous lipid anandamide is a full agonist at the human vanilloid receptor (hVR1). *British journal of pharmacology*, **129**, 227–230.

Smith, F.L., Cichewicz, D., Martin, Z.L., & Welch, S.P. (1998) The enhancement of morphine antinociception in mice by delta9-tetrahydrocannabinol. *Pharmacology, biochemistry, and behavior*, **60**, 559–566.

Smith, P.B., Compton, D.R., Welch, S.P., Razdan, R.K., Mechoulam, R., & Martin, B.R. (1994) The pharmacological activity of anandamide, a putative endogenous cannabinoid, in mice. *The Journal of pharmacology and experimental therapeutics*, **270**, 219–227.

Soghomonian, J.J. & Martin, D.L. (1998) Two isoforms of glutamate decarboxylase: why? *Trends in pharmacological sciences*, **19**, 500–505.

Song, C. & Howlett, A.C. (1995) Rat brain cannabinoid receptors are N-linked glycosylated proteins. *Life sciences*, **56**, 1983–1989.

Stella, N. & Piomelli, D. (2001) Receptor-dependent formation of endogenous cannabinoids in cortical neurons. *European journal of pharmacology*, **425**, 189–196.

Stella, N., Schweitzer, P., & Piomelli, D. (1997) A second endogenous cannabinoid that modulates long-term potentiation. *Nature*, **388**, 773–778.

Strangman, N.M. & Walker, J.M. (1999) Cannabinoid WIN 55,212-2 inhibits the activity-dependent facilitation of spinal nociceptive responses. *Journal of neurophysiology*, **82**, 472–477.

Streit, W.J. (1990) An improved staining method for rat microglial cells using the lectin from Griffonia simplicifolia (GSA I-B4). *The journal of histochemistry and cytochemistry : official journal of the Histochemistry Society*, **38**, 1683–1686.

Suárez, J., Bermúdez-Silva, F.J., Mackie, K., Ledent, C., Zimmer, A., Cravatt, B.F., & De Fonseca, F.R. (2008) Immunohistochemical description of the endogenous cannabinoid system in the rat cerebellum and functionally related nuclei. *The Journal of comparative neurology*, **509**, 400–421.

Suárez, J., Ortíz, O., Puente, N., Bermúdez-Silva, F.J., Blanco, E., Fernández-Llebrez, P., Grandes, P., De Fonseca, F.R., & Moratalla, R. (2011) Distribution of diacylglycerol lipase

alpha, an endocannabinoid synthesizing enzyme, in the rat forebrain. *Neuroscience*, **192**, 112–131.

Sugiura, T., Kobayashi, Y., Oka, S., & Waku, K. (2002) Biosynthesis and degradation of anandamide and 2-arachidonoylglycerol and their possible physiological significance. *Prostaglandins, leukotrienes, and essential fatty acids*, **66**, 173–192.

Sugiura, T., Kodaka, T., Kondo, S., Nakane, S., Kondo, H., Waku, K., Ishima, Y., Watanabe, K., & Yamamoto, I. (1997) Is the cannabinoid CB1 receptor a 2-arachidonoylglycerol receptor? Structural requirements for triggering a Ca2+ transient in NG108-15 cells. *Journal of biochemistry*, **122**, 890–895.

Sugiura, T., Kodaka, T., Nakane, S., Miyashita, T., Kondo, S., Suhara, Y., Takayama, H., Waku, K., Seki, C., Baba, N., & Ishima, Y. (1999) Evidence that the cannabinoid CB1 receptor is a 2-arachidonoylglycerol receptor. Structure-activity relationship of 2-arachidonoylglycerol, ether-linked analogues, and related compounds. *The Journal of biological chemistry*, **274**, 2794–2801.

Sugiura, T., Kondo, S., Kishimoto, S., Miyashita, T., Nakane, S., Kodaka, T., Suhara, Y., Takayama, H., & Waku, K. (2000) Evidence that 2-arachidonoylglycerol but not N-palmitoylethanolamine or anandamide is the physiological ligand for the cannabinoid CB2 receptor. Comparison of the agonistic activities of various cannabinoid receptor ligands in HL-60 cells. *The Journal of biological chemistry*, **275**, 605–612.

Sugiura, T., Kondo, S., Sukagawa, A., Nakane, S., Shinoda, A., Itoh, K., Yamashita, A., & Waku, K. (1995) 2-Arachidonoylglycerol: a possible endogenous cannabinoid receptor ligand in brain. *Biochemical and biophysical research communications*, **215**, 89–97.

Sugiura, T., Kondo, S., Sukagawa, A., Tonegawa, T., Nakane, S., Yamashita, A., & Waku, K. (1996) Enzymatic synthesis of anandamide, an endogenous cannabinoid receptor ligand, through N-acylphosphatidylethanolamine pathway in testis: involvement of Ca(2+)-dependent transacylase and phosphodiesterase activities. *Biochemical and biophysical research communications*, **218**, 113–117.

Sun, Y.-X., Tsuboi, K., Okamoto, Y., Tonai, T., Murakami, M., Kudo, I., & Ueda, N. (2004) Biosynthesis of anandamide and N-palmitoylethanolamine by sequential actions of phospholipase A2 and lysophospholipase D. *The Biochemical journal*, **380**, 749–756.

Suter, M.R., Wen, Y.-R., Decosterd, I., & Ji, R.-R. (2007) Do glial cells control pain? *Neuron glia biology*, **3**, 255–268.

Tanimura, A., Yamazaki, M., Hashimotodani, Y., Uchigashima, M., Kawata, S., Abe, M., Kita, Y., Hashimoto, K., Shimizu, T., Watanabe, M., Sakimura, K., & Kano, M. (2010) The endocannabinoid 2-arachidonoylglycerol produced by diacylglycerol lipase alpha mediates retrograde suppression of synaptic transmission. *Neuron*, **65**, 320–327.

Todd, A.J., Hughes, D.I., Polgár, E., Nagy, G.G., Mackie, M., Ottersen, O.P., & Maxwell, D.J. (2003) The expression of vesicular glutamate transporters VGLUT1 and VGLUT2 in neurochemically defined axonal populations in the rat spinal cord with emphasis on the dorsal horn. *The European journal of neuroscience*, **17**, 13–27.

Tornqvist, H. & Belfrage, P. (1976) Determination of protein in adipose tissue extracts. *Journal of lipid research*, **17**, 542–545.

Tran, T.S., Alijani, A., & Phelps, P.E. (2003) Unique developmental patterns of GABAergic neurons in rat spinal cord. *The Journal of comparative neurology*, **456**, 112–126.

Traub, R.J., Solodkin, A., & Ruda, M.A. (1989) Calcitonin gene-related peptide immunoreactivity in the cat lumbosacral spinal cord and the effects of multiple dorsal rhizotomies. *The Journal of comparative neurology*, **287**, 225–237.

Tsou, K., Brown, S., Sañudo-Peña, M.C., Mackie, K., & Walker, J.M. (1998) Immunohistochemical distribution of cannabinoid CB1 receptors in the rat central nervous system. *Neuroscience*, **83**, 393–411.

Tsou, K., Lowitz, K.A., Hohmann, A.G., Martin, W.J., Hathaway, C.B., Bereiter, D.A., & Walker, J.M. (1996) Suppression of noxious stimulus-evoked expression of Fos protein-like immunoreactivity in rat spinal cord by a selective cannabinoid agonist. *Neuroscience*, **70**, 791–798.

Tsuboi, K., Zhao, L.-Y., Okamoto, Y., Araki, N., Ueno, M., Sakamoto, H., & Ueda, N. (2007) Predominant expression of lysosomal N-acylethanolamine-hydrolyzing acid amidase in macrophages revealed by immunochemical studies. *Biochimica et biophysica acta*, **1771**, 623–632.

Turu, G. & Hunyady, L. (2010) Signal transduction of the CB1 cannabinoid receptor. *Journal of molecular endocrinology*, **44**, 75–85.

Twitchell, W., Brown, S., & Mackie, K. (1997) Cannabinoids inhibit N- and P/Q-type calcium channels in cultured rat hippocampal neurons. *Journal of neurophysiology*, **78**, 43–50.

Uchigashima, M., Narushima, M., Fukaya, M., Katona, I., Kano, M., & Watanabe, M. (2007) Subcellular arrangement of molecules for 2-arachidonoyl-glycerol-mediated retrograde signaling and its physiological contribution to synaptic modulation in the striatum. *The Journal of neuroscience : the official journal of the Society for Neuroscience*, **27**, 3663–3676.

Ueda, H., Kobayashi, T., Kishimoto, M., Tsutsumi, T., & Okuyama, H. (1993) A possible pathway of phosphoinositide metabolism through EDTA-insensitive phospholipase A1 followed by lysophosphoinositide-specific phospholipase C in rat brain. *Journal of neurochemistry*, **61**, 1874–1881.

Van der Stelt, M., Trevisani, M., Vellani, V., De Petrocellis, L., Schiano Moriello, A., Campi, B., McNaughton, P., Geppetti, P., & Di Marzo, V. (2005) Anandamide acts as an intracellular messenger amplifying Ca2+ influx via TRPV1 channels. *The EMBO journal*, **24**, 3026–3037.

Van Sickle, M.D., Duncan, M., Kingsley, P.J., Mouihate, A., Urbani, P., Mackie, K., Stella, N., Makriyannis, A., Piomelli, D., Davison, J.S., Marnett, L.J., Di Marzo, V., Pittman, Q.J., Patel, K.D., & Sharkey, K.A. (2005) Identification and functional characterization of brainstem cannabinoid CB2 receptors. *Science (New York, N.Y.)*, **310**, 329–332.

Veldhuis, W.B., Van der Stelt, M., Wadman, M.W., Van Zadelhoff, G., Maccarrone, M., Fezza, F., Veldink, G.A., Vliegenthart, J.F.G., Bär, P.R., Nicolay, K., & Di Marzo, V. (2003) Neuroprotection by the endogenous cannabinoid anandamide and arvanil against in vivo excitotoxicity in the rat: role of vanilloid receptors and lipoxygenases. *The Journal of neuroscience : the official journal of the Society for Neuroscience*, **23**, 4127–4133.

Venance, L., Sagan, S., & Giaume, C. (1997) (R)-methanandamide inhibits receptor-induced calcium responses by depleting internal calcium stores in cultured astrocytes. *Pflügers Archiv : European journal of physiology*, **434**, 147–149.

Villeda, S.A., Akopians, A.L., Babayan, A.H., Basbaum, A.I., & Phelps, P.E. (2006) Absence of Reelin results in altered nociception and aberrant neuronal positioning in the dorsal spinal cord. *Neuroscience*, **139**, 1385–1396.

Vogel, Z., Barg, J., Levy, R., Saya, D., Heldman, E., & Mechoulam, R. (1993) Anandamide, a brain endogenous compound, interacts specifically with cannabinoid receptors and inhibits adenylate cyclase. *Journal of neurochemistry*, **61**, 352–355.

Volterra, A. & Bezzi, P. (2002) The tripartite synapse: Glia. In Volterra, A., Magistretti, P.J. & Haydon, P.G. (Eds.) *Synaptic Transmission*, Oxford University Press, New York, pp.164–168.

Walter, L., Dinh, T., & Stella, N. (2004) ATP induces a rapid and pronounced increase in 2-arachidonoylglycerol production by astrocytes, a response limited by monoacylglycerol lipase. *The Journal of neuroscience : the official journal of the Society for Neuroscience*, **24**, 8068–8074.

Walter, L., Franklin, A., Witting, A., Moller, T., & Stella, N. (2002) Astrocytes in culture produce anandamide and other acylethanolamides. *The Journal of biological chemistry*, **277**, 20869–20876.

Walter, L., Franklin, A., Witting, A., Wade, C., Xie, Y., Kunos, G., Mackie, K., & Stella, N. (2003) Nonpsychotropic cannabinoid receptors regulate microglial cell migration. *The Journal of neuroscience : the official journal of the Society for Neuroscience*, **23**, 1398–1405.

Walter, L. & Stella, N. (2003) Endothelin-1 increases 2-arachidonoyl glycerol (2-AG) production in astrocytes. *Glia*, **44**, 85–90.

Walter, L. & Stella, N. (2004) Cannabinoids and neuroinflammation. *British journal of pharmacology*, **141**, 775–785.

Wang, H., Matsumoto, H., Guo, Y., Paria, B.C., Roberts, R.L., & Dey, S.K. (2003) Differential G protein-coupled cannabinoid receptor signaling by anandamide directs blastocyst activation for implantation. *Proceedings of the National Academy of Sciences of the United States of America*, **100**, 14914–14919.

Wang, J. & Ueda, N. (2009) Biology of endocannabinoid synthesis system. *Prostaglandins & other lipid mediators*, **89**, 112–119.

Wei, B.Q., Mikkelsen, T.S., McKinney, M.K., Lander, E.S., & Cravatt, B.F. (2006) A second fatty acid amide hydrolase with variable distribution among placental mammals. *The Journal of biological chemistry*, **281**, 36569–36578.

Willis, W.D. & Coggeshall, R.E. (2004) *Sensory Mechanisms of the Spinal Cord. Vol 1. Primary Afferent Neurons and the Spinal Dorsal Horn*. Kluwer Academic/Plenum Publishers, New York.

Wilson, R.I. & Nicoll, R.A. (2001) Endogenous cannabinoids mediate retrograde signalling at hippocampal synapses. *Nature*, **410**, 588–592.

Wilson, R.I. & Nicoll, R.A. (2002) Endocannabinoid signaling in the brain. *Science (New York, N.Y.)*, **296**, 678–682.

Witting, A., Walter, L., Wacker, J., Möller, T., & Stella, N. (2004) P2X7 receptors control 2-arachidonoylglycerol production by microglial cells. *Proceedings of the National Academy of Sciences of the United States of America*, **101**, 3214–3219.

Woodward, D.F., Carling, R.W.C., Cornell, C.L., Fliri, H.G., Martos, J.L., Pettit, S.N., Liang, Y., & Wang, J.W. (2008) The pharmacology and therapeutic relevance of endocannabinoid derived cyclo-oxygenase (COX)-2 products. *Pharmacology & therapeutics*, **120**, 71–80.

Yazulla, S., Studholme, K.M., McIntosh, H.H., & Deutsch, D.G. (1999) Immunocytochemical localization of cannabinoid CB1 receptor and fatty acid amide hydrolase in rat retina. *The Journal of comparative neurology*, **415**, 80–90.

Yoshida, T., Fukaya, M., Uchigashima, M., Miura, E., Kamiya, H., Kano, M., & Watanabe, M. (2006) Localization of diacylglycerol lipase-alpha around postsynaptic spine suggests close proximity between production site of an endocannabinoid, 2-arachidonoyl-glycerol, and presynaptic cannabinoid CB1 receptor. *The Journal of neuroscience : the official journal of the Society for Neuroscience*, **26**, 4740–4751.

Yoshida, T., Uchigashima, M., Yamasaki, M., Katona, I., Yamazaki, M., Sakimura, K., Kano, M., Yoshioka, M., & Watanabe, M. (2011) Unique inhibitory synapse with particularly rich endocannabinoid signaling machinery on pyramidal neurons in basal amygdaloid nucleus. *Proceedings of the National Academy of Sciences of the United States of America*, **108**, 3059–3064.

Zhang, F., Vadakkan, K.I., Kim, S.S., Wu, L.-J., Shang, Y., & Zhuo, M. (2008) Selective activation of microglia in spinal cord but not higher cortical regions following nerve injury in adult mouse. *Molecular pain*, **4**, 15.

Zhang, J., Hoffert, C., Vu, H.K., Groblewski, T., Ahmad, S., Donnell, D.O., & O'Donnell, D. (2003) Induction of CB2 receptor expression in the rat spinal cord of neuropathic but not inflammatory chronic pain models. *European Journal of Neuroscience*, **17**, 2750–2754.

Zygmunt, P.M., Petersson, J., Andersson, D.A., Chuang, H., Sørgård, M., Di Marzo, V., Julius, D., & Högestätt, E.D. (1999) Vanilloid receptors on sensory nerves mediate the vasodilator action of anandamide. *Nature*, **400**, 452–457.

9. LIST OF PUBLICATIONS

DEENK www.lib.unideb.hu
UNIVERSITY AND NATIONAL LIBRARY UNIVERSITY OF DEBRECEN
KENÉZY LIFE SCIENCES LIBRARY

Register Number: DEENKÉTK/162/2013.
Item Number:
Subject: Ph.D. List of Publications

Candidate: Zoltán Hegyi
Neptun ID: PC5PRJ
Doctoral School: Doctoral School of Neurosciences

List of publications related to the dissertation

1. **Hegyi, Z.**, Holló, K., Kis, G., Mackie, K., Antal, M.: Differential distribution of diacylglycerol lipase-alpha and N-acylphosphatidylethanolamine-specific phospholipase D immunoreactivity in the superficial spinal dorsal horn of rats.
Glia. 60 (9), 1316-1329, 2012.
DOI: http://dx.doi.org/10.1002/glia.2235
IF:4.82 (2011)

2. **Hegyi, Z.**, Kis, G., Holló, K., Ledent, C., Antal, M.: Neuronal and glial localization of the cannabinoid-1 receptor in the superficial spinal dorsal horn of the rodent spinal cord.
Eur. J. Neurosci. 30 (2), 251-262, 2009.
DOI: http://dx.doi.org/10.1111/j.1460-9568.2009.06816.x
IF:3.418

List of other publications

3. Karosi, T., Csomor, P., **Hegyi, Z.**, Sziklai, I.: The presence of CD209 expressing dendritic cells correlates with biofilm positivity in chronic rhinosinusitis with nasal polyposis.
Eur. Arch. Oto-Rhino-Laryn. Epub ahead of print (2013)
DOI: http://dx.doi.org/10.1007/s00405-013-2372-9
IF:1.287 (2011)

DEBRECENI EGYETEM KENÉZY EMLÉKTUDOMÁNYI KÖNYVTÁRA EGYETEMI ÉS NEMZETI KÖNYVTÁR

H-4032 Debrecen, Egyetem tér 1. e-mail: publikaciok@lib.unideb.hu

4. Szalai, E., Felszeghy, S., **Hegyi, Z.**, Módis, L., Berta, A., Kaarniranta, K.: Fibrillin-2, tenascin-C, matrilin-2, and matrilin-4 are strongly expressed in the epithelium of human granular and lattice type I corneal dystrophies.
Mol. Vis. 18, 1927-1936, 2012.
IF:2.205 (2011)

Total IF: 11.73

Total IF (publications related to the dissertation): 8.238

The Candidate's publication data submitted to the Publication Database of the University of Debrecen have been validated by Kenezy Life Sciences Library on the basis of Web of Science, Scopus and Journal Citation Report (Impact Factor) databases.

02 May, 2013

Conference abstracts

1. **Hegyi Z**, Kis G, Antal M: Neuronal and glial localization of the cannabinoid-1 receptor in the superficial dorsal horn of the rodent spinal cord. *IBRO International Workshop*, Debrecen, 2008.
2. **Hegyi Z**, Kis G, Holló K, Ledent C, Antal M: Neuronal and glial localization of the cannabinoid-1 receptor in the superficial dorsal horn of the rodent spinal cord. *6th FENS Forum*, Geneva, 2008.
3. **Hegyi Z**, Antal M: Reorganization of cannabinoid-1 receptor expression in the superficial spinal dorsal horn of rats in inflammatory pain. *Annual Conference of the Hungarian Neuroscience Society*, 2008.
4. **Hegyi Z**, Holló K, Kis G, Mackie K, Antal, M: Differential distribution of DGL-alpha and NAPE-PLD immunoreactivity in the superficial spinal dorsal horn of rodents. *IBRO Workshop*, Pécs, 2010.
5. **Hegyi Z**, Kis G, Holló K, Ledent C, Mackie K, Antal M: Differential distribution of CB1 receptor, DGL-alpha and NAPE-PLD immunoreactivity in the superficial spinal dorsal horn of rodents. *Workshop on the endocannabinoid system*, Bonn, 2010
6. **Hegyi Z**, Kis G, Holló K, Mackie K, Antal M: Differential distribution of DGL-alpha and NAPE-PLD immunoreactivity in the superficial spinal dorsal horn of rodents. *FENS Forum*, 2010, Amsterdam
7. **Hegyi Z**, Kis G, Holló K, Mackie K, Antal M: Differential distribution of diacylglycerol lipase-alpha and N-acyl-phosphatidyl-ethanolamine-hydrolyzing phospholipase D immunoreactivity in the superficial spinal dorsal horn of rodent. *Joint Conference of the LXXV. Meeting of the Hungarian Physiological Society with participation of the Hungarian Society of Anatomists, the Experimental Section of the Hungarian Society for Experimental and Clinical Pharmacology and the Hungarian Society for Microcirculation and Vascular Biology*, Pécs, 2011.
8. **Hegyi Z**, Holló K, Antal M: Co-expression of CB1 receptors and the major endocannabinoid-synthesizing enzymes, DGL-α and NAPE-PLD by astrocytes in the rat spinal cord. *FENS Forum*, 2012, Barcelona

9. Holló K, Ducza L, Bakk E, Hegedus K, **Hegyi Z**, Antal M: Expression And Cellular Localization Of Interleukin-1 Receptor Type-1 In The Spinal Dorsal Horn In The Freund Adjuvant-Evoked Inflammatory Pain. *FENS Forum*, 2012, Barcelona
10. **Hegyi Z**, Oláh T, Docova K, Holló K, Csernoch L, Antal M: Endocannabinoid-mediated calcium signaling in spinal astrocytes. *Annual Conference of the Hungarian Neuroscience Society*, 2013, Budapest

11. Holló K, Gajtkó A, Hegedűs K, Bakk E, **Hegyi Z**, Antal M: IL-1 beta production by cultured spinal cord astrocytes upon LPS treatment is influenced by ATP and glutamate. *Annual Conference of the Hungarian Neuroscience Society*, 2013, Budapest
12. Docova K, **Hegyi Z**, Holló K, Kis G, Mackie K, Antal M: Distribution of monoacylglycerol lipase (MGL) immunoreactivity in the superficial spinal dorsal horn of rodents. *Annual Conference of the Hungarian Neuroscience Society*, 2013, Budapest

10. KEY WORDS

presynaptic CB1 receptors, DGL-α, NAPE-PLD, nociceptive primary afferents, interneurons, astrocytes, microglia, glial cells

11. ACKNOWLEDGEMENT

I would like to express my appreciation for the help and support of the people who have contributed to this work.

First and foremost I owe a great deal of sincere gratitude to my supervisor Prof. Dr. Miklós Antal for his valuable guidance, motivation and for the support of my research.

I would also like to thank my former and present colleagues in the Department of Anatomy for the scientific and personal support, especially to Dr. Krisztina Holló, Gréta Kis, Mrs. Mária Varga, Krisztina Hegedűs and Erzsébet Bakk.

I am grateful to Prof. Dr. Catherine Ledent for providing transgenic mice, and to Prof. Dr. Ken Mackie who provided excellent antibodies for my experiments.

Most importantly, I am much obliged to my parents for encouraging and supporting me my entire life.

Above all, I would like to acknowledge my wife Kata – there is nothing I can do to thank her enough for the continuous support, patience, understanding and endless love.